Carbon nanotubes and graphene as THz emitters and detectors

Mikhail Portnoi

School of Physics
University of Exeter
United Kingdom

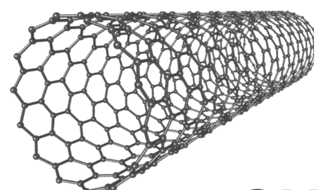

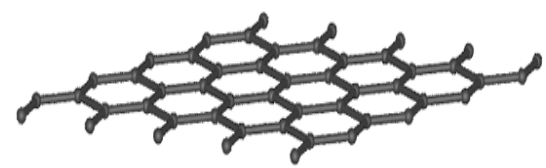

ISNP-V, April 2012

UNIVERSITY OF EXETER

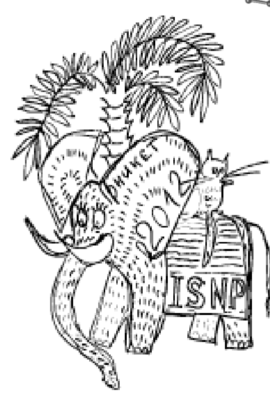

Terahertz radiation and the ‘THz gap’

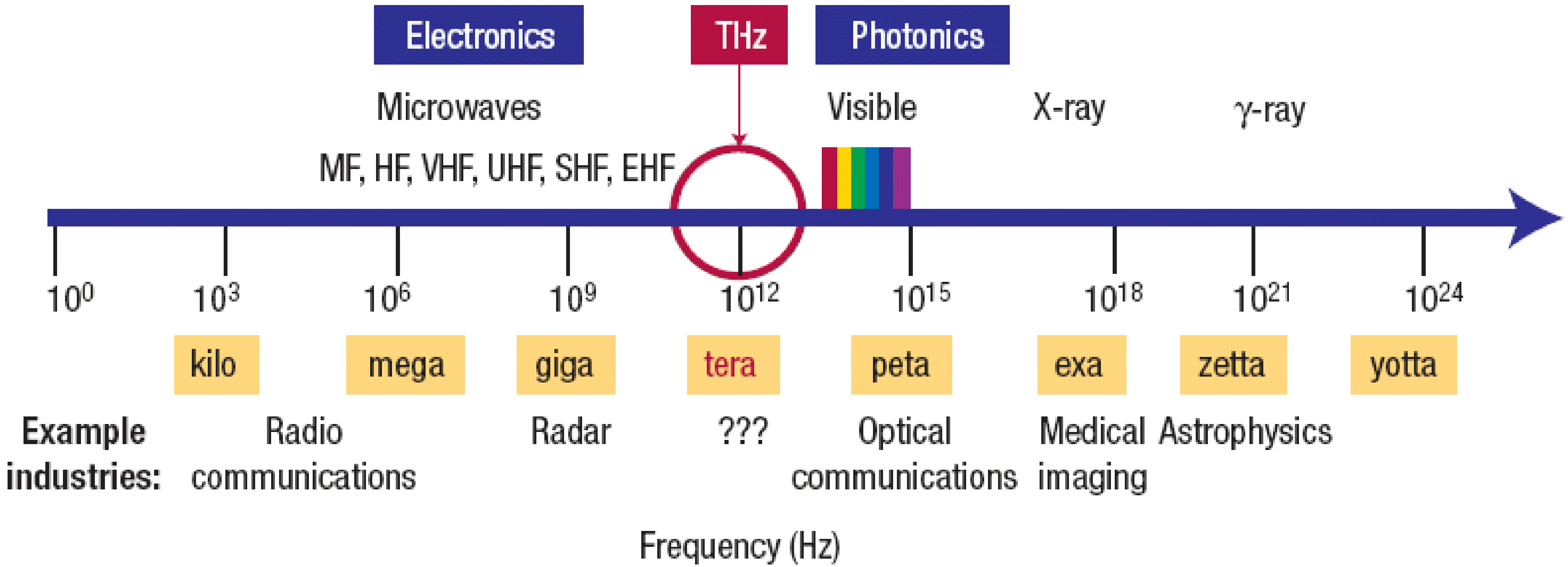

From B. Ferguson and X.-Ch. Zhang, Nature Materials **1**, 26 (2002)

Terahertz radiation and the 'THz gap'

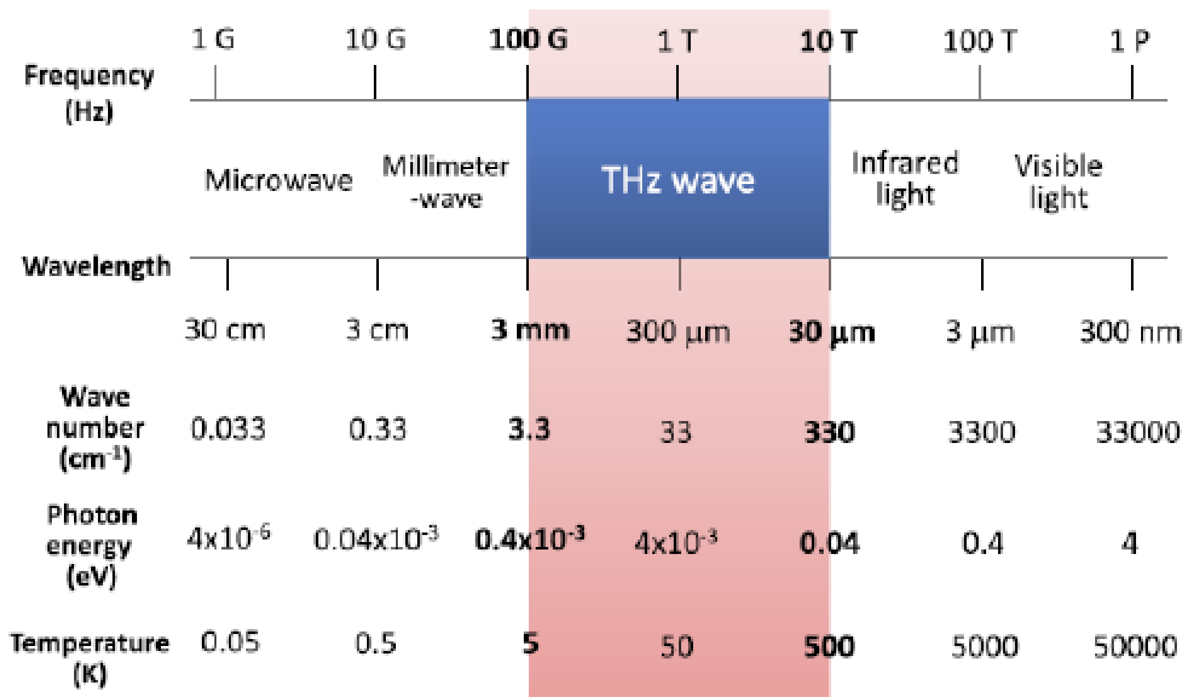

Recent review: T. Nagatsuma, IEICE Electronics Express **8**, 1127 (July 25, 2011)

Why is the THz range important?

Examples from the DOE-NSF-NIH Workshop Report, 2004

- Electrons in highly-excited atomic Rydberg states orbit at THz frequencies
- Small molecules rotate at THz frequencies
- Collisions between gas phase molecules at room temperature last about 1 ps
- Biologically-important collective modes of proteins vibrate at THz frequencies
- Frustrated rotations and collective modes cause polar liquids (such as water) to absorb at THz frequencies

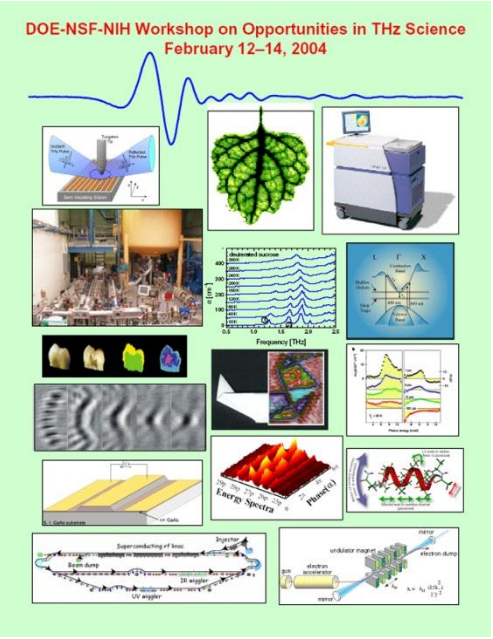

More examples from the DOE-NSF-NIH Workshop Report

- Electrons in semiconductors and their nanostructures resonate at THz frequencies
- Superconducting energy gaps are found at THz frequencies
- Gaseous and solid-state plasmas oscillate at THz frequencies
- Matter at temperatures above 10 K emits black-body radiation at THz frequencies
- An electron in Intel's THz Transistor races under the gate in ~1 ps …

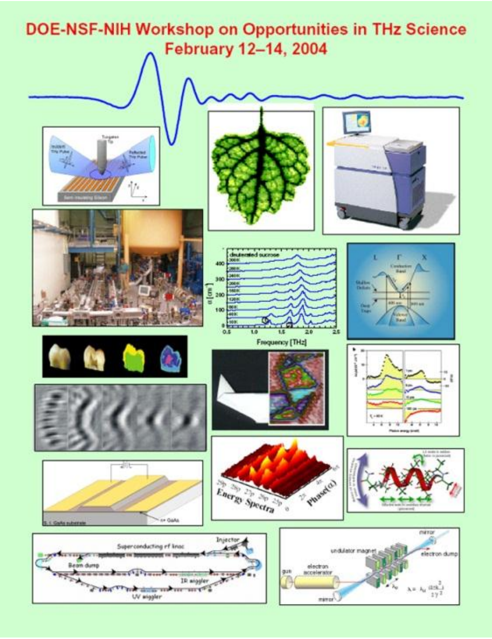

Transition region between photonics and electronics => unprecedented creativity in source development!

Free-electron laser (FELIX)

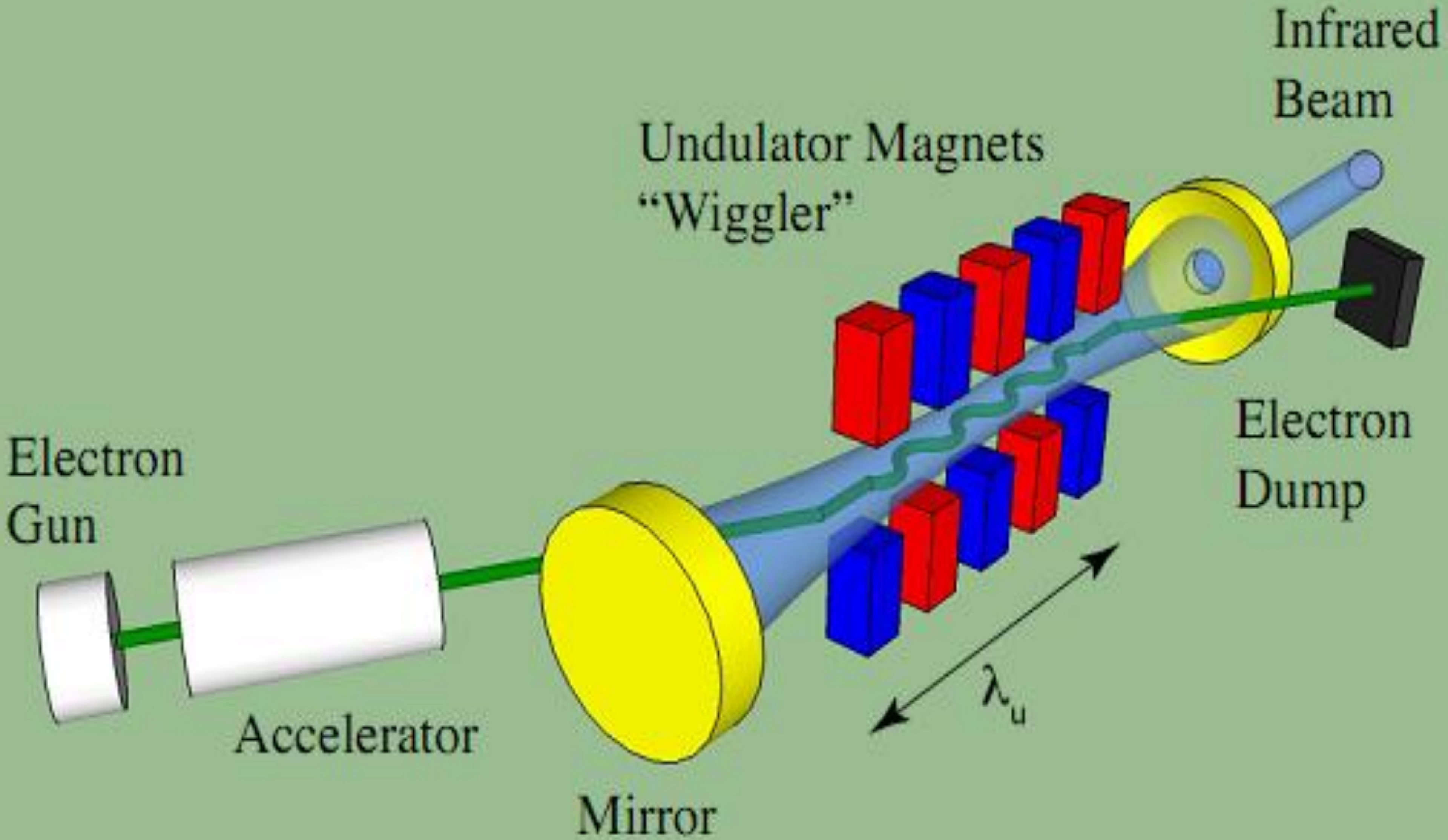
Infrared
Beam
Undulator Magnets
"Wiggler"
Electron
Dump
Electron
Gun
Accelerator
Mirror
λ_u

TeraView scanner ~ $500K

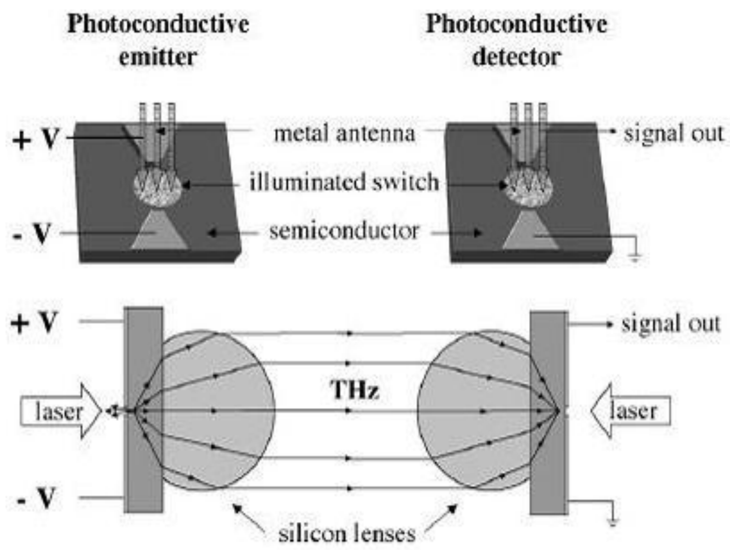

Quantum cascade laser

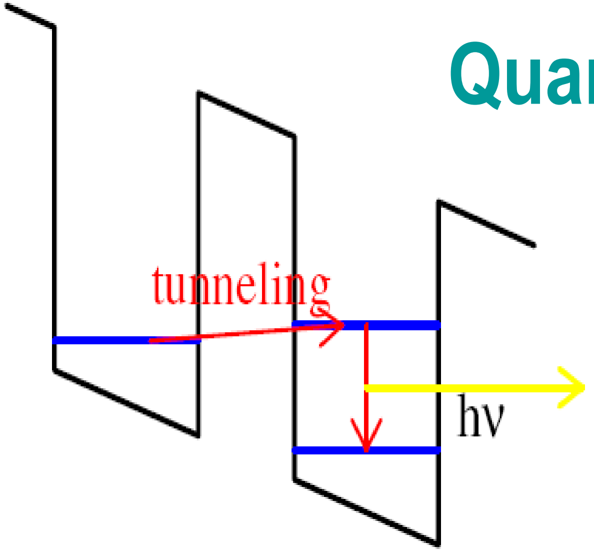

Kazarinov and Suris, 1971

It took 23 years to achieve this laser!

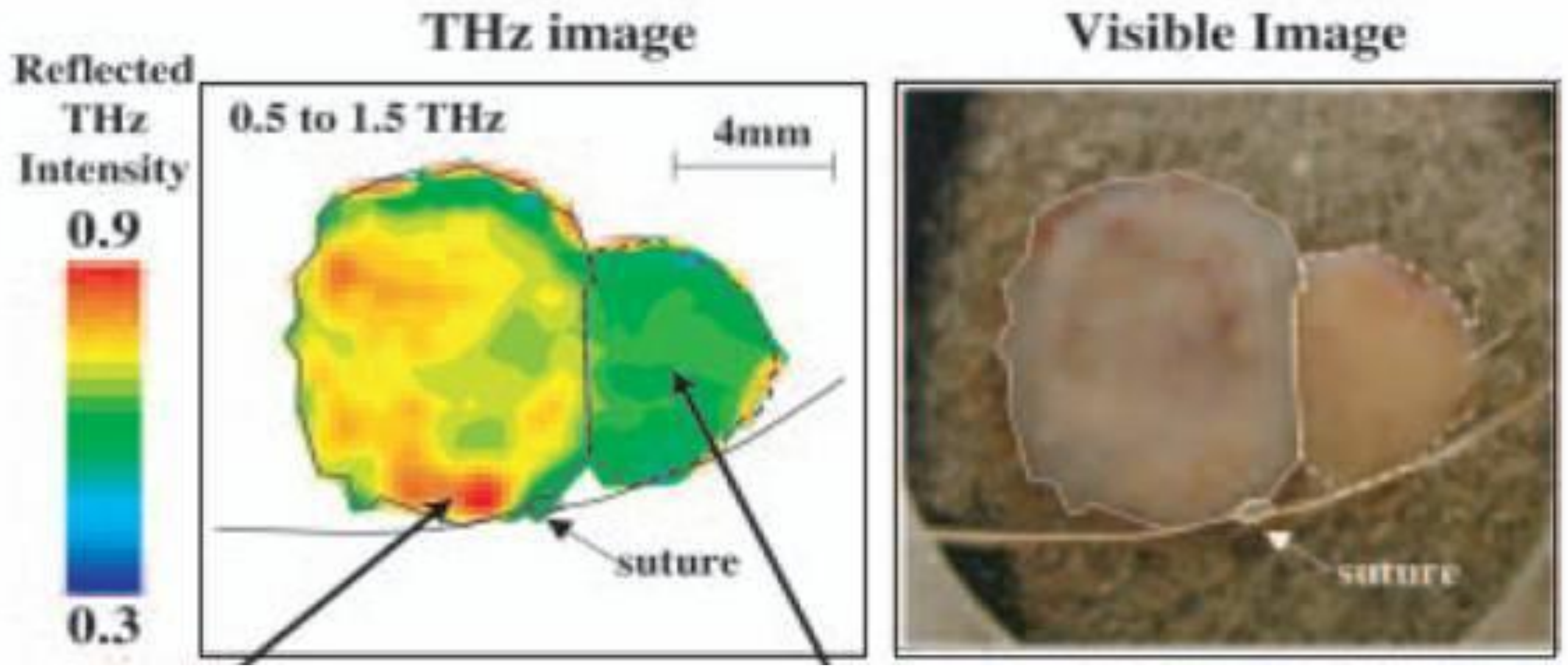

Diseased tissue

Healthy tissue

Images from TeraView Limited

Visible image of human tooth

Terahertz image of cavity in human tooth

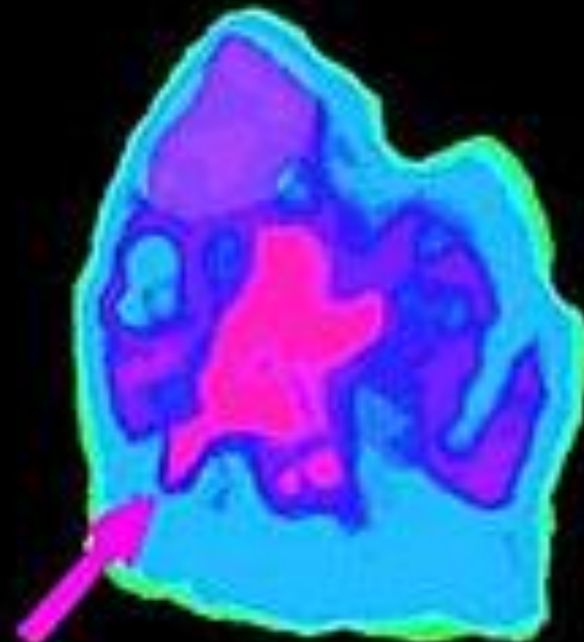

Cavity

Image composed from absorption data

Security applications of THz Imaging

: HMGCC

Security applications of THz Imaging

: HMGCC

Security applications of THz Imaging

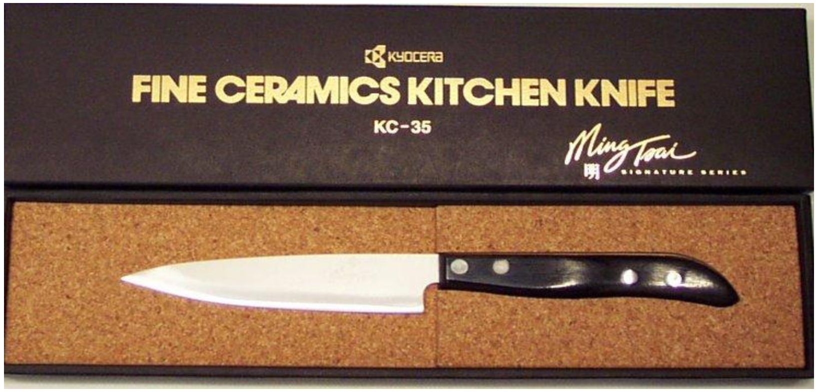

Acknowledgement: HMGCC

Anthrax

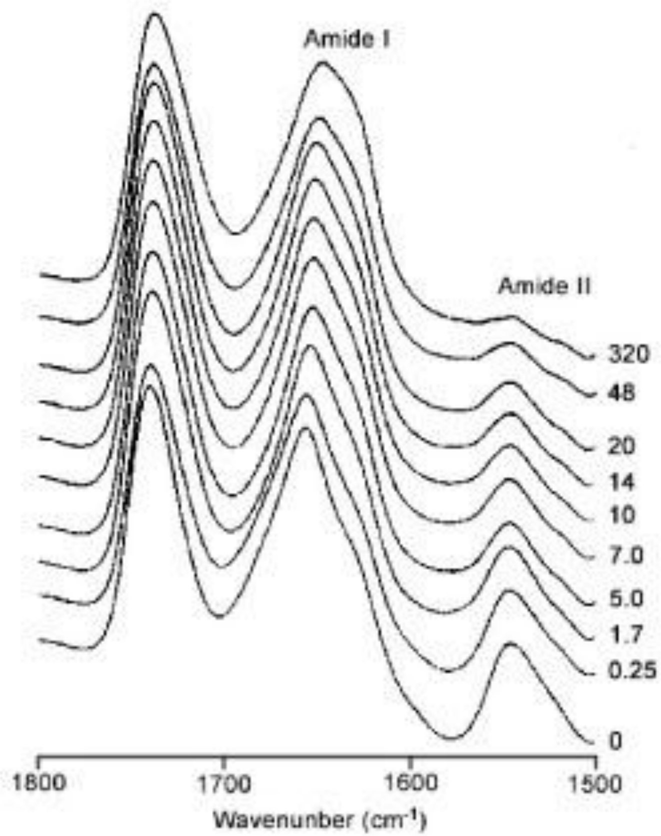

L. A. Vanderberg. Detection of biological agents : Looking for bugs in all the wrong places. *Applied Spectroscopy*, 54:376A, 2000.

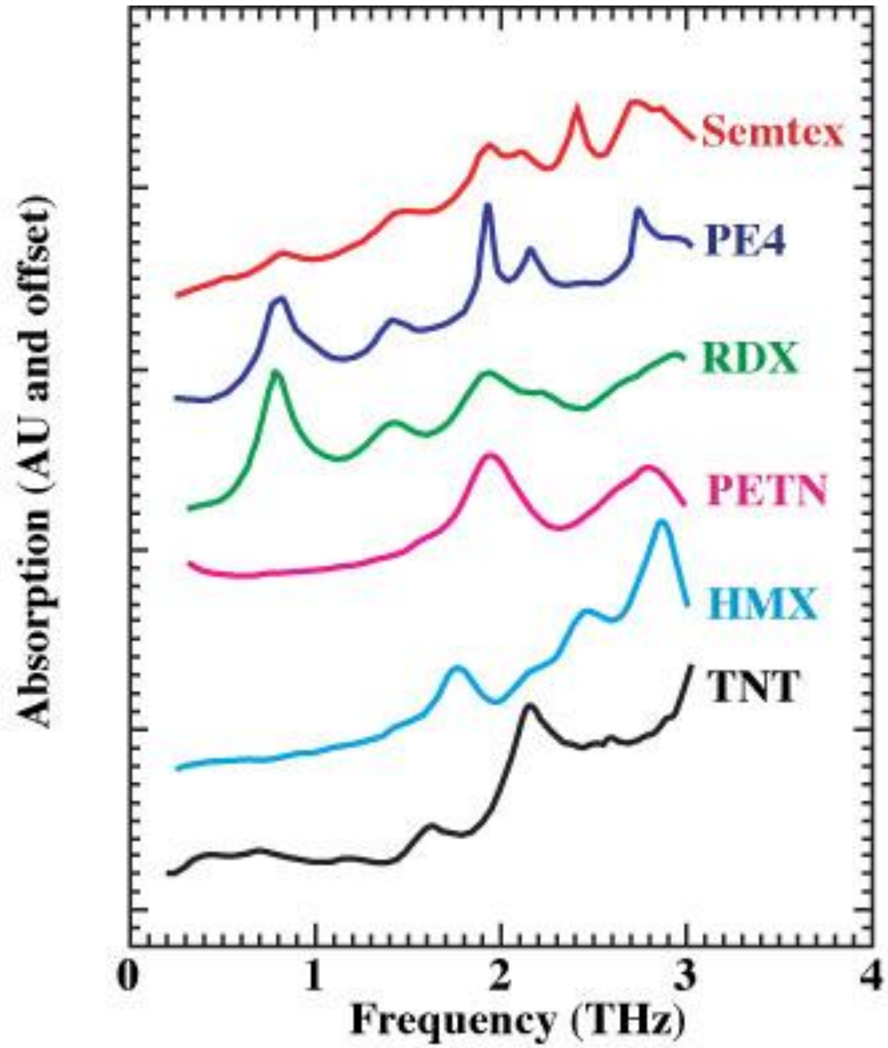

Image courtesy of TeraView Ltd.

Latest proposals – polaritonics

APPLIED PHYSICS LETTERS **97**, 201111 (2010)

Stimulated emission of terahertz radiation by exciton-polariton lasers

K. V. Kavokin,[1,2] M. A. Kaliteevski,[3] R. A. Abram,[3] A. V. Kavokin,[4] S. Sharkova,[5] and I. A. Shelykh[2,5,6]

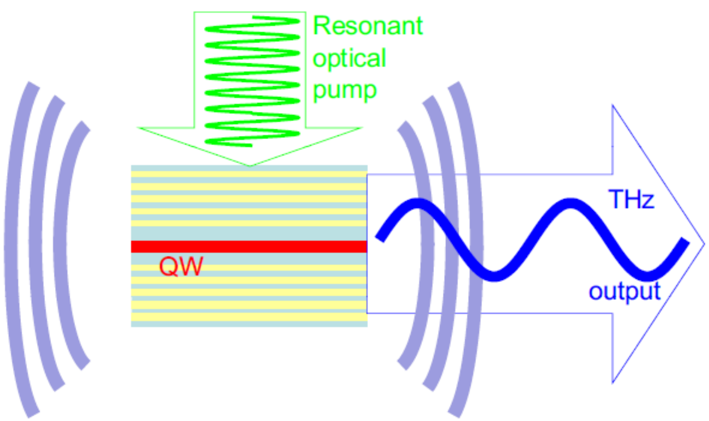

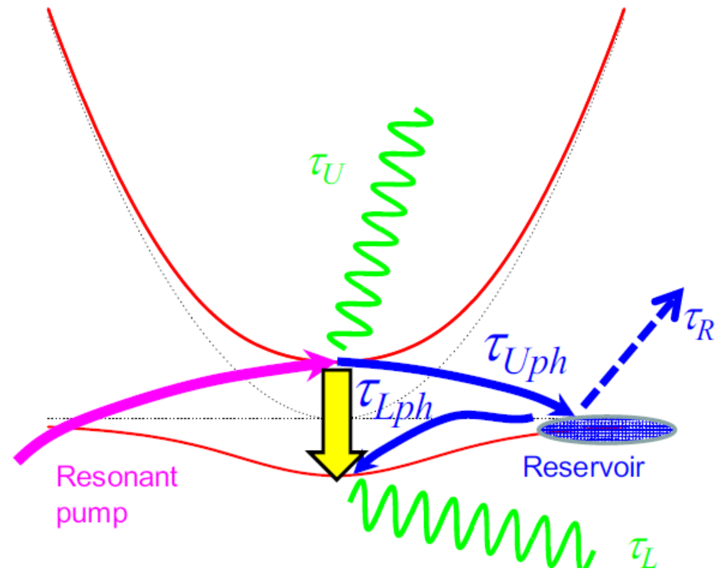

PHYSICAL REVIEW B **83**, 193303 (2011)

Terahertz lasing in a polariton system: Quantum theory

Elena del Valle* and Alexey Kavokin

PRL **107**, 027401 (2011) PHYSICAL REVIEW LETTERS week ending 8 JULY 2011

Nonlinear Terahertz Emission in Semiconductor Microcavities

Allotropes of Carbon

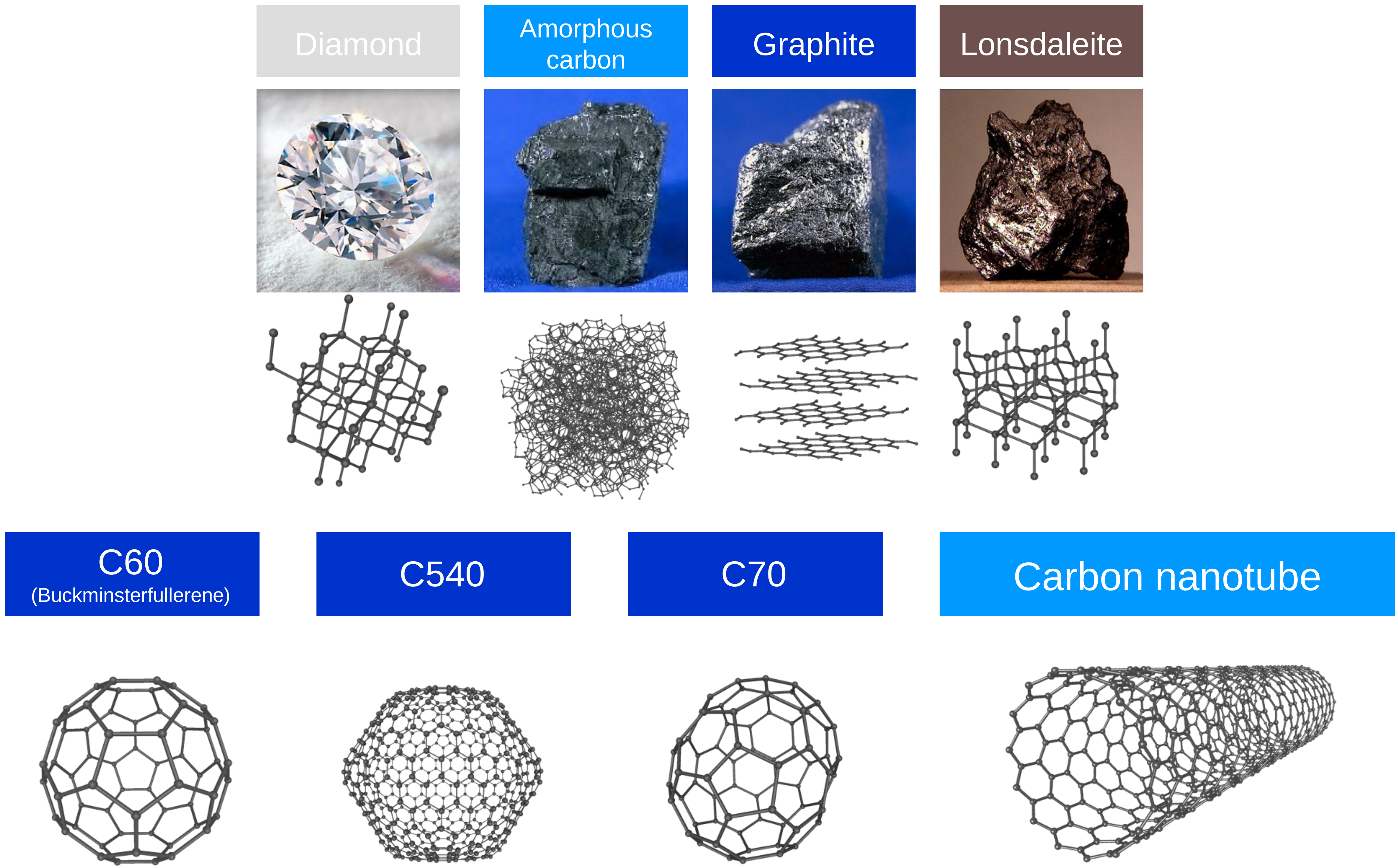

Graphene

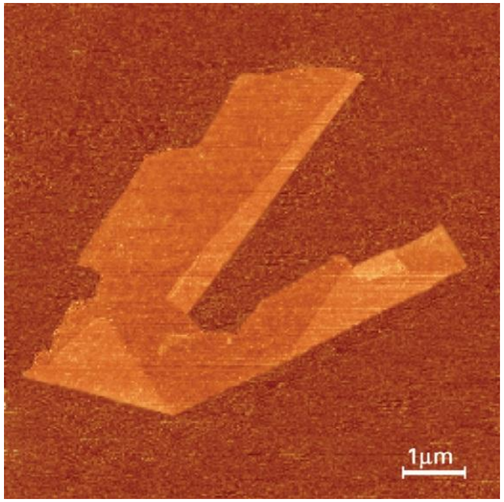

Atomic force microscopy image of a graphene flake.

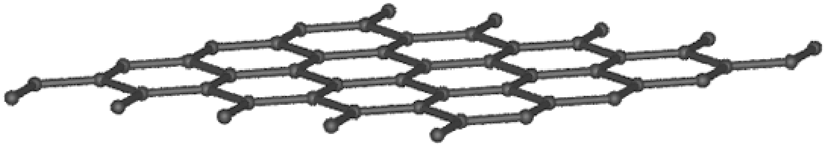

Graphite to Graphene

Graphite

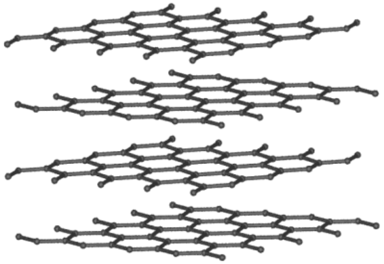

Graphene

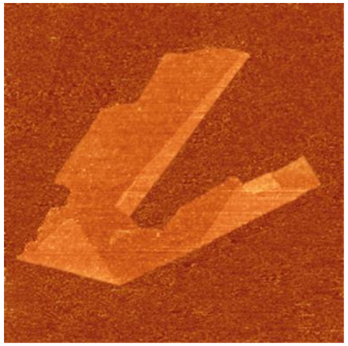

K.S. Novoselov et al., Science **306**, 666 (2004).

THE RISE OF GRAPHENE

K.S. Novoselov, A.K.Geim, S.V.Morozov, D. Jiang, Y.Zhang, S.V.Dubonos, I.V.Grigorieva, A.A.Firsov, 'Electric field effect in atomically thin carbon films', Science **306**, 666 (2004)

Citations (ISI): 2005 – 21; 06 – 92; 07 – 257; 08 – 643; 09 – 1071; 10 – 1657 11 – 2349 (total – 6645)

K.S. Novoselov, A.K.Geim, S.V.Morozov, D. Jiang, M.I.Katsnelson, S.V.Dubonos, I.V.Grigorieva, A.A.Firsov, 'Two-dimensional gas of massless Dirac fermions in graphene', Nature **438**, 197 (2005)

Citations: 05 – 1; 06 – 99; 07 – 329; 08 – 576; 09 – 762; 10 – 944; 11 – 1098

Review (already out of date): A.H.Castro Neto, F.Guinea, N.M.R.Peres, K.S.Novoselov, A.K.Geim, Rev.Mod.Phys. **81**, 109 (2009)

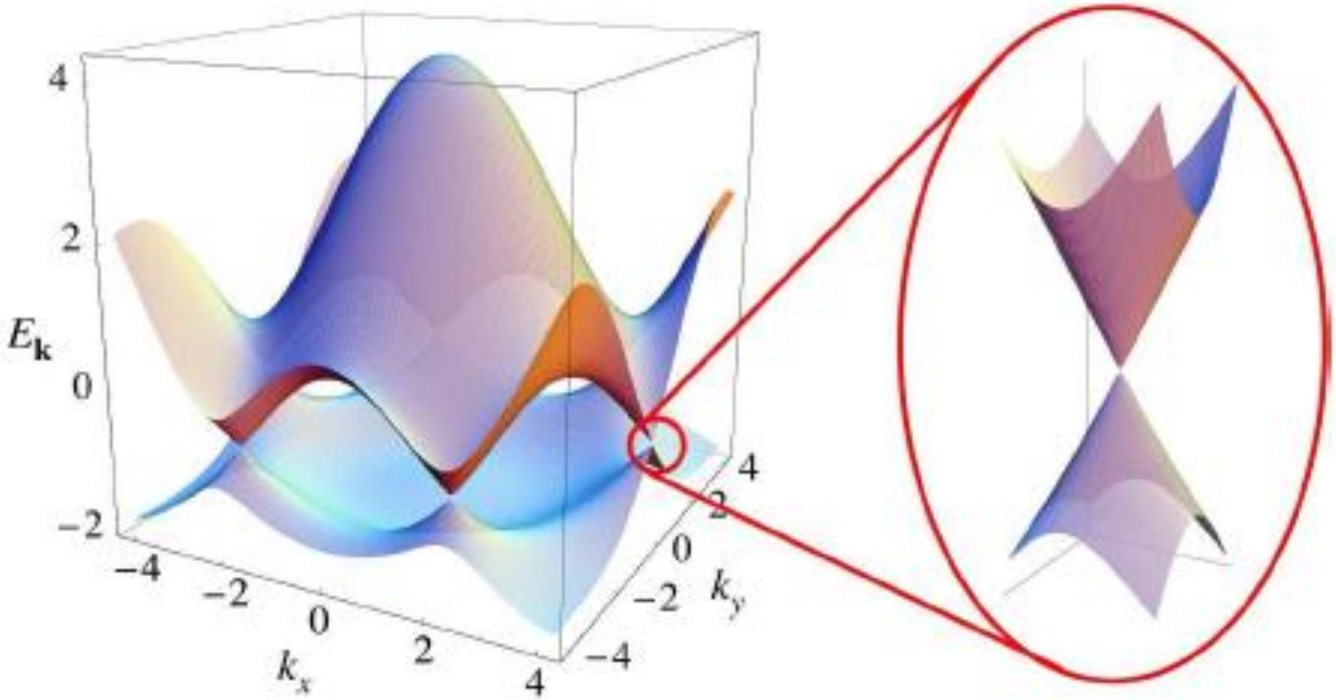

Graphene dispersion

P.R. Wallace, 'The band theory of graphite', Phys. Rev. 71, 622 (1947).

Unconventional QHE; huge mobility (suppression of backscattering); minimal conductivity despite of vanishing density of states… **Theory**: use of 2D relativistic QM, optical analogies, Klein paradox, valleytronics…

Graphene's

Crystal Structure

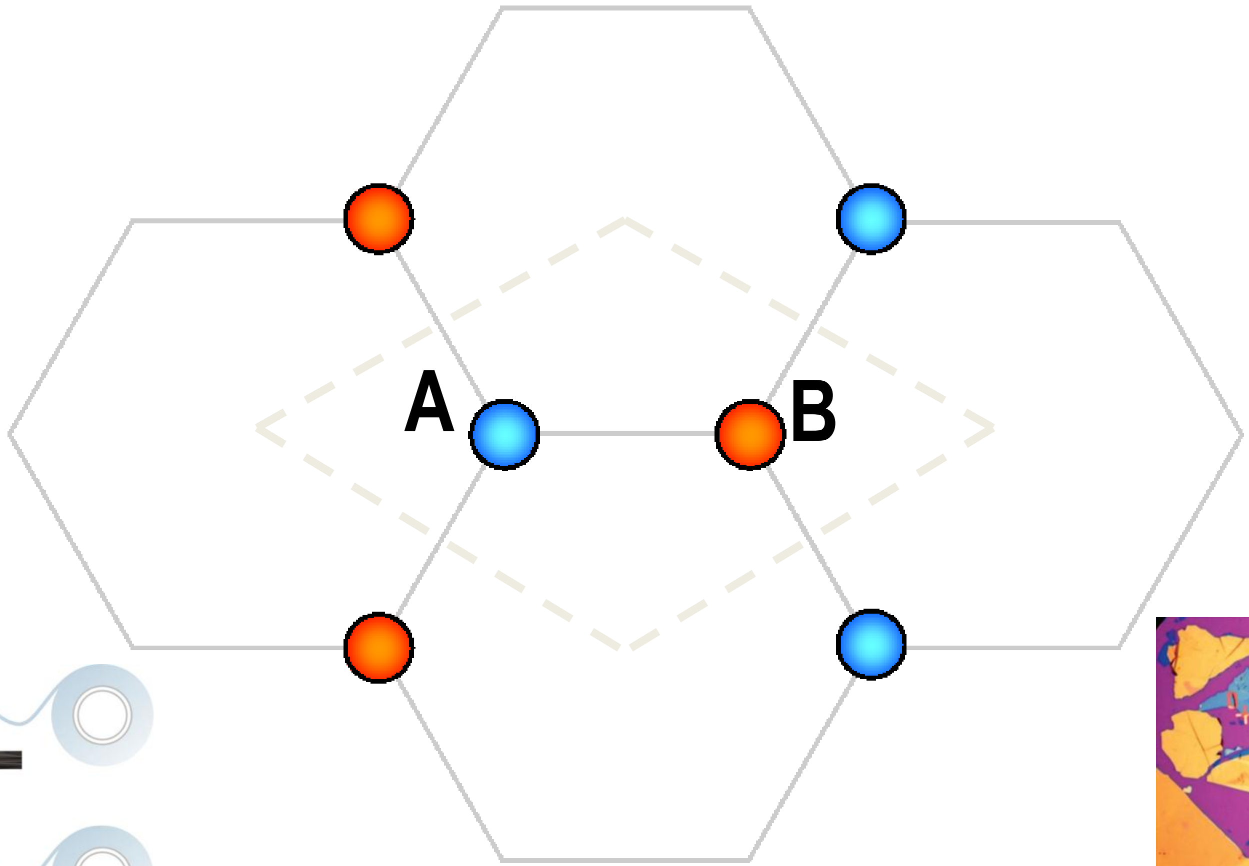

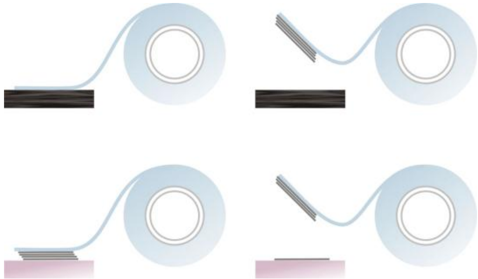

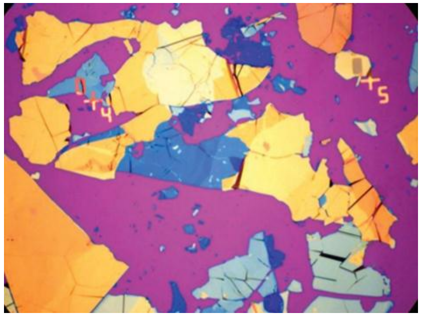

P. R. Wallace "The band theory of graphite", Phys. Rev. **71**, 622 (1947)

Dispersion Relat $E = \pm\gamma_0\sqrt{|f(\underline{k})|}$

$$f(\underline{k}) = e^{i\left(\frac{a}{\sqrt{3}}k_x\right)} + 2e^{i\left(-\frac{a}{2\sqrt{3}}k_x\right)}\cos\left(k_y\frac{a}{2}\right)$$

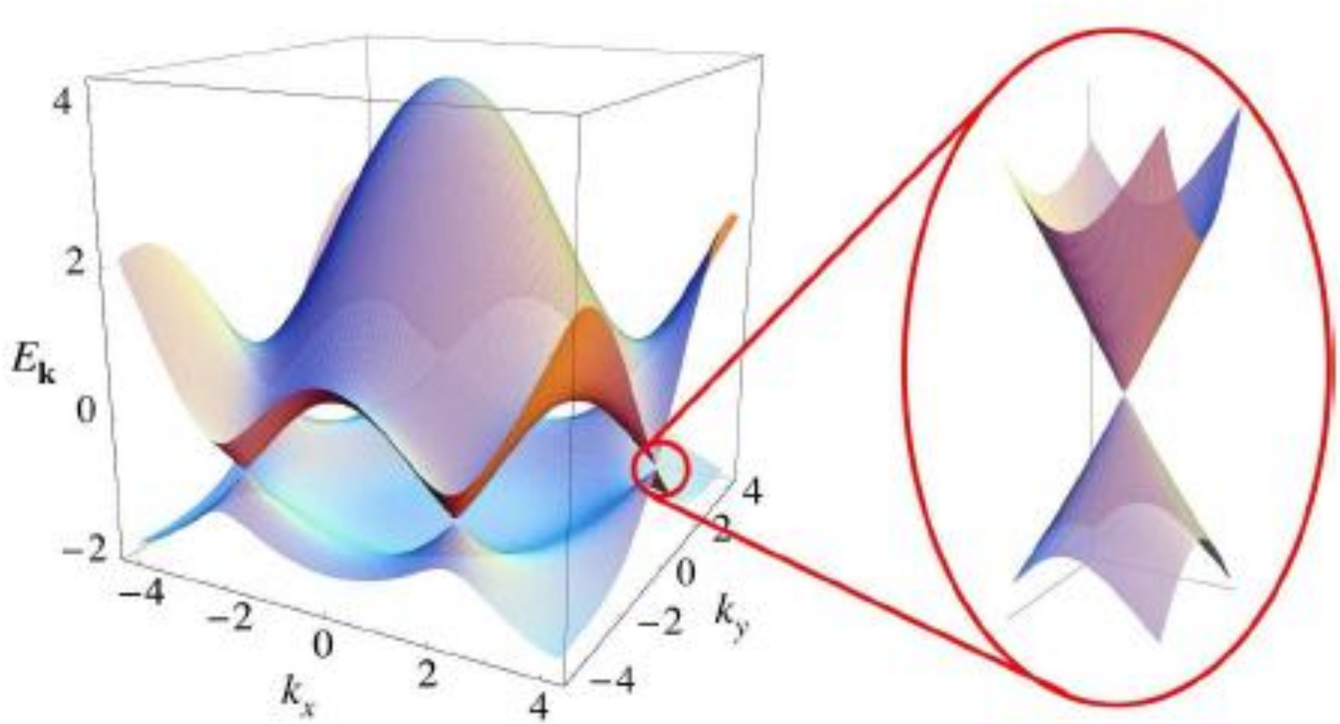

$$E = \hbar v_F k \qquad c/v_F \approx 300$$

“Dirac Points”

Expanding around the K points in terms of small q

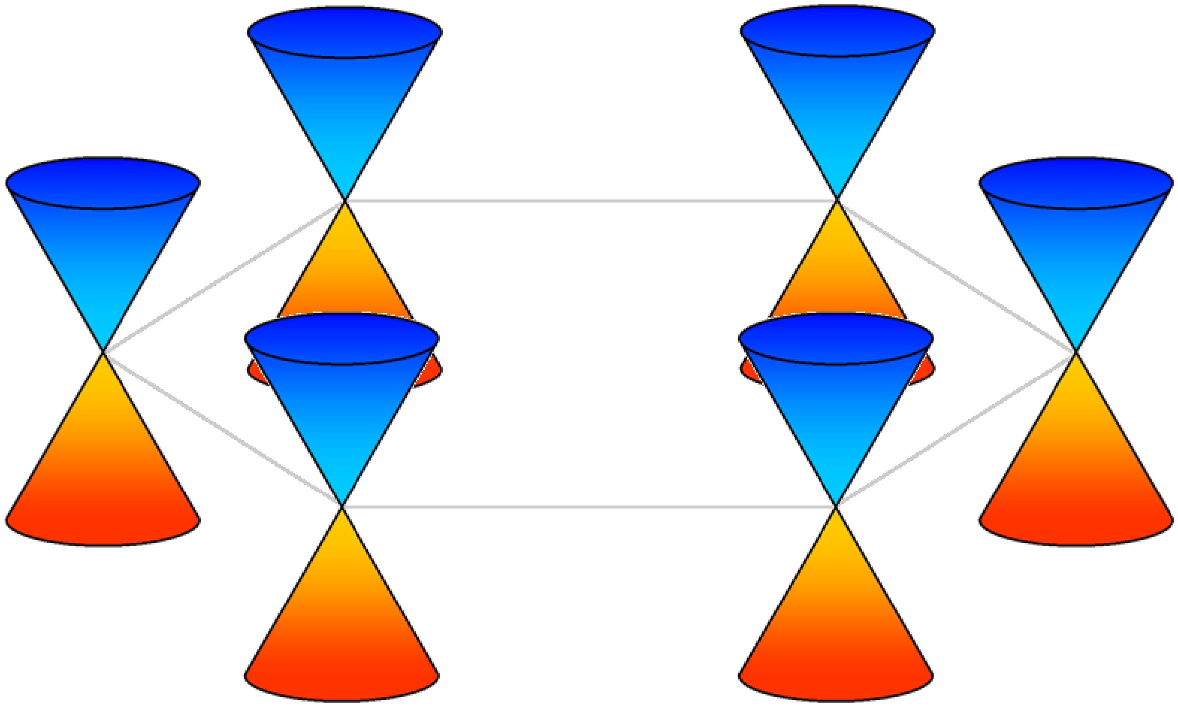

$$\widehat{H} = \hbar v_{\mathrm{F}} \begin{pmatrix} 0 & \widehat{q}_x - i\widehat{q}_y \\ \widehat{q}_x + i\widehat{q}_y & 0 \end{pmatrix}$$

Carbon nanotubes

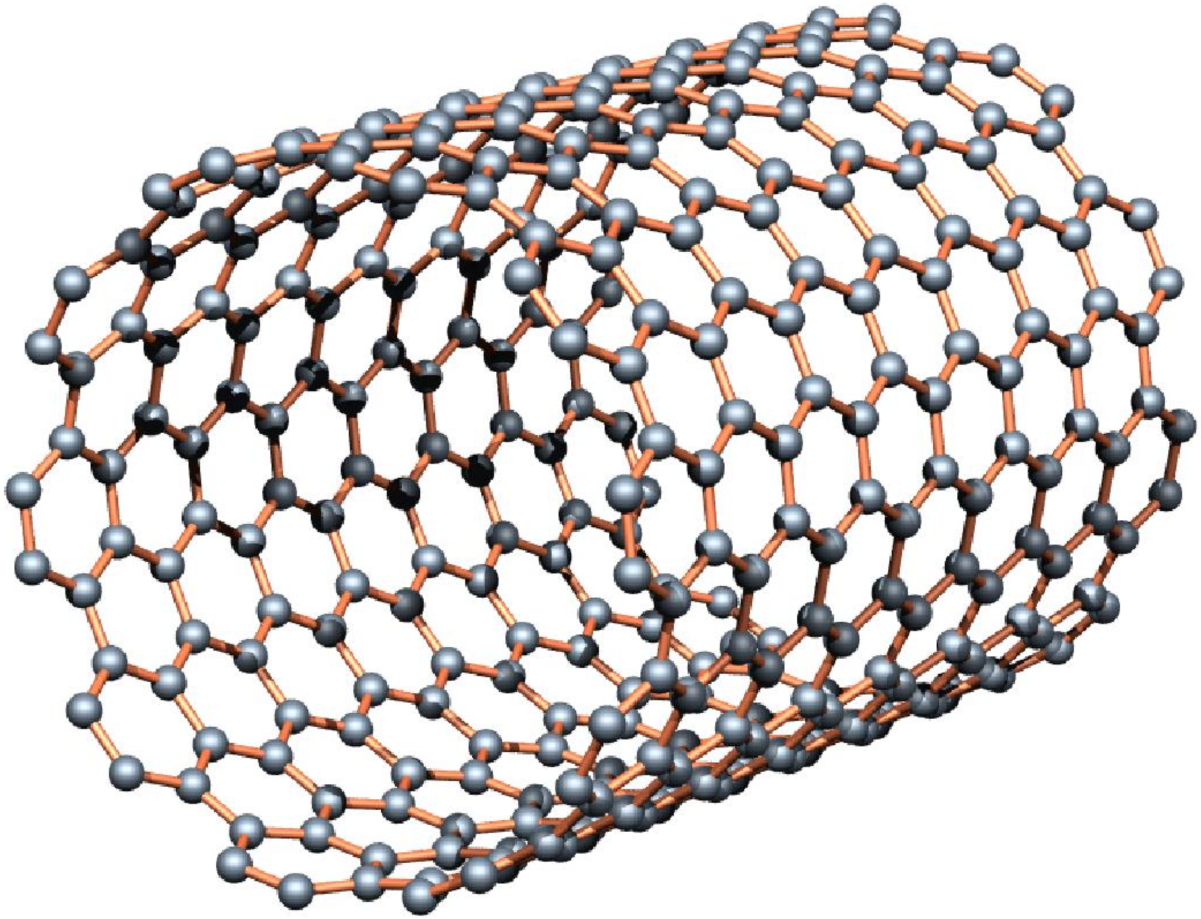

S. Iijima, “Helical Microtubules of Graphitic Carbon” Nature, Vol. 354, pp. 56-58, 1991. [ISI-13075 citations]

Carbon nanotubes: Classification

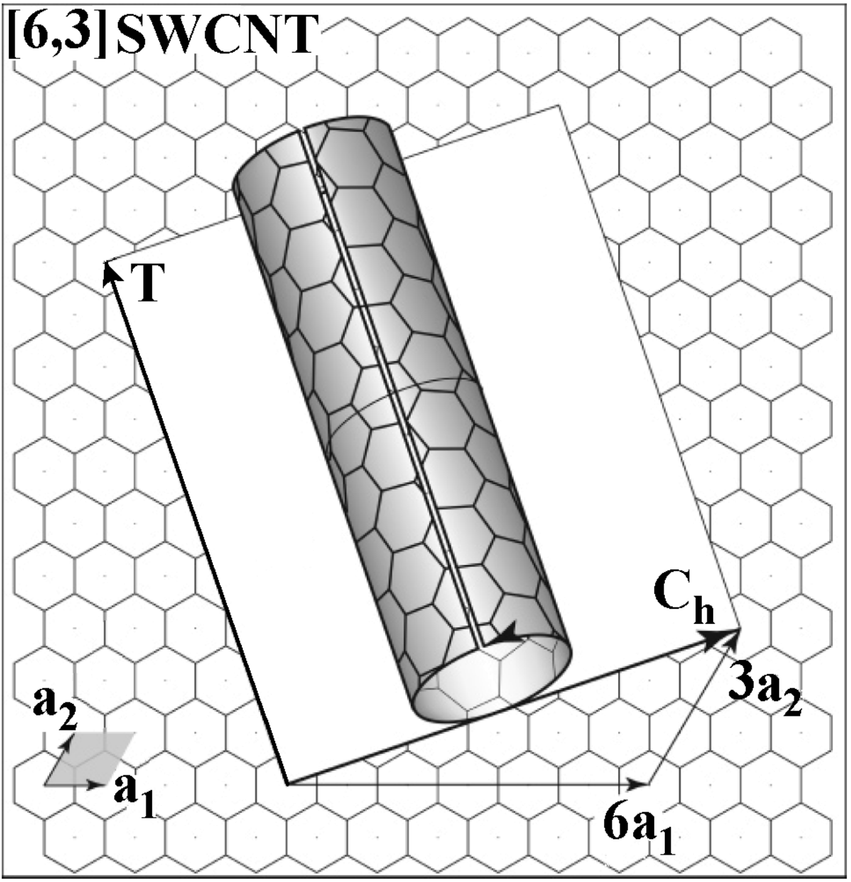

(n,m) :

$$\mathbf{C_h} = n\mathbf{a}_1 + m\mathbf{a}_2$$

$$|\mathbf{T}| = \sqrt{3}\,|\mathbf{C_h}|\,/d_R$$

$$d_R = \gcd\left[2n+m, 2m+n\right]$$

Achiral Nanotubes:

Zig-zag $(n,0)$

Armchair (n,n)

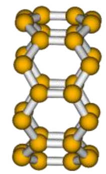

(8,0)

$$T_{[n,0]} = \sqrt{3}a$$

$$T_{[n,n]} = a$$

$$a = 2.49\mathring{A}$$

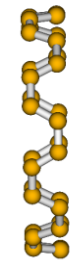

(8,8)

Chiral Nanotubes:

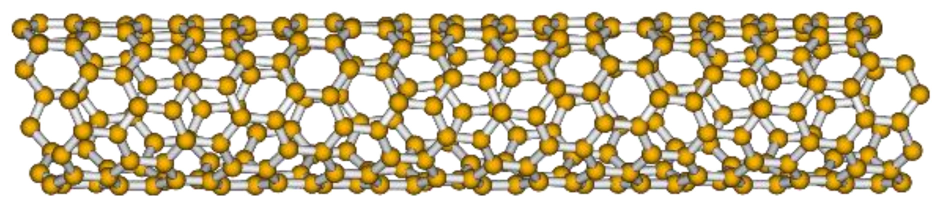

(8,1)

$$T_{[8,1]} = 14.8a = 36.8\mathring{A}$$

Ideal and real CNTs

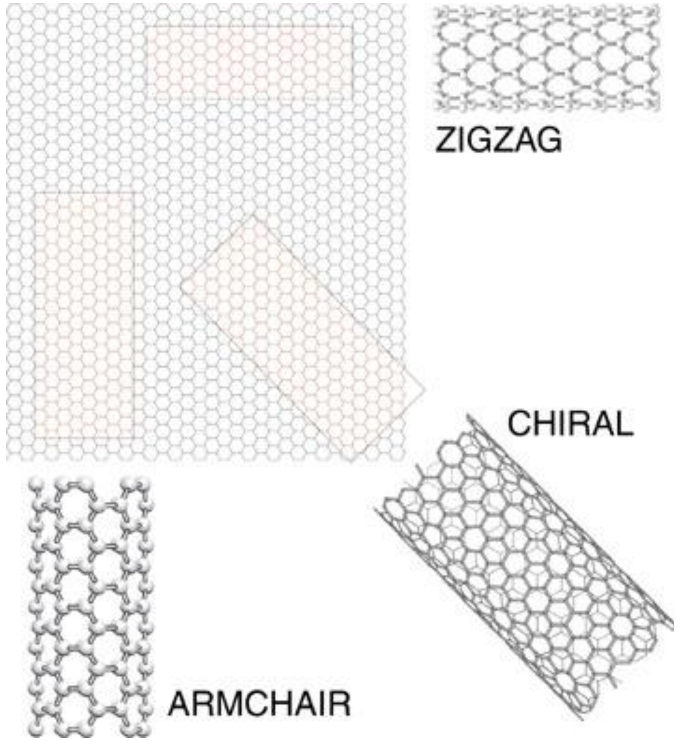

[from www.seas.upenn.edu]

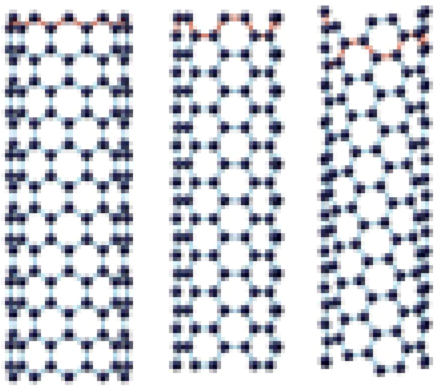

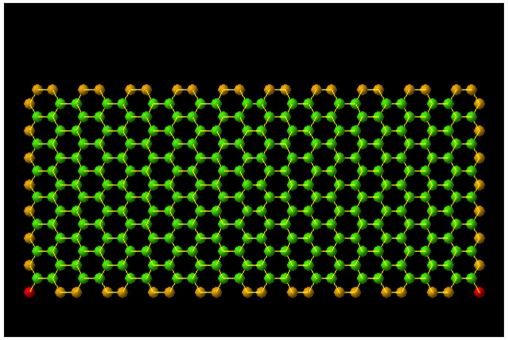

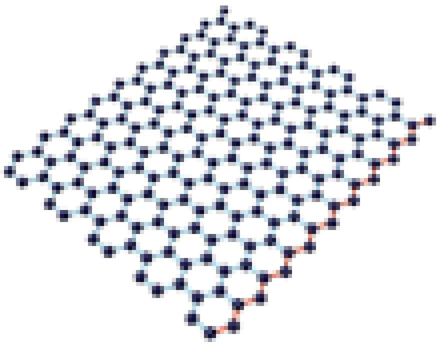

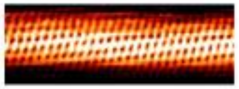

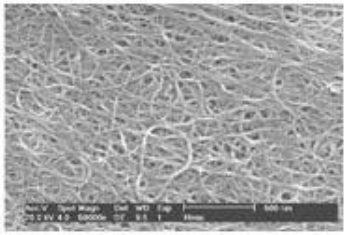

CNTs produced by laser ablation of a graphite target containing metal catalyst additives

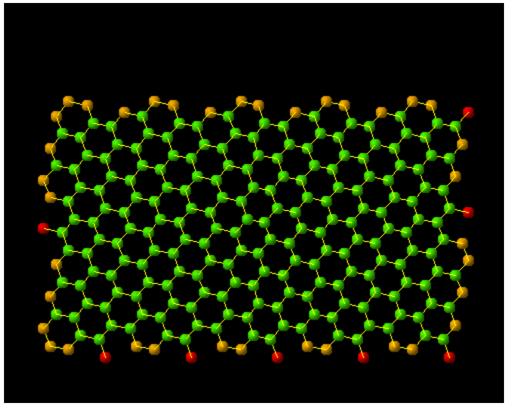

[from www.surf.nuqe.nagoya-u.ac.jp and www.photon.t.u-tokyo.ac.jp]

Carbon nanotubes:

Applications

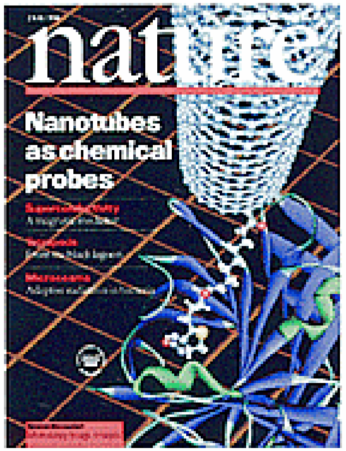

Chemical/Biological

Electronic

Mechanical

THz?

Previous proposals

Nanoklystron utilizing efficient high-field electron emission from nanotubes:

D. Dragoman and M. Dragoman, Progr. Quant. Electron. 28, 1 (2004);

H.M. Manohara *et.al*., J. Vac. Sci. Technol. B 23, 157 (2005);

Aldo Di Carlo *et.al*., Proc. SPIE 632808 (2006).

Devices based on negative differential conductivity in large-diameter semiconducting CNTs:

A.S. Maksimenko and G.Ya. Slepyan, Phys. Rev. Lett. 84, 362 (2000);

G. Pennington and N. Goldsman, Phys. Rev. B 68, 045426 (2003).

High-frequency resonant-tunneling and Schottky diodes:

A.A. Odintsov, Phys. Rev. Lett. 85, 150 (2000);

F. Leonard and J. Tersoff, Phys. Rev. Lett. 85, 4767 (2000);

D. Dragoman and M. Dragoman, Physica E 24, 282 (2004).

THz frequency multipliers, amplifiers and antennas:

G.Ya. Slepyan *et. al.* , Phys. Rev. A 60, 777 (1999); *ibid.* 63, 53808 (2000);

D. Dragoman and M. Dragoman, Physica E 25, 492 (2005);

G.Ya. Slepyan *et.al*., Phys. Rev. B 73, 195416 (2006); Proc. SPIE 632806 (2006).

OUTLINE

- Introduction
- Generation of THz radiation by hot electrons in quasi-metallic CNTs
- Chiral CNTs as frequency multipliers
- Armchair CNTs in a magnetic field as tunable THz sources and detectors
- Quasi-metallic CNTs as THz amplifiers
- Polarization-sensitive THz detectors based on graphene p-n junctions

Generation of THz radiation by hot carriers in quasi-metallic CNTs

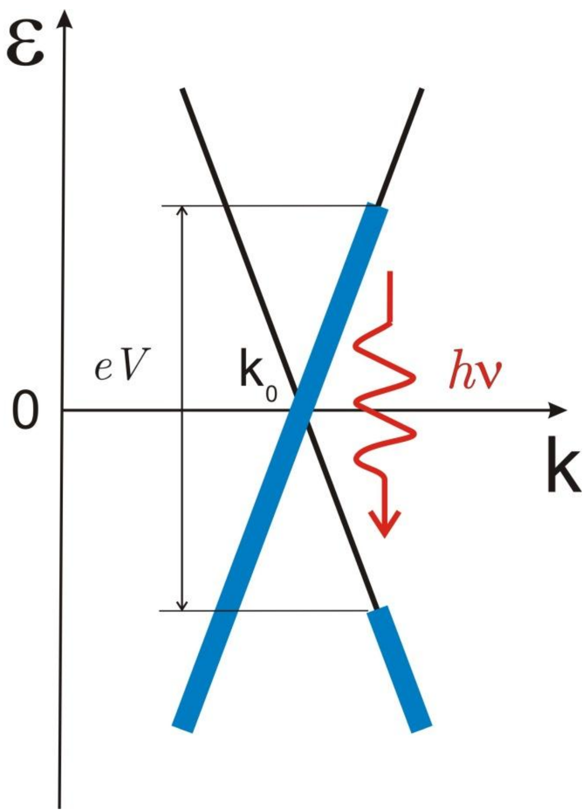

$$\varepsilon(k) = \pm v_F |k - k_0|$$

$$L < l_{ac}$$ (acoustic scattering mean free path, approximately 2 μm)

$$eV < \hbar\Omega$$

(energy of zone-boundary / optical phonons of around 160 / 200 meV)

The scheme of THz photon generation by hot carriers in quasi-metallic CNTs in the ballistic regime.

$$f_e(k) = \begin{cases} 1, & 0 < k - k_0 < \Delta\varepsilon/2\hbar v_F \\ 0, & k - k_0 > \Delta\varepsilon/2\hbar v_F \end{cases}$$

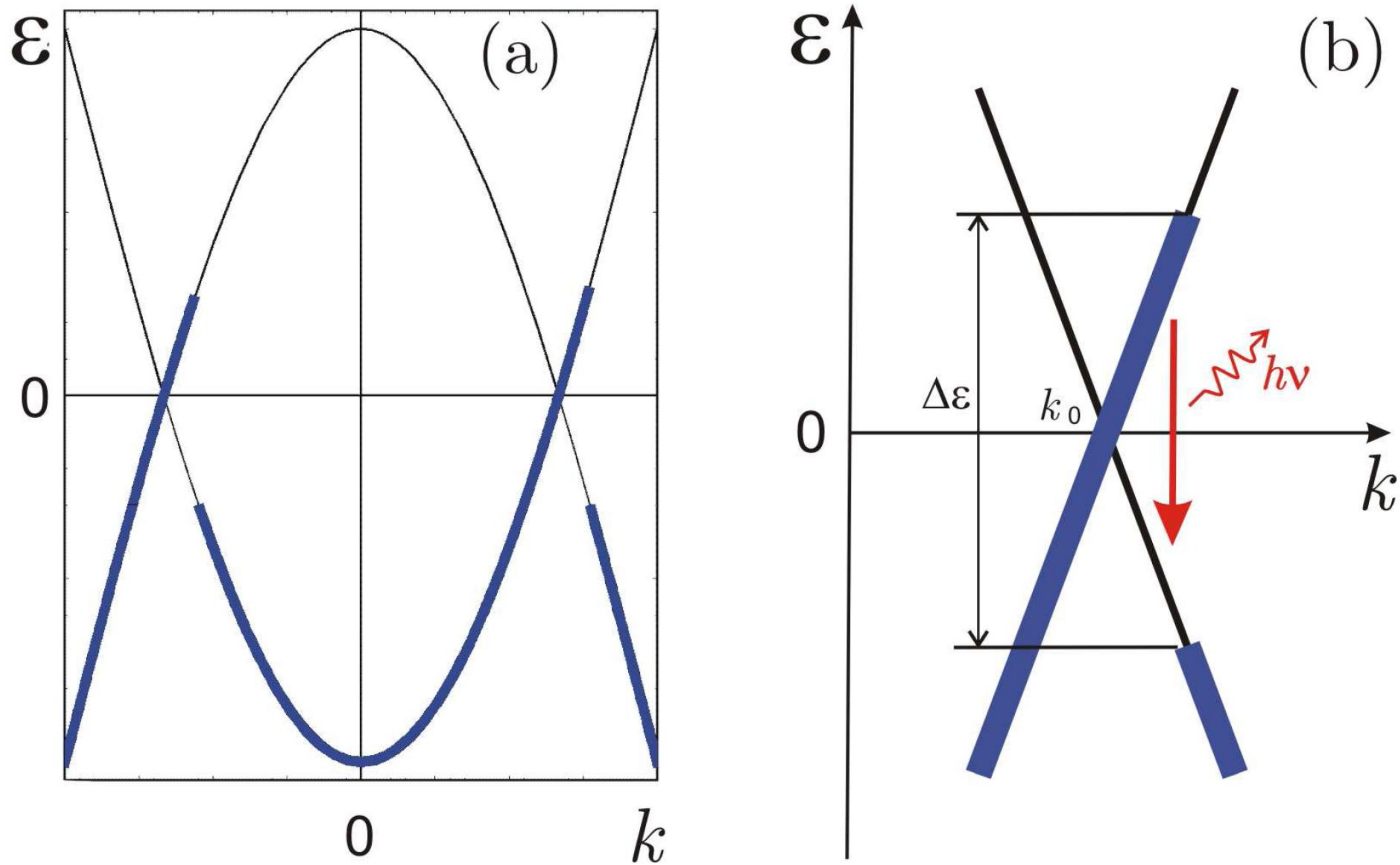

ε
(a)
0
0
k
ε
(b)
Δε
k_0
0
hν
k

Ballistic transport and phonon scattering: Key publications

T. Ando, t. Nakanishi, and R. Saito, J. Phys. Soc. Jpn. 67, 1704 (1997)

Z. Yao, C.L. Kane, and C. Dekker, Phys. Rev. Lett. 84, 2941 (2000)

A. Javey *et. al.*, Phys. Rev. Lett. 92, 106804 (2005)

J.-Y. Park *et. al.*, Nano Lett. 4, 517 (2004)

M. Freitag *et. al.*, Nano Lett 4, 1063 (2004)

V.Perebeinos, J.Tersoff, and P. Avouris, Phys.Rev.Lett. 94, 86802 (2004)

M.P.Anantram and F.Léonard, Rep. Prog. Phys. 69, 507 (2006)

Ballistic transport and phonon scattering

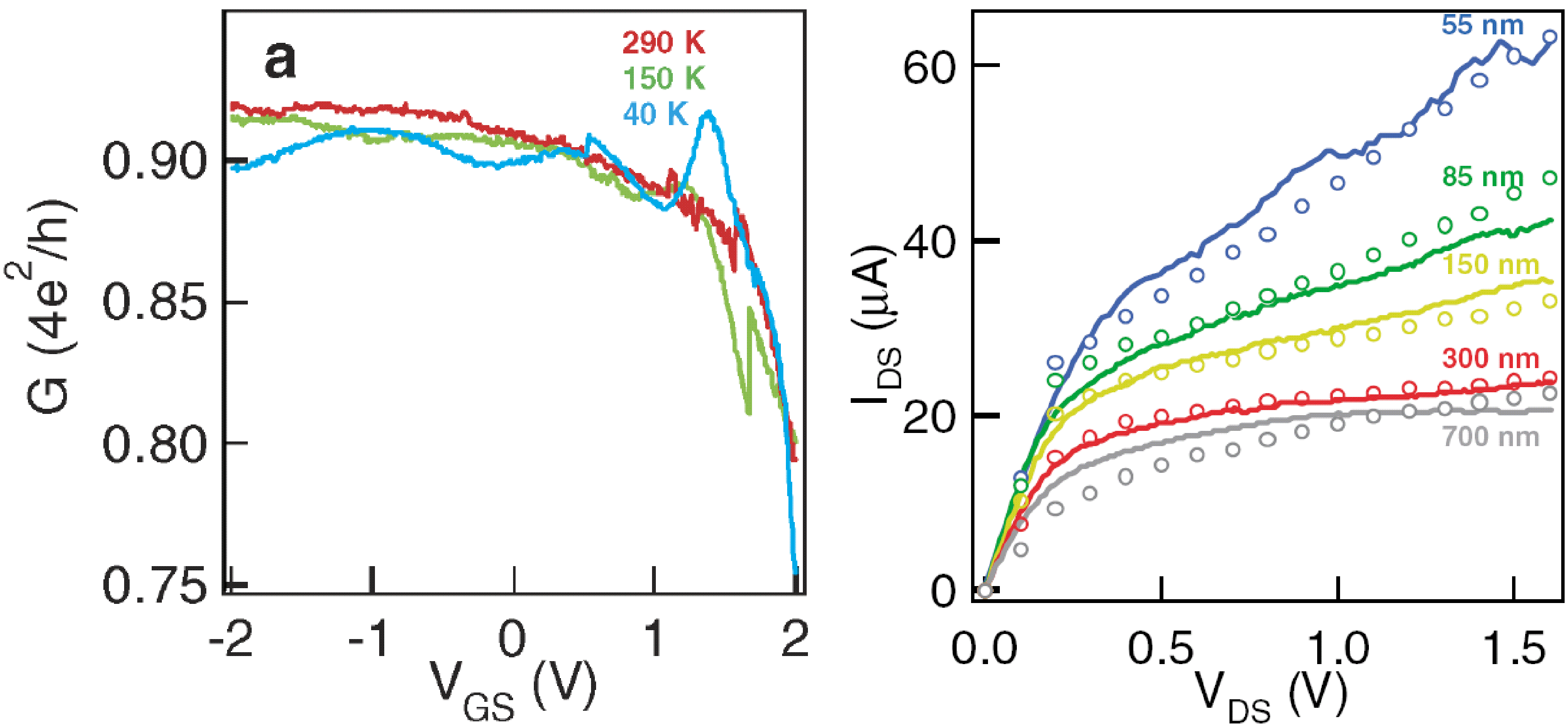

From A. Javey *et. al*., Phys. Rev. Lett. 92, 106804 (2004)

Optical transitions in CNTs (recent papers only)

I. Milošević *al*., Phys. Rev. B 67, 165418 (2003)

J. Jiang *et. al*., Carbon 42, 3169 (2004)

A. Grüneis *et. al*., Phys. Rev. B 67, 165402 (2003)

V.N. Popov and L. Henrard, Phys. Rev. B 70, 115407 (2004)

R. Saito *et. al*., Appl. Phys. A 78, 1099 (2004)

S.V. Goupalov, Phys. Rev. B 72, 195403 (2005)

Y. Oyama, Carbon 44, 873 (2006)

Optical transitions between the lowest conduction subband and the top valence subband of a true metallic (armchair) CNT are forbidden!

Quasi-metallic nanotubes

are (n,m) SWNTs with n-m=$3p$, where p is a non-zero integer.

Their bandgap is given by $$\varepsilon_g = \frac{\hbar v_F a_{\text{C-C}} \cos 3\theta}{8R^2},$$

where $a_{\text{C-C}} = 1.42$ Å is the nearest-neighbor distance between two carbon aroms, R is the CNT radius, and $\theta = \arctan[\sqrt{3}m/(2n+m)]$ is a chiral angle.

[See, e.g., C.L. Kane and E.J. Mele, Phys. Rev. Lett. 78, 1932 (1997)]

Zener tunneling

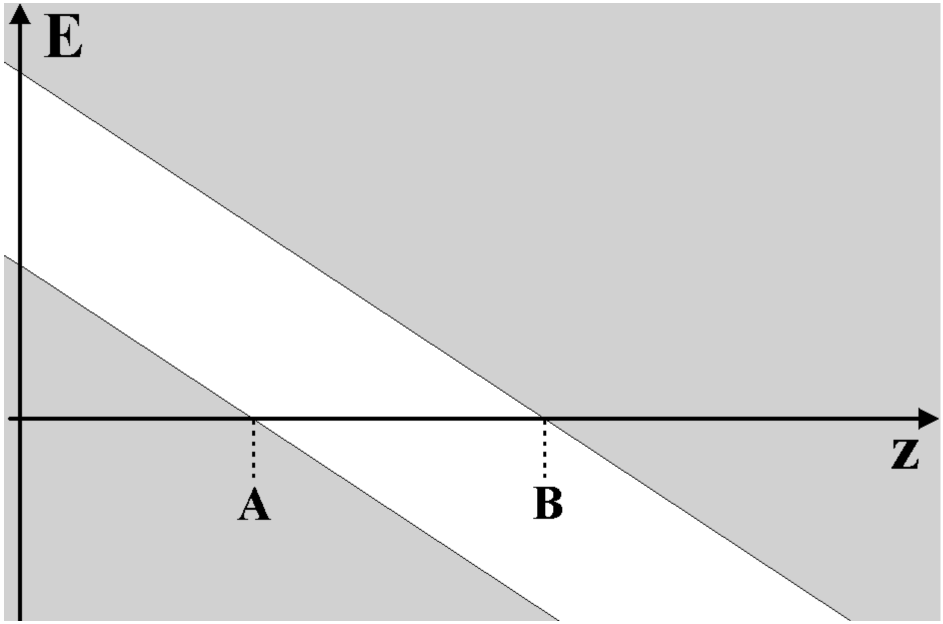

For the energy spectrum near the gap given by

$$\varepsilon = \pm\sqrt{\varepsilon_g^2 / 4 + \hbar^2 v_F^2 k^2}$$

the tunneling exponent is

$$\exp\left(-\frac{\pi}{4}\frac{\varepsilon_g^2}{eE\hbar v_F}\right)$$

For example, for a zig-zag (30,0) CNT the gap is about 6meV and the Zener breakdown occurs for the electric field of about 0.1 V/μm.

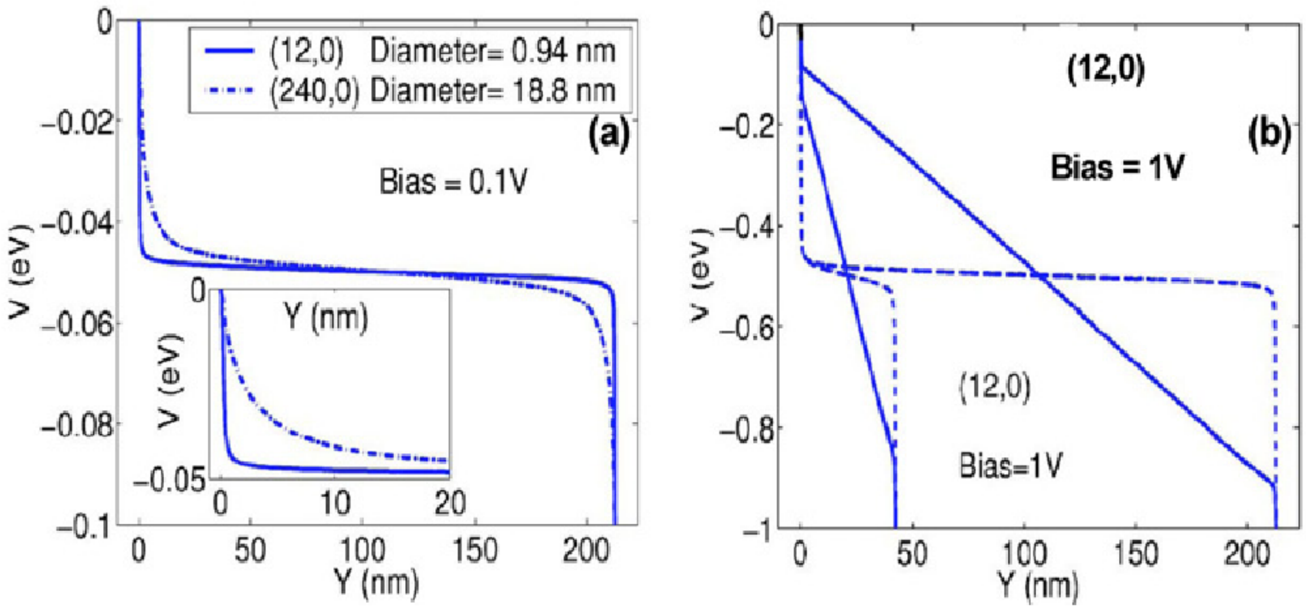

Figure 17. Electrostatic potential versus length along nanotube axis. (*a*) Low bias potential versus position for (12,0) and (240,0) nanotubes, which have diameters of 0.94 nm and 18.8 nm, respectively. The applied bias is 100 mV. The screening for the large-diameter nanotube is significantly poorer. The inset magnifies the potential close to the nanotube–contact interface, showing that in contrast to the nanotube bulk the electric field is smaller at the edges when the diameter is larger (density of states is smaller). The nanotube length is 213 nm. (*b*) The potential as a function of position is shown for (12,0) nanotubes of lengths 42.6 and 213 nm in the presence of scattering (——). The potential profile in the ballistic limit (- - - -) is shown for comparison.

From M.P.Anantram and F.Léonard, Rep. Prog. Phys. 69, 507 (2006)

Dipole optical transitions in CNTs

I. Milošević *al*., Phys. Rev. B 67, 165418 (2003)

A. Grüneis *et. al*., Phys. Rev. B 67, 165402 (2003)

J. Jiang *et. al*., Carbon 42, 3169 (2004)

V.N. Popov and L. Henrard, Phys. Rev. B, 70, 115407 (2004)

R. Saito *et. al*., Appl. Phys. A 78, 1099 (2004)

S.V. Goupalov, Phys. Rev. B 72, 195403 (2005)

Y. Oyama, Carbon 44, 873 (2006)

Nearest-neighbor orthogonal π-electron tight-binding model

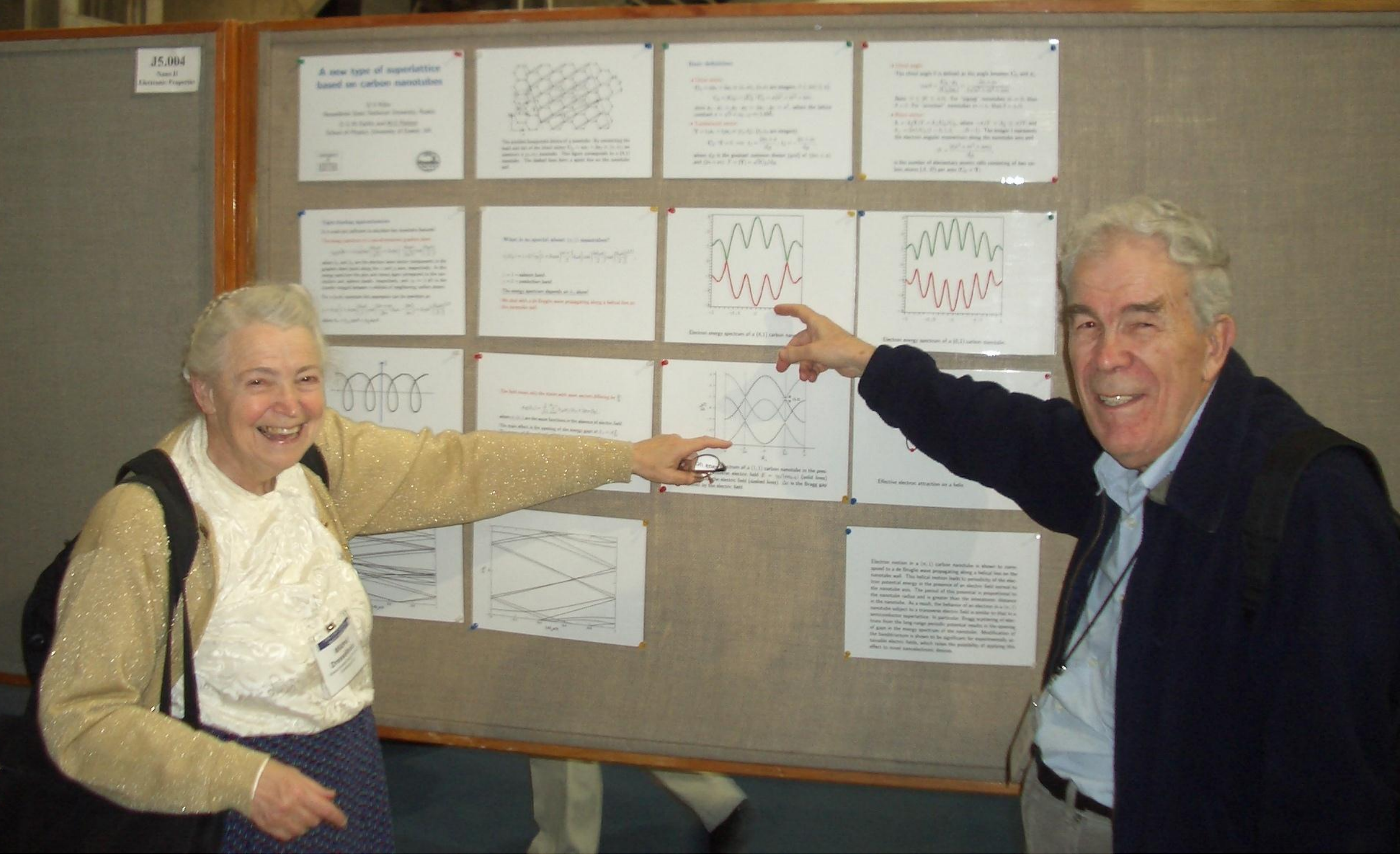

M.S. Dresselhaus & G. Dresselhaus, Fort Collins, Arizona, August 2004

Dipole optical transitions polarized along the CNT axis

The spectral density of spontaneous emission:

$$I_\nu = \frac{8\pi e^2 \nu}{3c^3} \sum_{i,f} f_e(k_i) f_h(k_f) \left| \langle \Psi_f | \hat{v}_z | \Psi_i \rangle \right|^2 \delta(\varepsilon_i - \varepsilon_f - h\nu).$$

Using $v_z = i/\hbar[H,r]$ and the properties of the tight-binding Hamiltonian we get for the transitions between the lowest conduction and the highest valence subband of a (3p,0) zigzag CNT:

$$\langle \Psi_f | \hat{v}_z | \Psi_i \rangle = \frac{a_{\text{C-C}} \omega_{if}}{8} \delta_{k_f, k_i},$$ **where** $\hbar\omega_{if} = \varepsilon_i - \varepsilon_f$. **Finally,**

$$I_\nu = L f_e(\pi\nu/v_F) f_h(\pi\nu/v_F) \frac{\pi^2 e^2 a_{\text{C-C}}^2 \nu^3}{6c^3 \hbar v_F}.$$

A similar expression (corrected by a numerical factor depending on a chiral angle θ) is valid for any quasi-metallic CNT.

$$\varepsilon(k) = \pm v_F |k - k_0|$$

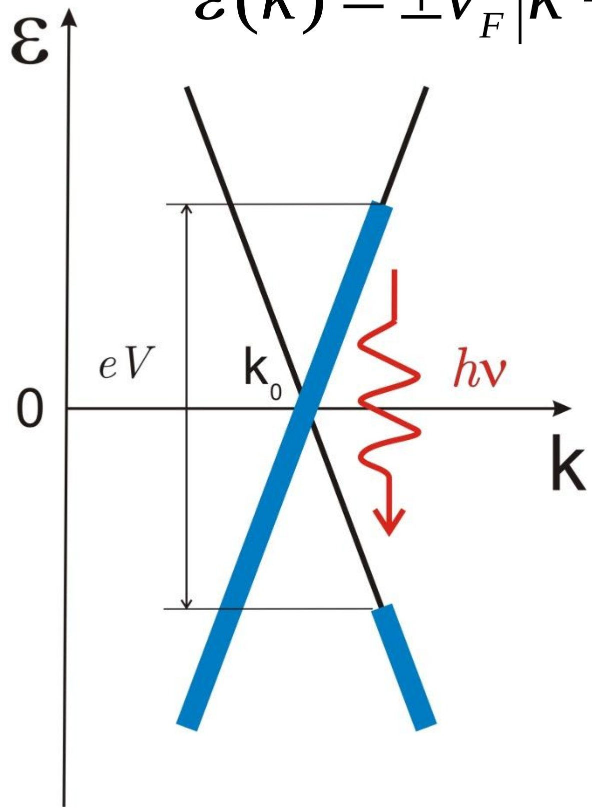

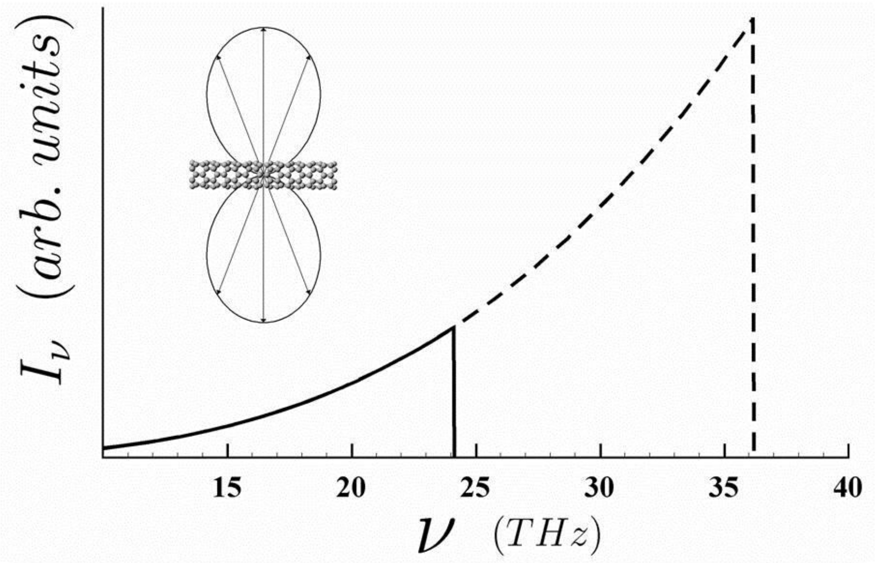

The scheme of THz photon generation by hot carriers in quasi-metallic CNTs in the ballistic regime.

[O.V.Kibis, M.Rosenau da Costa, M.E.Portnoi, Nano Lett. 7, 3414 (2007)]

The spectral density of spontaneous emission as a function of frequency for two values of applied voltage: solid line for *V*=0.1V; dashed line for *V*=0.15V. The inset shows the directional radiation pattern of the THz emission with respect to the nanotube axis.

Chiral CNTs as frequency multipliers

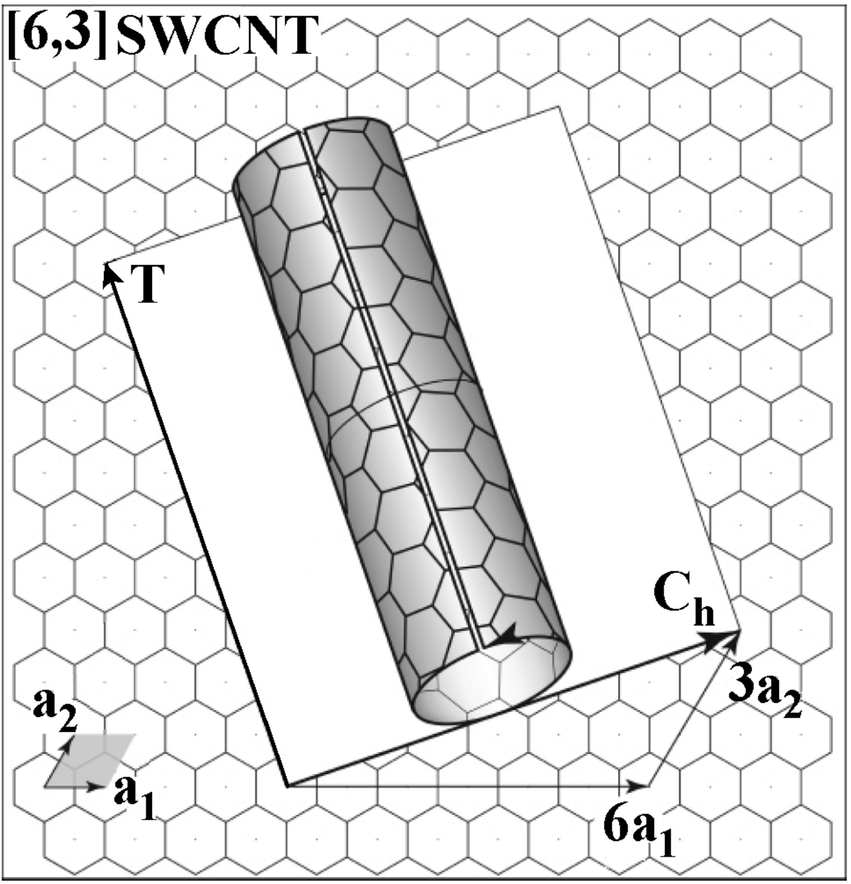

Achiral nanotubes:

Zig-zag $(n,0)$

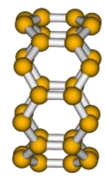

(8,0)

$$T_{[n,0]} = \sqrt{3}a$$

$$T_{[n,n]} = a$$

$$a = 2.49\AA$$

Armchair (n,n)

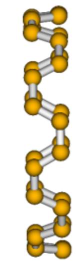

(8,8)

Chiral nanotubes:

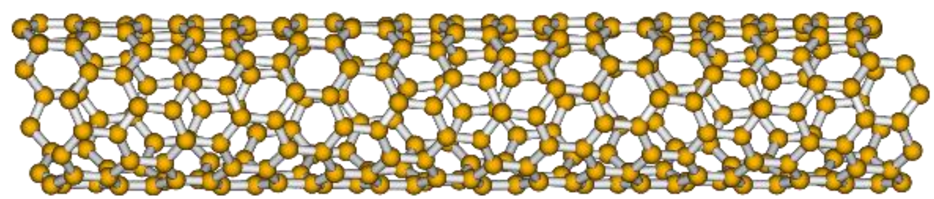

(8,1)

$$T_{[8,1]} = 14.8a = 36.8\AA$$

(n,m) :

$$\mathbf{C_h} = n\mathbf{a}_1 + m\mathbf{a}_2$$

$$|\mathbf{T}| = \sqrt{3}\,|\mathbf{C_h}|\,/d_R$$

$$d_R = \gcd\left[2n+m, 2m+n\right]$$

Helical symmetries in chiral CNTs

C.T. White, D.H. Hoberstons and J.W. Mintmire, PRB 47, 5485 (1993).

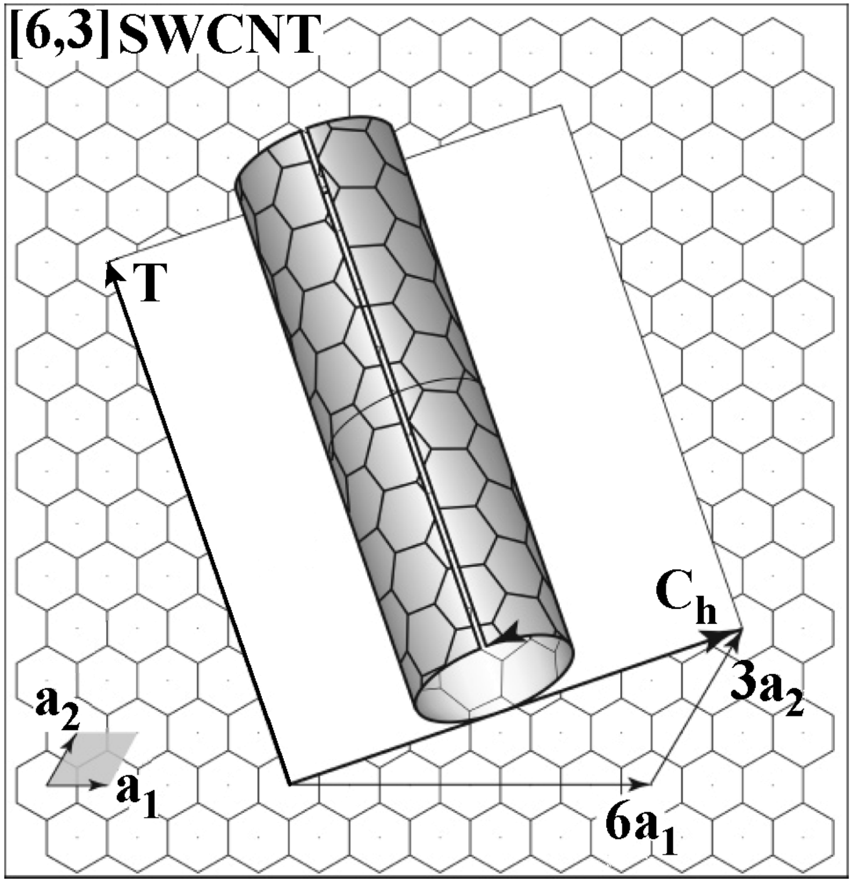

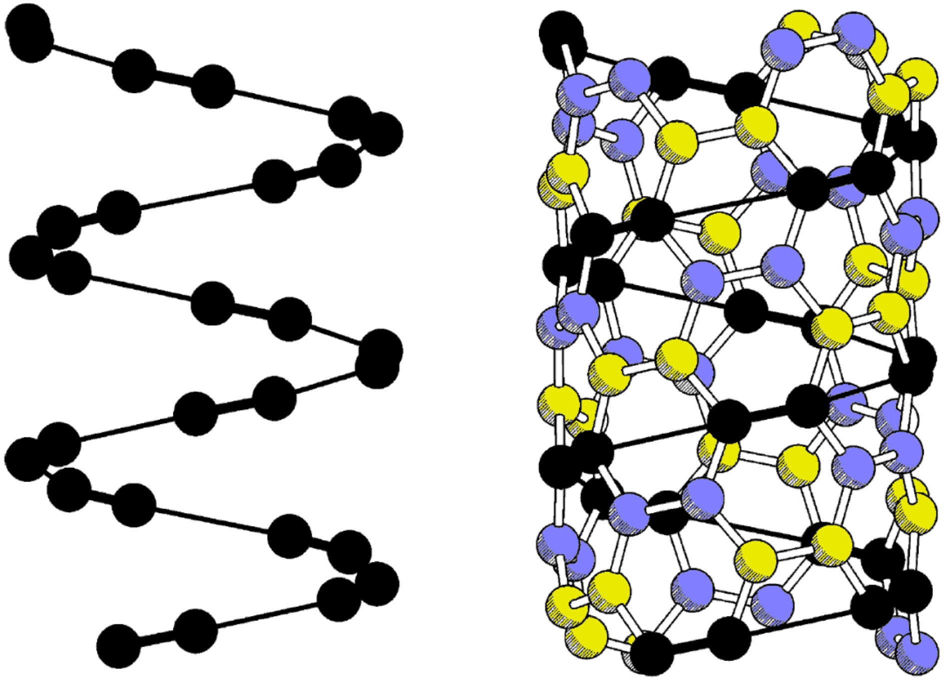

The number of helices is:

$$N_{Helix} = \gcd[n, m]$$

Superlattice properties of chiral CNTs in a transverse Electric Field

O.V. Kibis, D.G.W. Parfitt and M.E. Portnoi, PRB 71, 35411 (2005).

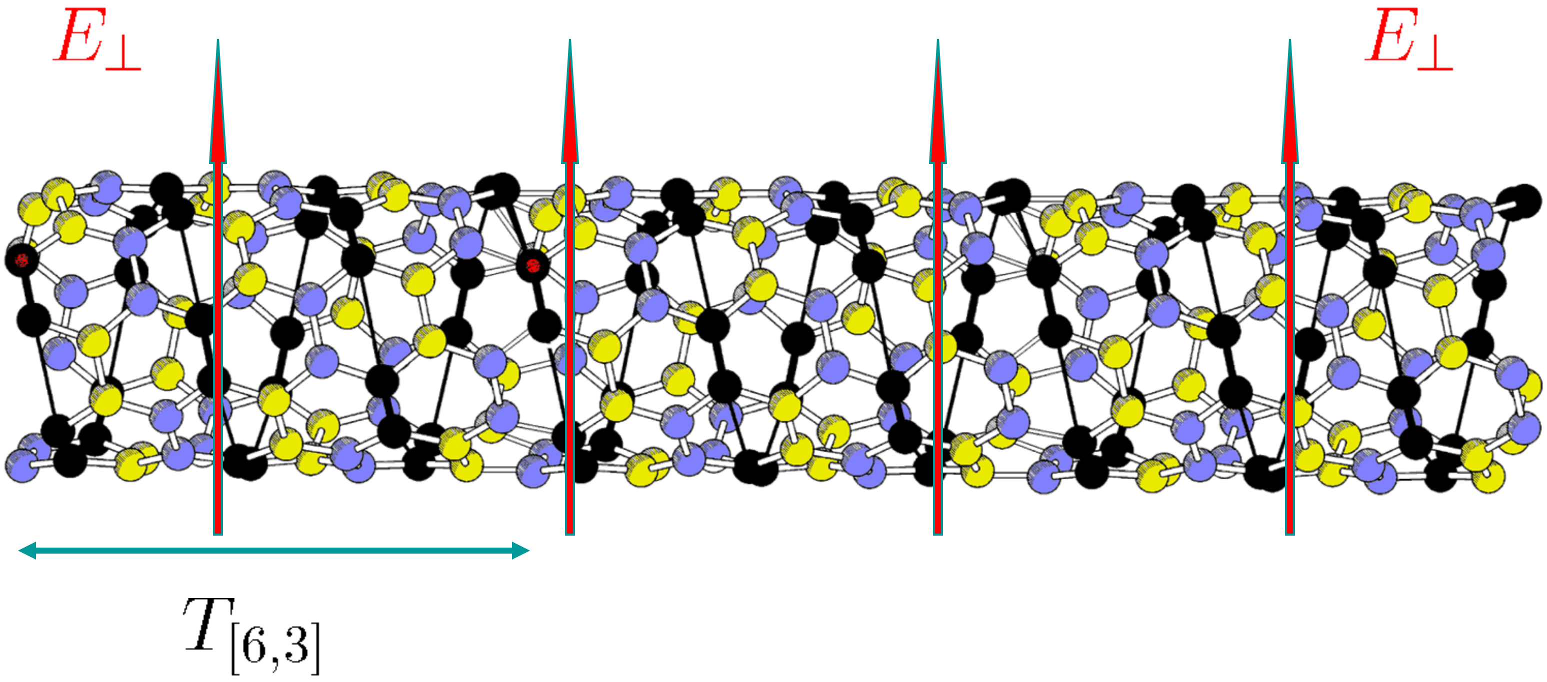

The helical symmetry provides an idea of the origin of the superlattice properties.

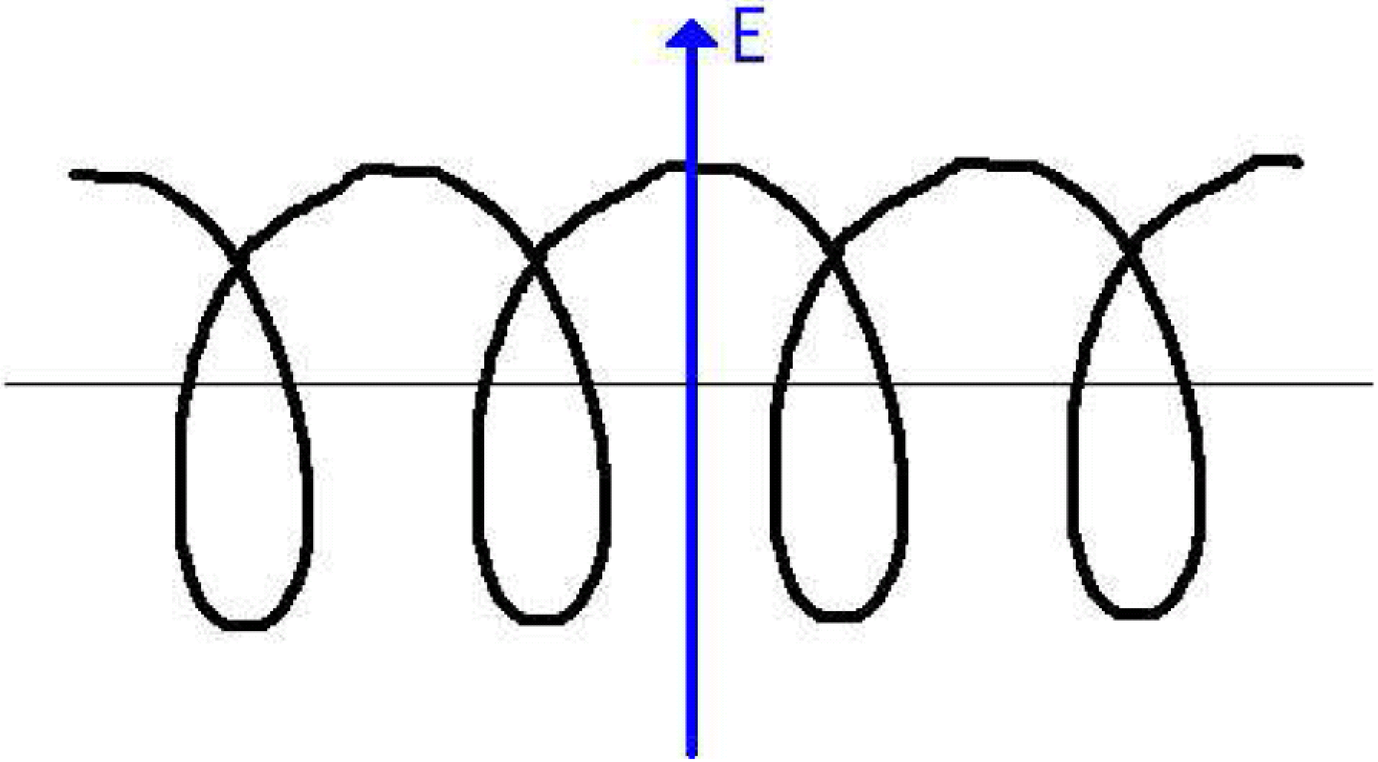

Helix in a transverse electric field

The potential energy of an electron on a helix subject to a transverse electric field takes the form $U = eER\cos(2\pi s/l_0)$, where e is the electron charge, E is the electric field strength, R is the radius of the helix, l_0 is the length of the single coil and s is the electron coordinate along the spiral line.

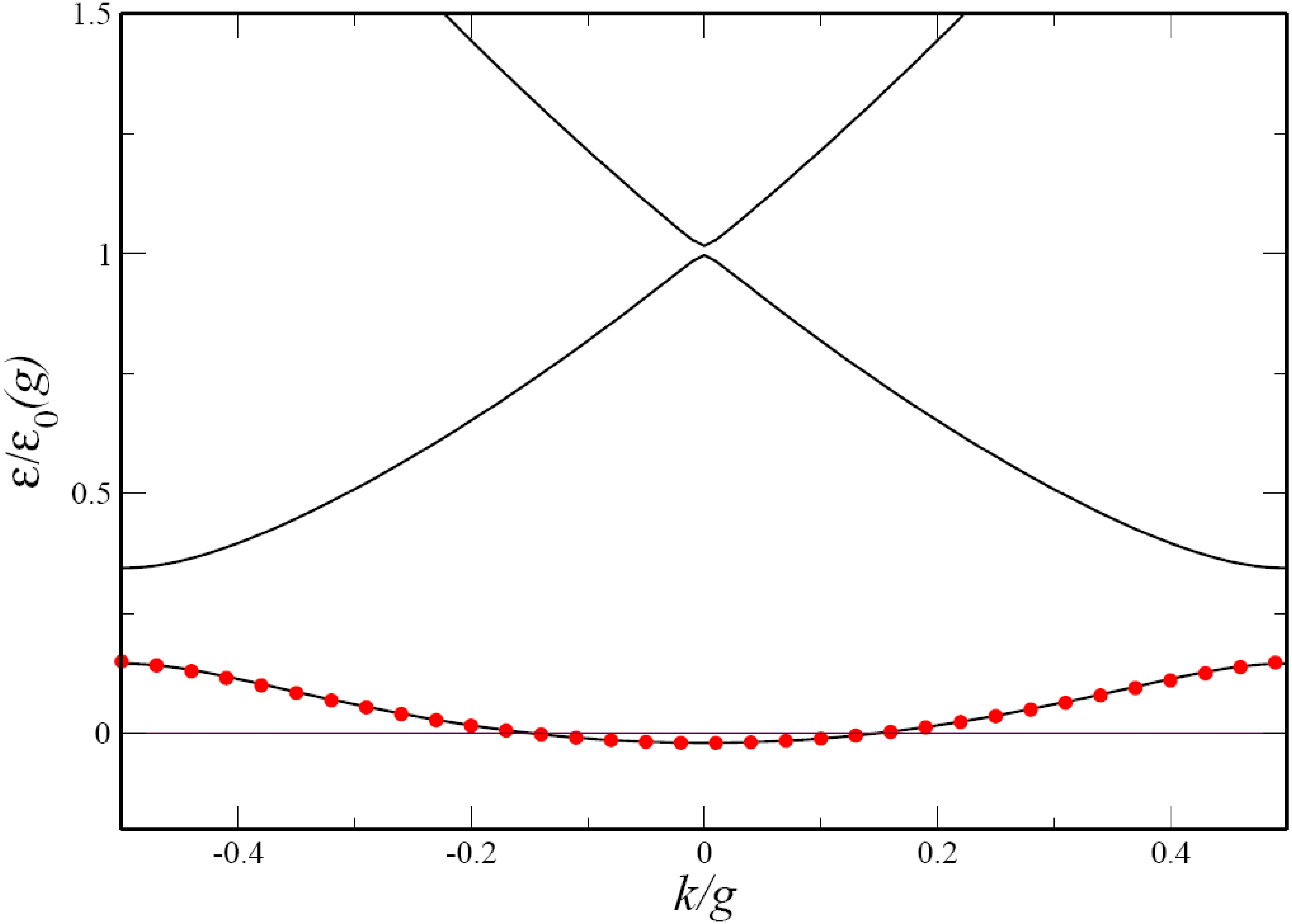

Electron energy spectrum of a nanohelix in the presence of a transverse electric field $E = 0.2\varepsilon_0(g)/(eR)$: solid lines – result of numerical diagonalisation of a 7×7 matrix; red circles – simple analytic approximation.

Bloch oscillations (BOs) and criterion of their existance

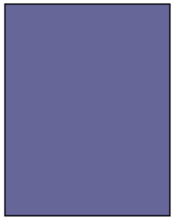

Bulk Semiconductor

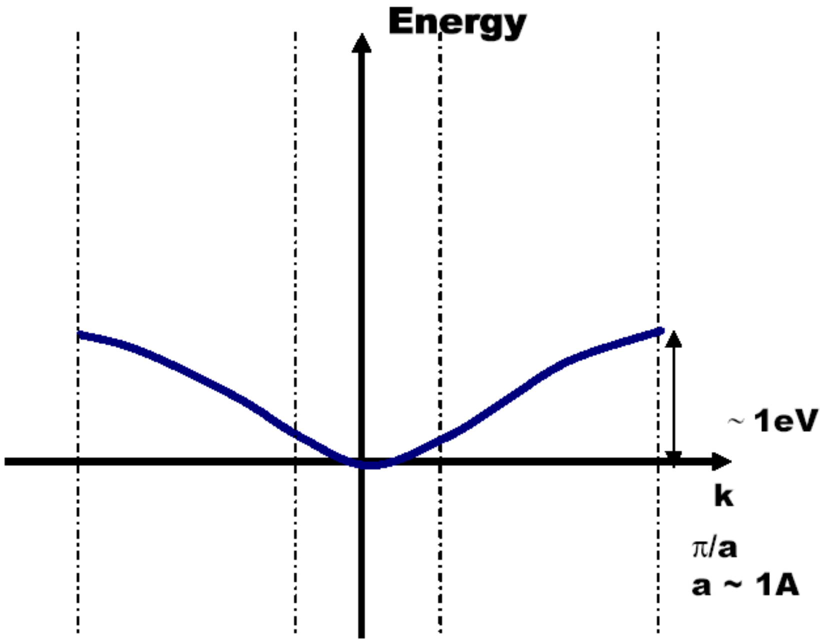

$$\hbar \frac{dk}{dt} = eE_{dc}$$ **Bloch, 1928**

A particle which is accelerated through k-space performs an oscillation in real space.

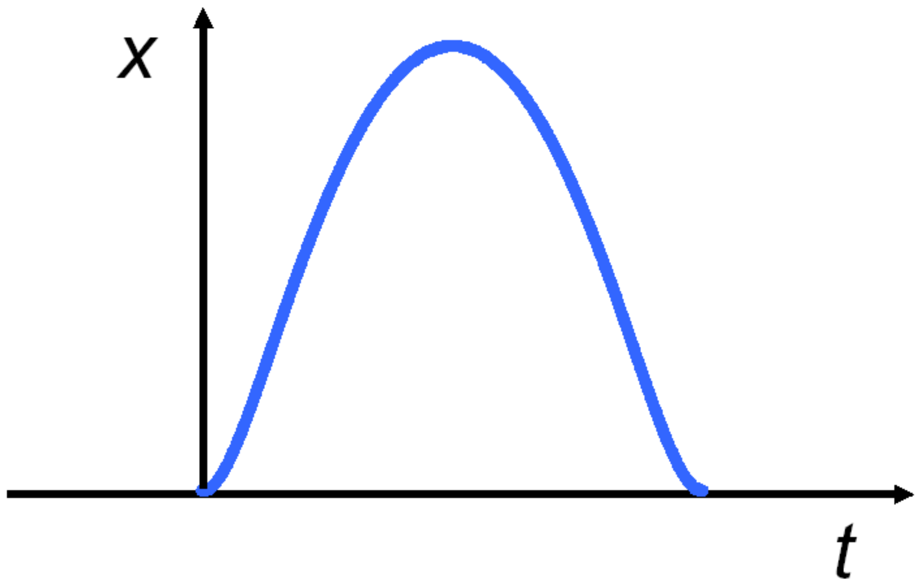

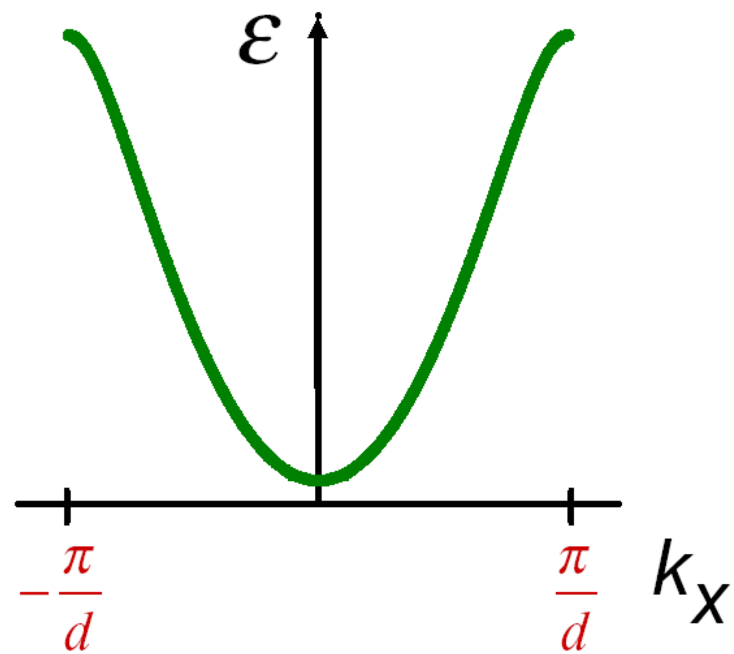

This is known as a Bloch oscillation.

$$V = \frac{dx}{dt} = \frac{1}{\hbar}\frac{d\varepsilon}{dk_x}$$

$$\hbar\frac{dk_x}{dt} = eE_{dc}$$

A particle which is accelerated through k-space performs an oscillation in real space.

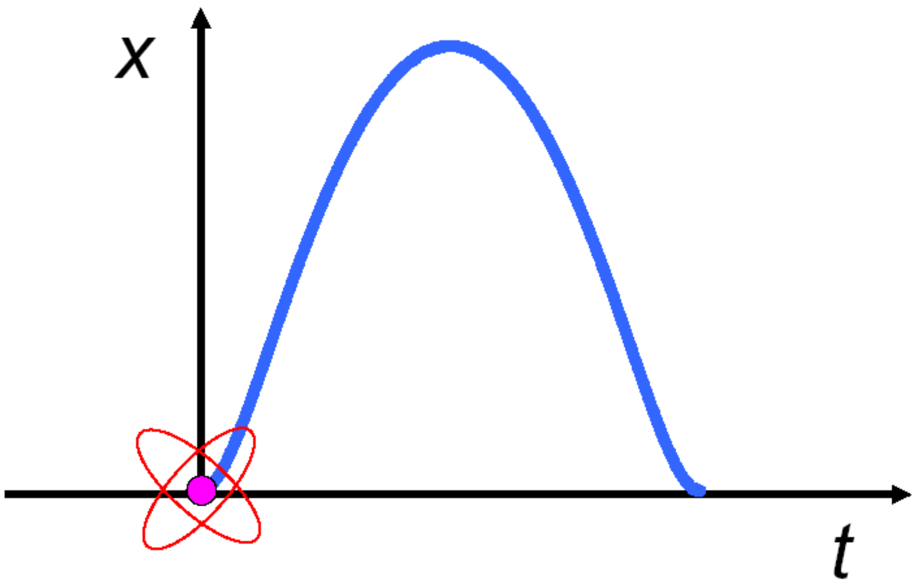

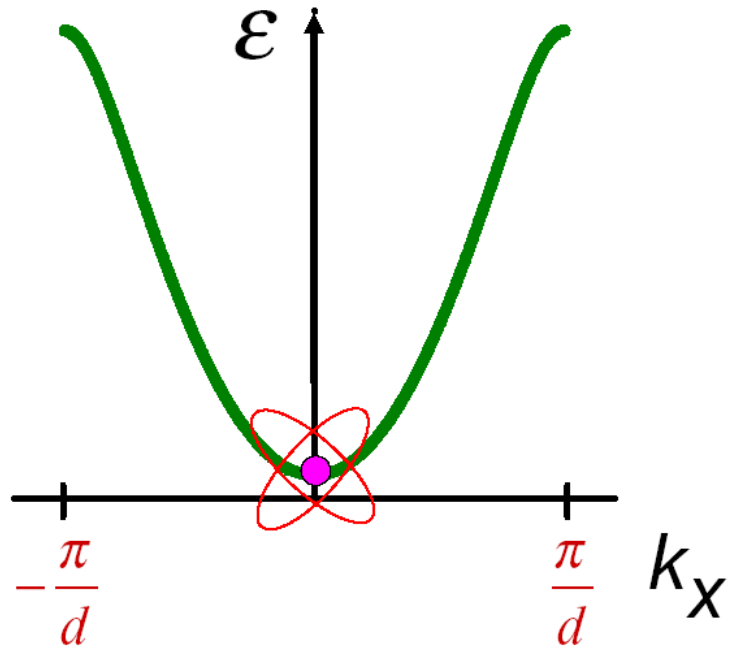

This is known as a Bloch oscillation.

$$V = \frac{dx}{dt} = \frac{1}{\hbar}\frac{d\varepsilon}{dk_x}$$

$$\hbar\frac{dk_x}{dt} = eE_{dc}$$

A particle which is accelerated through k-space performs an oscillation in real space.

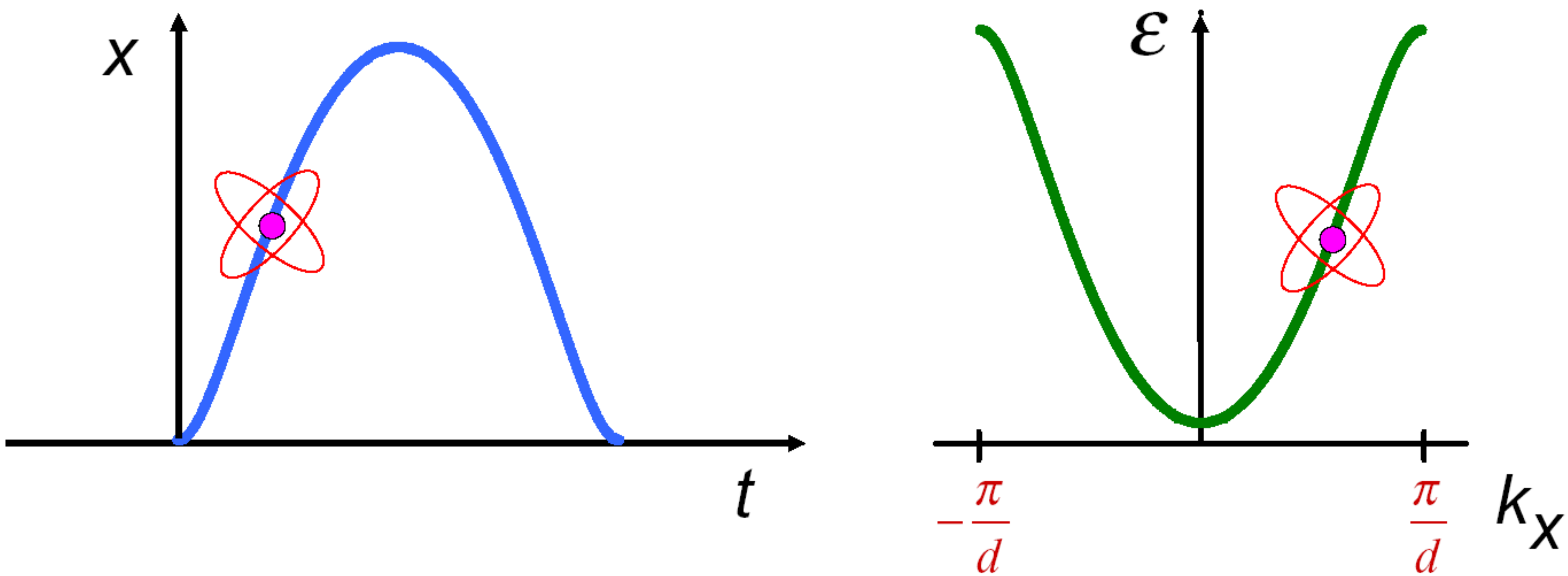

This is known as a Bloch oscillation.

$$V = \frac{dx}{dt} = \frac{1}{\hbar}\frac{d\varepsilon}{dk_x}$$

$$\hbar\frac{dk_x}{dt} = eE_{dc}$$

A particle which is accelerated through k-space performs an oscillation in real space.

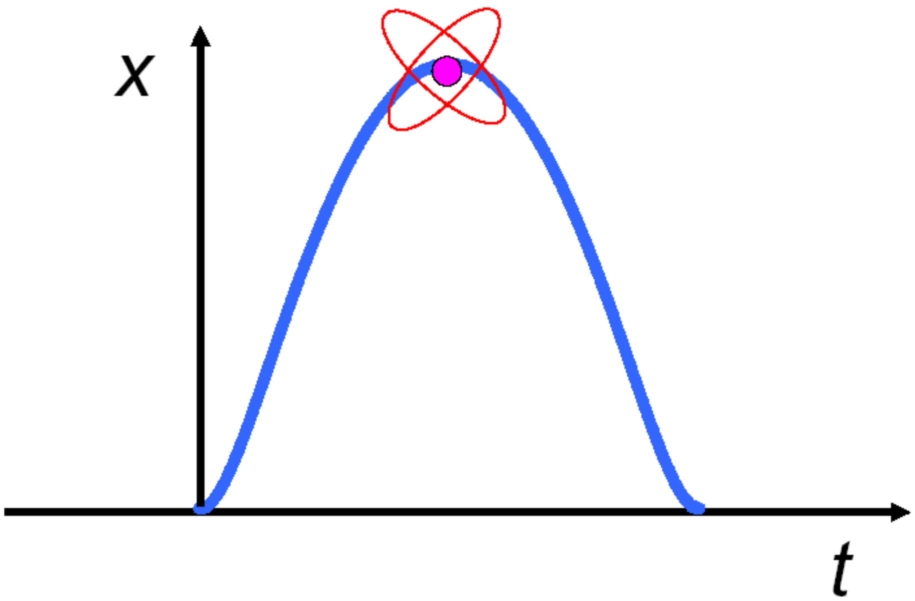

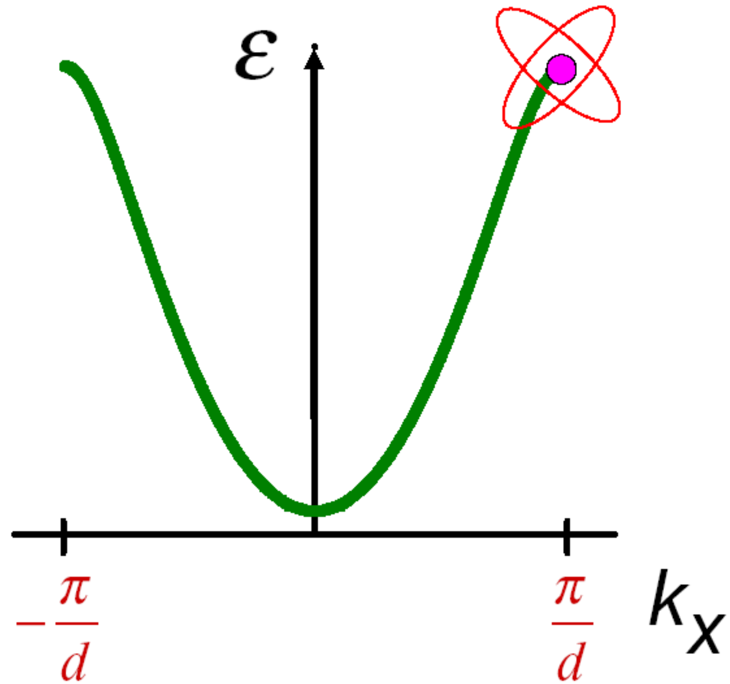

$$V = \frac{dx}{dt} = \frac{1}{\hbar}\frac{d\varepsilon}{dk_x}$$

$$\hbar\frac{dk_x}{dt} = eE_{dc}$$

This is known as a Bloch oscillation.

A particle which is accelerated through k-space performs an oscillation in real space.

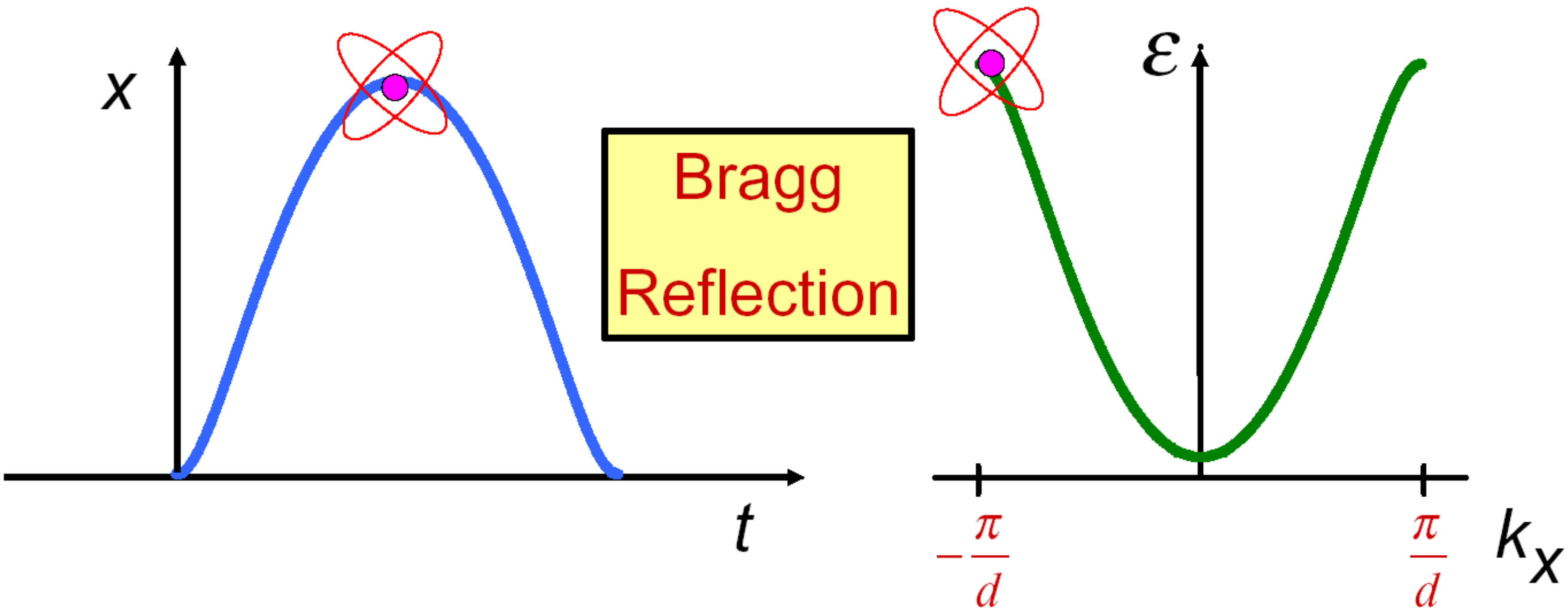

This is known as a Bloch oscillation.

$$V = \frac{dx}{dt} = \frac{1}{\hbar}\frac{d\varepsilon}{dk_x}$$

$$\hbar\frac{dk_x}{dt} = eE_{dc}$$

A particle which is accelerated through k-space performs an oscillation in real space.

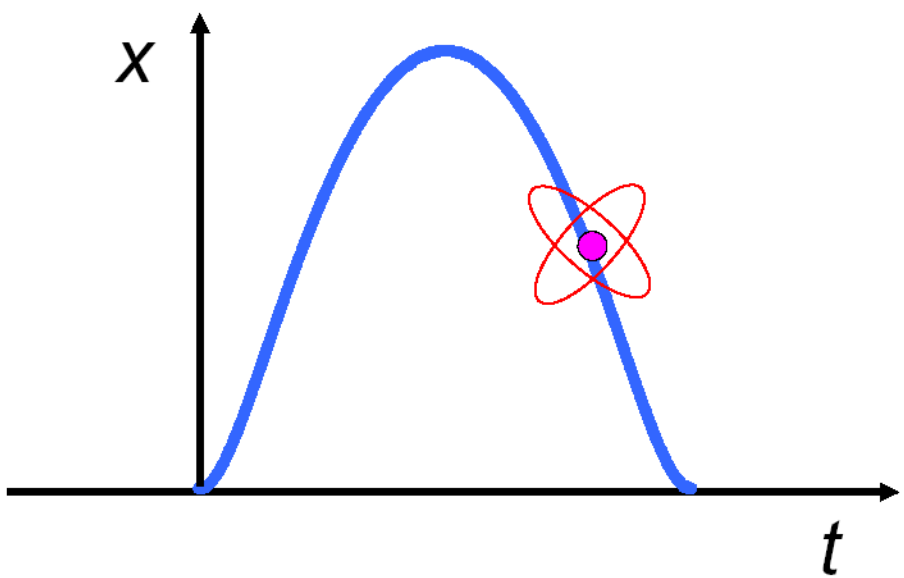

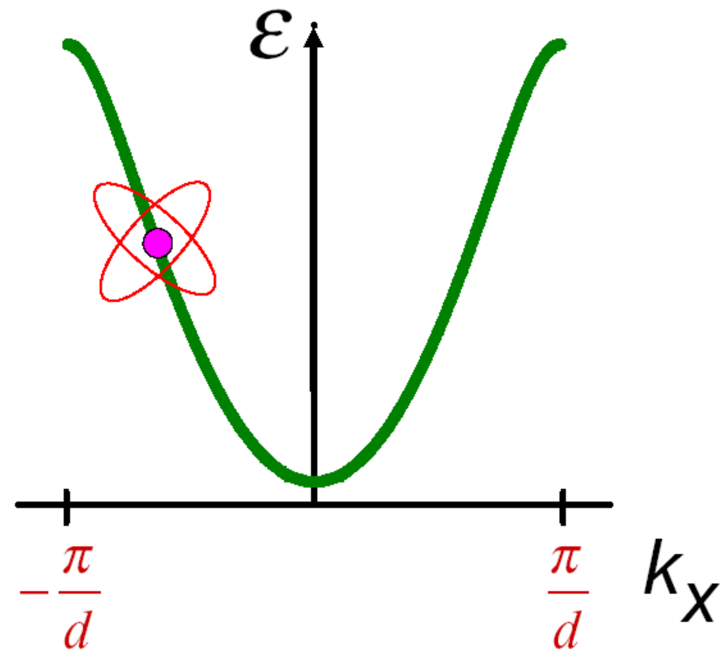

$$V = \frac{dx}{dt} = \frac{1}{\hbar}\frac{d\varepsilon}{dk_x}$$

$$\hbar \frac{dk_x}{dt} = eE_{dc}$$

This is known as a Bloch oscillation.

A particle which is accelerated through k-space performs an oscillation in real space.

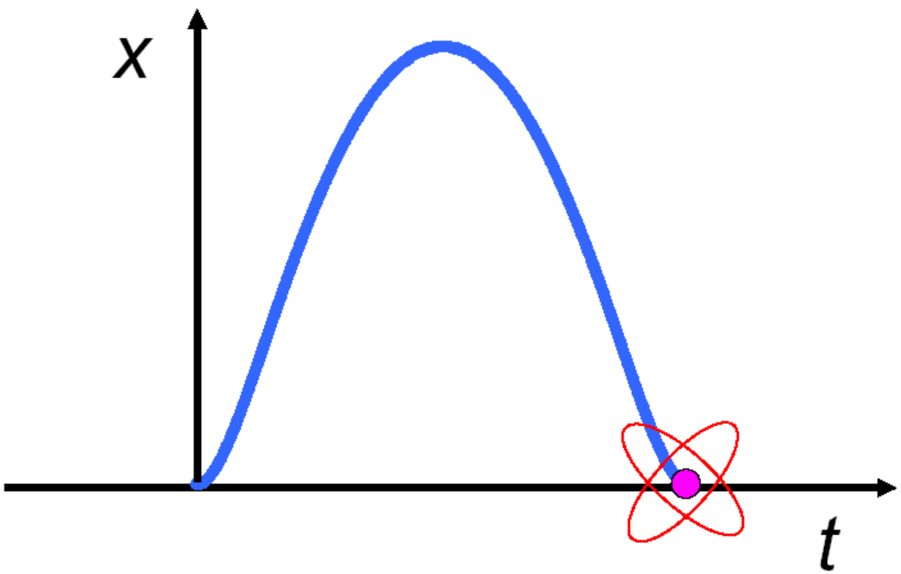

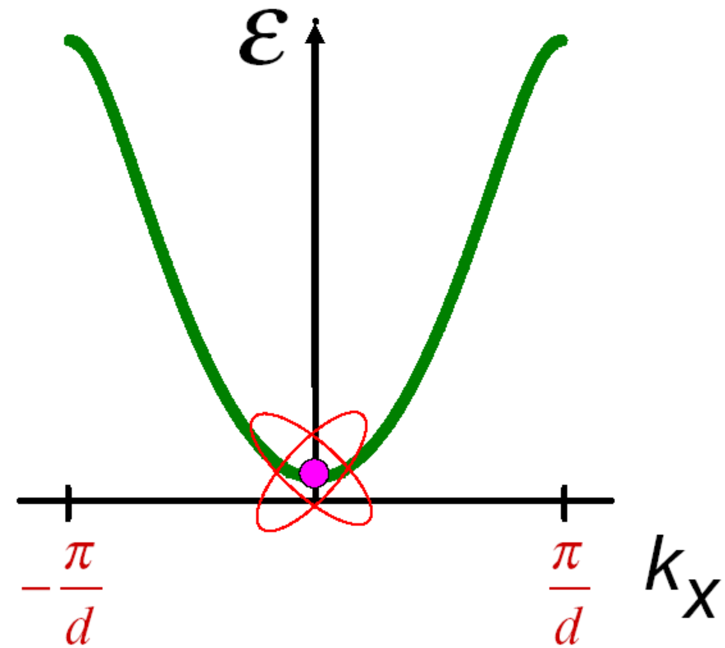

This is known as a Bloch oscillation.

$$V = \frac{dx}{dt} = \frac{1}{\hbar}\frac{d\varepsilon}{dk_x}$$

$$\hbar\frac{dk_x}{dt} = eE_{dc}$$

Time period of BOs:

$$\tau_B = \frac{h}{eaE_{dc}}$$

Frequency of BOs:

$$\omega_B = \frac{eaE_{dc}}{\hbar}$$

Criterion of BOs existance

high fields
and/or
long scattering times

$$\tau >> \tau_B$$

$$\omega_B \tau \geq 1$$

Zone-folding method in a single π–band tight binding model

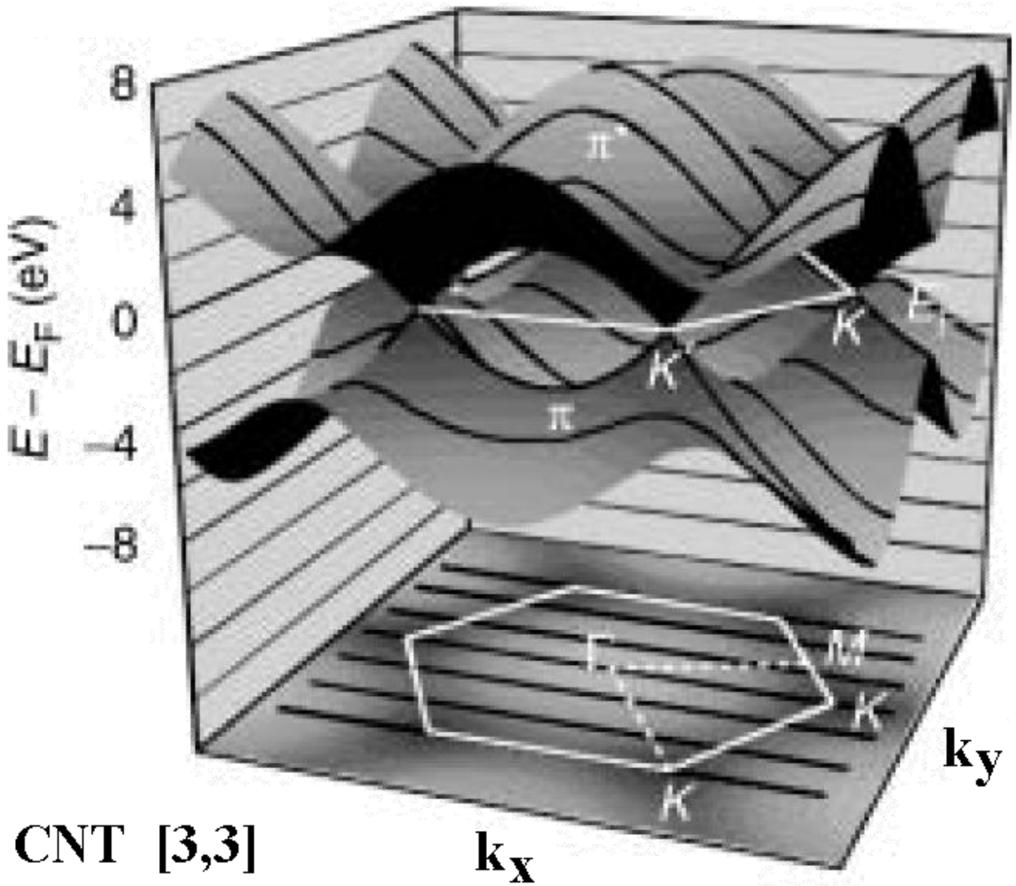

The allowed values of k are:

$$\mathbf{k} = k_{\parallel}\hat{\mathbf{T}} + k_{\perp}\hat{\mathbf{C}}_{\mathbf{h}},$$

with

$$-\pi/T < k_{\parallel} \leq \pi/T,$$

$$k_{\perp} = \frac{2\pi}{C_h} l,$$

where

$$l = -N/2+1, ..., 0, 1, ..., N/2.$$

N is the number of hexagons in the CNT unit cell.

Transverse electric field opens gaps in the CNT energy spectrum

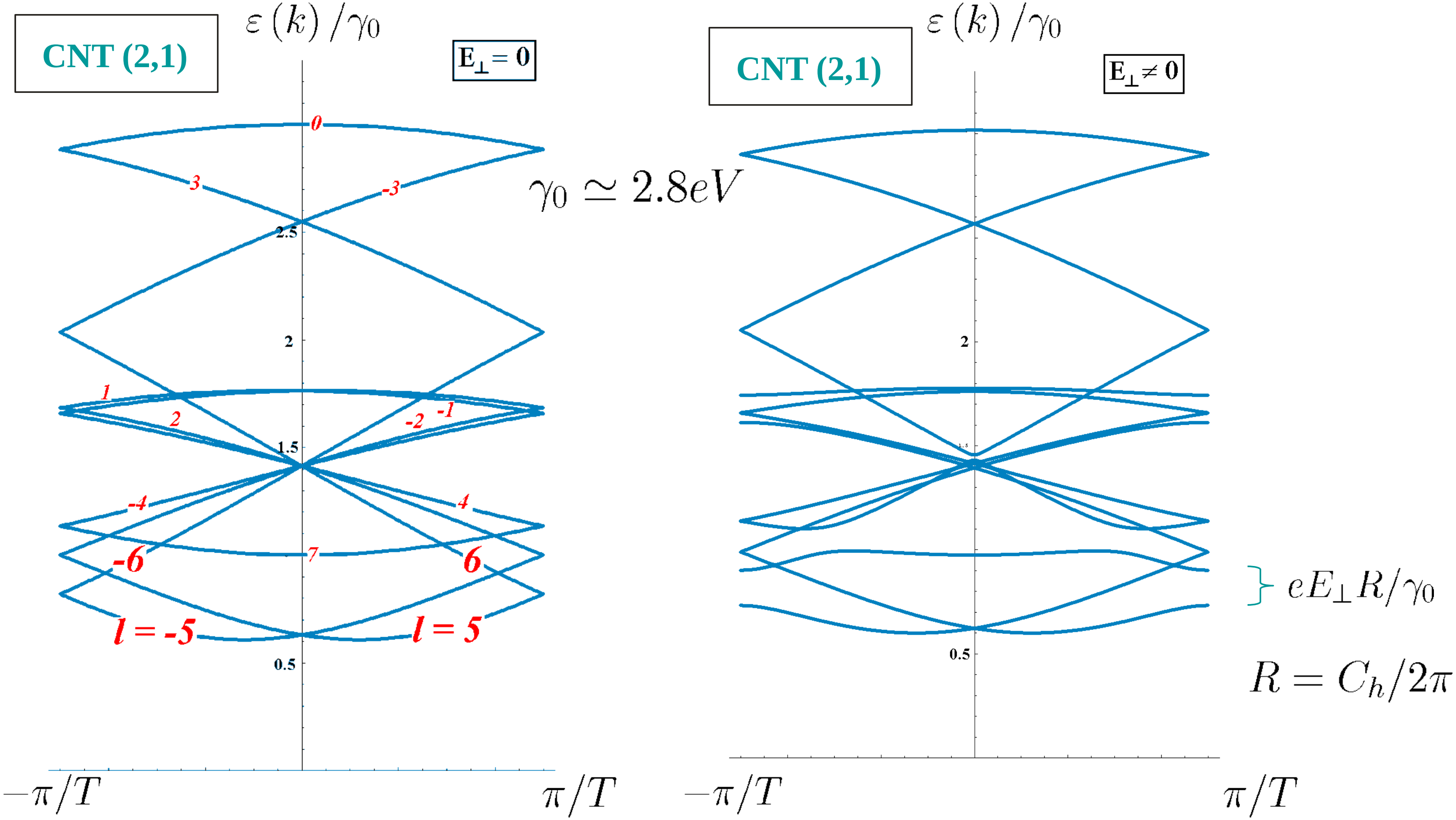

First order gaps between the subbands such that: $l' = l \pm 1$

For the lowest band and other chiral nanotubes there are only higher order gaps: $\Delta_{Gap}^{1^a\,B} \propto \left(\frac{eE_\perp C_h}{2\pi\gamma_0}\right)^n$.

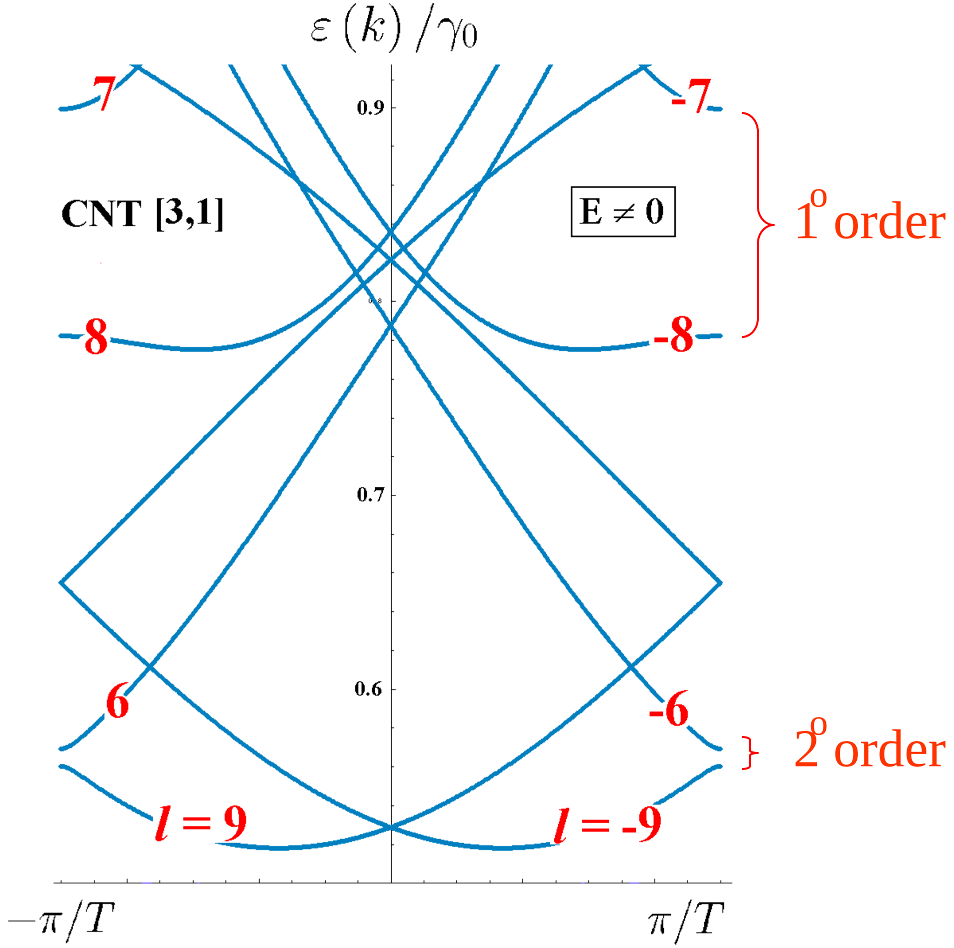

For the (n,1) family we have:

CNT	Gap Order	T / a
(2,1)	1	4.6
(3,1)	2	6.3
(4,1)	2	2.6
(5,1)	2	9.6
(6,1)	3	11.4
(7,1)	3	4.4
(8,1)	3	14.8
(9,1)	4	16.5
(10,1)	4	6.1

Repeated-zone scheme

CNT (6,1) $E_{\perp} = 0.39\ V/A$ $eE_{\perp}a/\gamma_0 = 0.35$

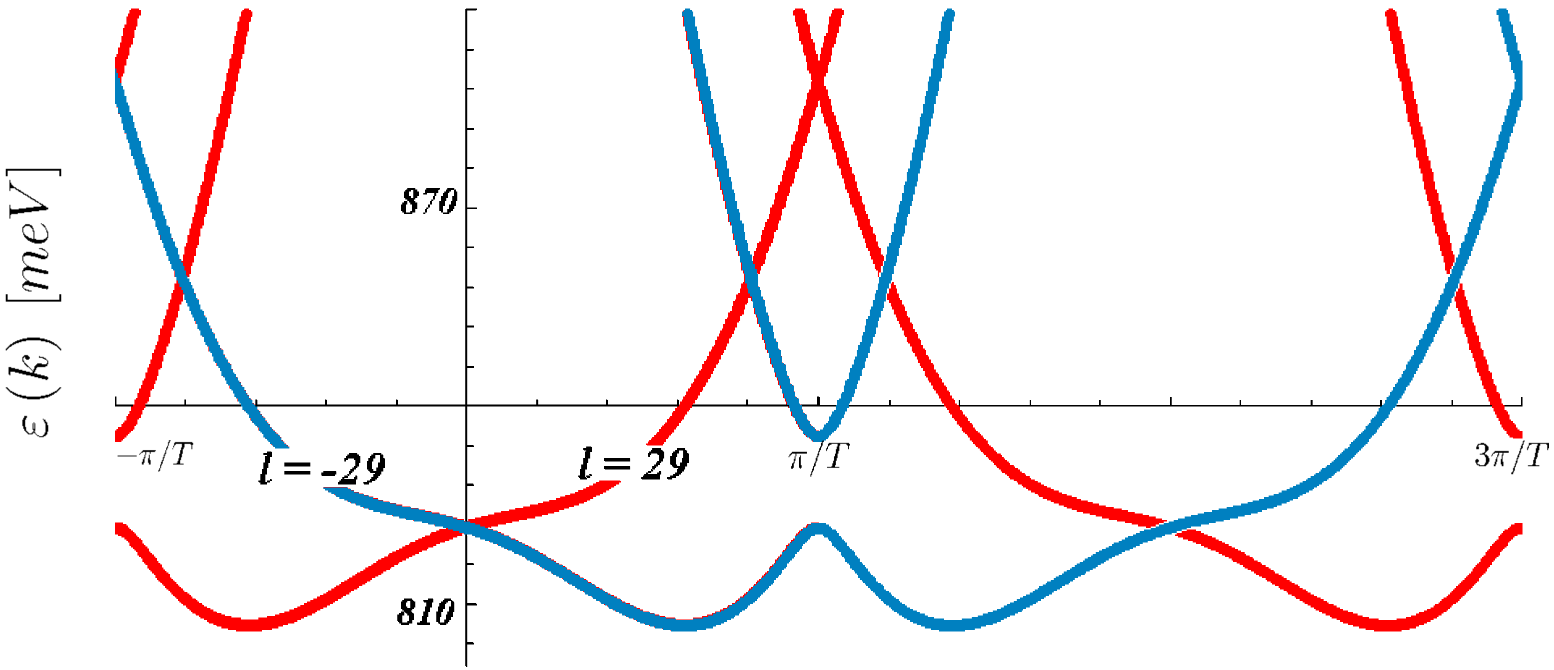

Response to a DC Parallel Electric Field

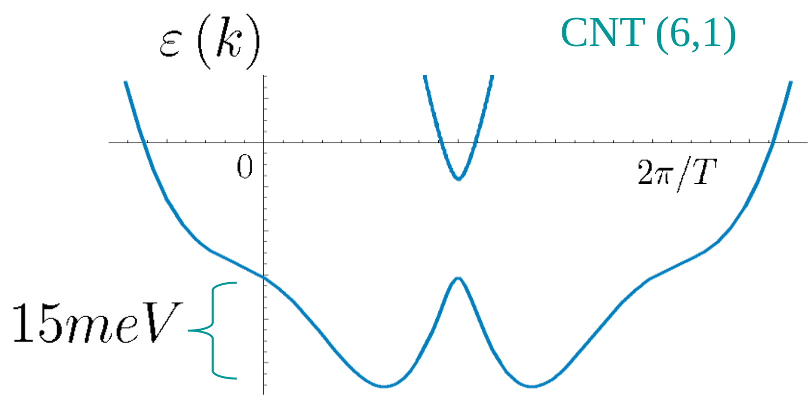

$$\varepsilon_{op.\ phon.} \simeq 160meV$$

In the semiclassical description:

$$v_T(t) = v_1(t) + v_2(t)\,,$$

$$v_i(t) = v_i(k_i(t)) = v\left(k_{0,i} + \frac{eE_\parallel}{\hbar}t\right).$$

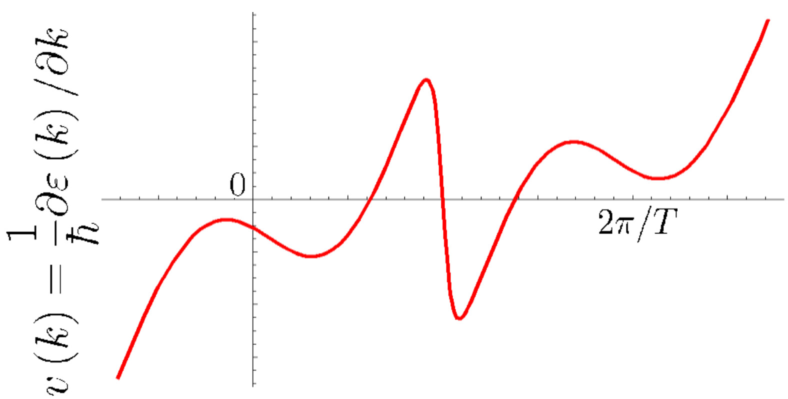

For the drift velocity (Esaki-Tsu):

$$v_{drift} = \int_0^\infty e^{-t/\tau}\frac{d}{dt}v_T(t)\,dt.$$

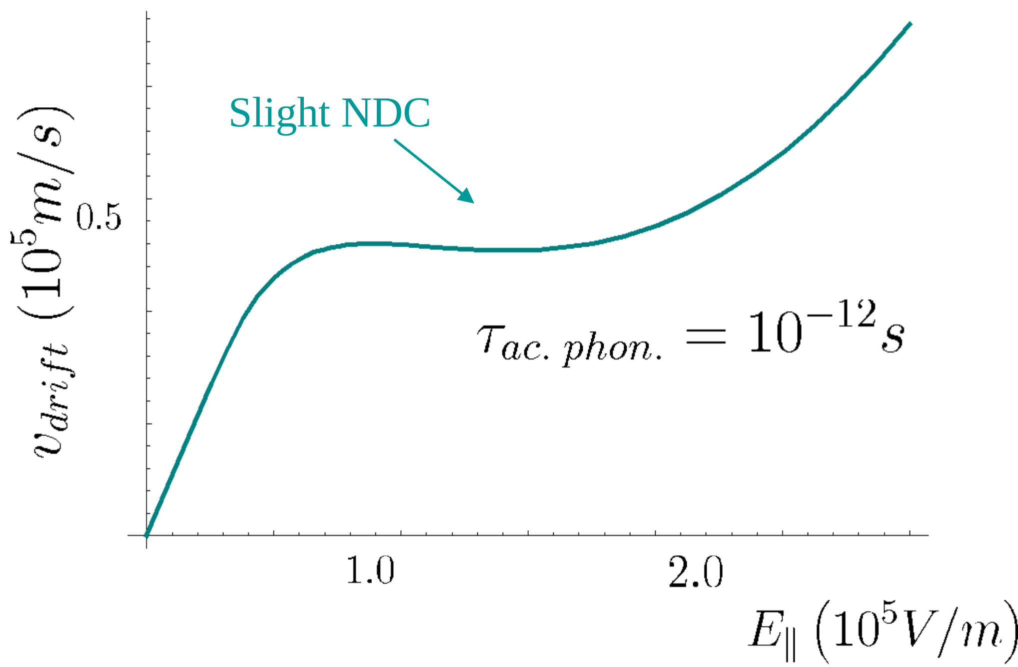

Response to an AC parallel electric field

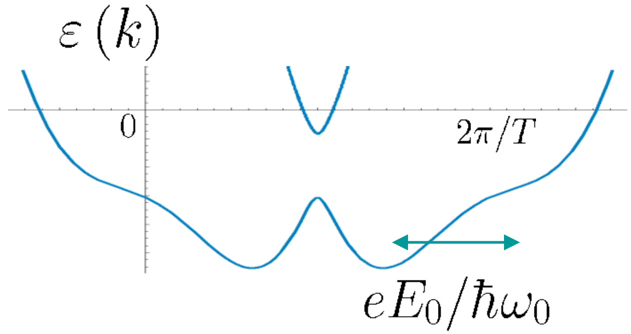

Applying an AC field:

$$E_{\|}(t) = E_0 \sin[\omega_0 t]$$

$$k(t) = k_0 + \frac{eE_0}{\hbar\omega_0}\sin(\omega_0 t)\,.$$

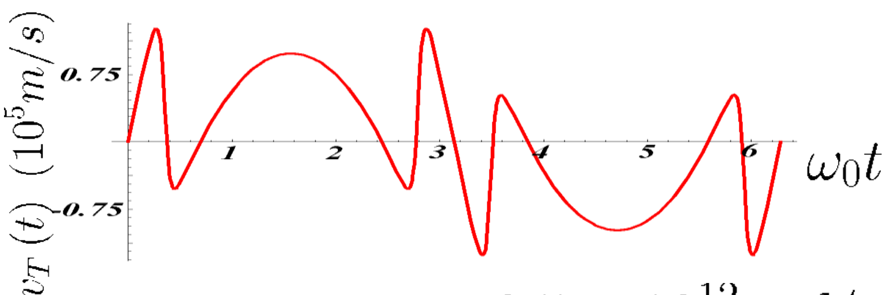

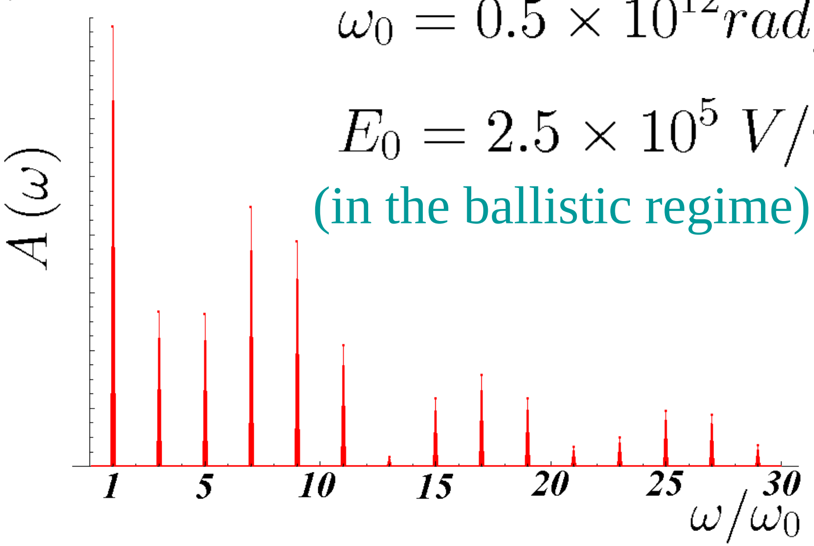

$$\omega_0 = 0.5 \times 10^{12} rad/s$$

$$E_0 = 2.5 \times 10^5\ V/m$$

(in the ballistic regime)

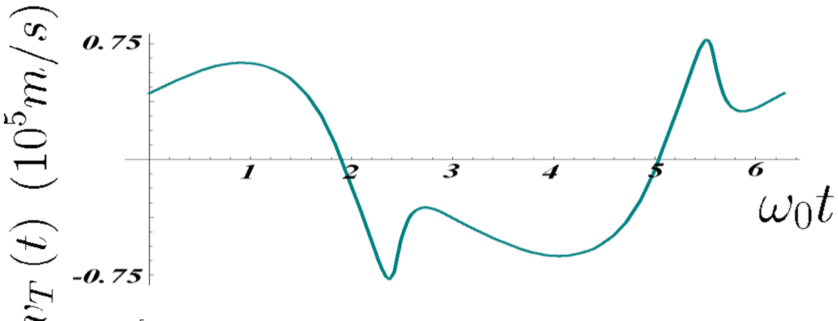

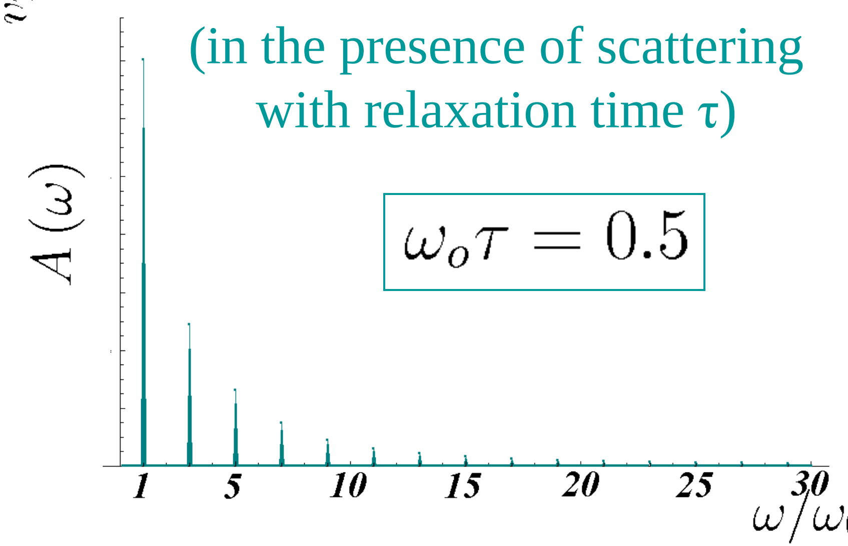

(in the presence of scattering with relaxation time τ)

$$\omega_o \tau = 0.5$$

Armchair CNT in a magnetic field

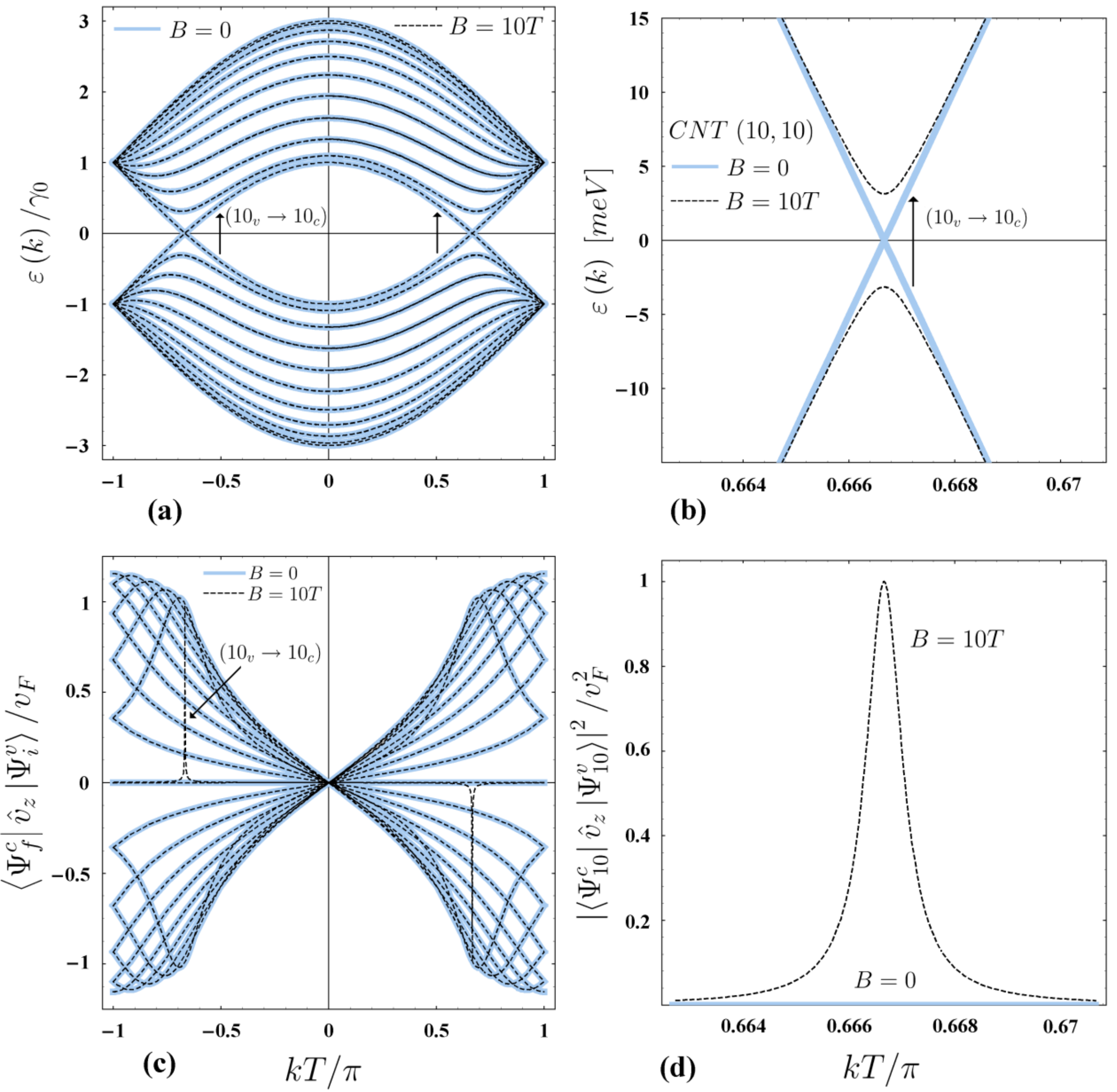

Energy spectra and matrix elements of optical tranzitions polarized alond the nanotube axis for a (10,10) CNT in a magnetic field B=10T along the nanotube axis and without the field.

Magnetic-field induced gap in an armchair (n,n) CNT:

$$\varepsilon_g = 2\gamma_0 \left| \sin\left(\frac{f}{n} \pi \right) \right|$$, where $$f = \Phi / \Phi_0$$.

Matrix element of velocity at the band edge:

$$\left| \left\langle \Psi_C \right| \hat{v}_z \left| \Psi_V \right\rangle \right| = v_F \frac{2}{\sqrt{3}} \left[1 - \frac{1}{4} \cos^2\left(\frac{f}{n} \pi \right) \right]^{1/2} \approx v_F$$

Absorbtion intensity: $$I(\varepsilon) \propto \frac{1}{\varepsilon^2} \frac{\varepsilon_g^{5/2}}{\sqrt{\varepsilon - \varepsilon_g}} \theta(\varepsilon - \varepsilon_g)$$.

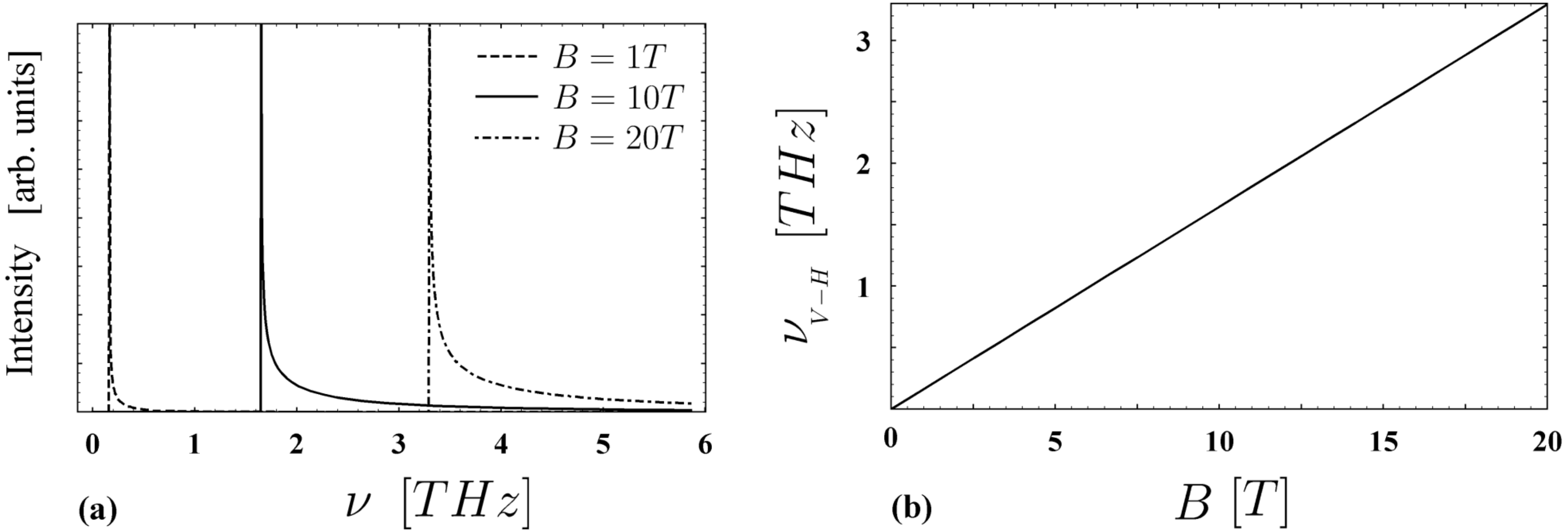

(a) Absorption intensity (taking into account the van-Hove singularity in the reduced density of states) for several magnetic field values.

(b) The magnetic field dependence of the peak frequency for a (10,10) CNT.

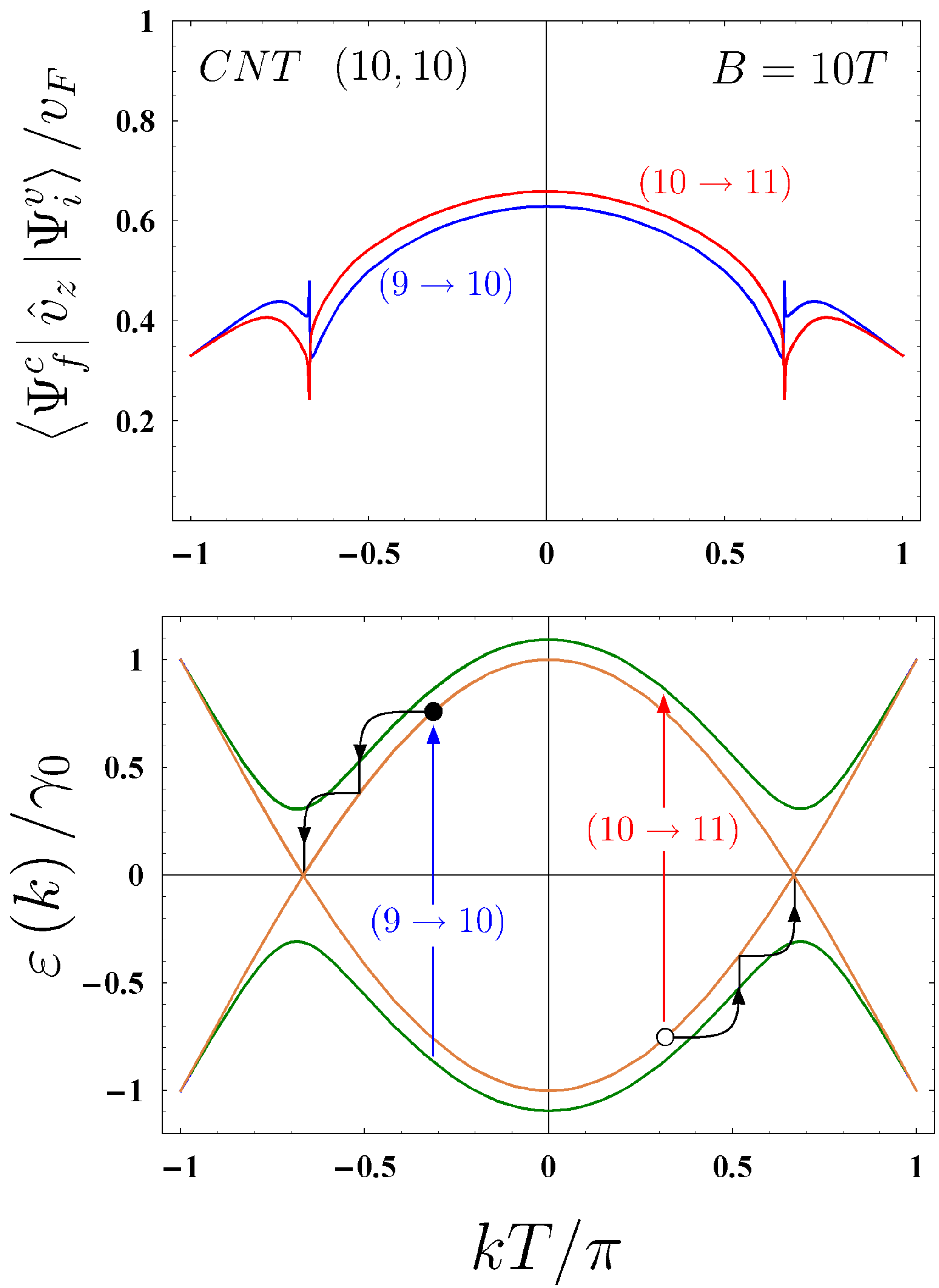

The scheme for creating inversion of population in tunable THz emitters based on armchair CNTs in a magnetic field.

cond-mat/0608596;
Proc. SPIE 632805 (2006);
Superlattices and Microstructures (2007);
Int. J. Mod. Phys. B (2009)

Quasi-metallic nanotubes (revisited)

are (n,m) CNTs with $n\text{-}m=3p$, where p is a non-zero integer.

Their bandgap is given by $$\varepsilon_g = \frac{\hbar v_F a_{\text{C-C}} \cos 3\theta}{8R^2},$$

where $a_{\text{C-C}} = 1.42\ \text{Å}$ is the nearest-neighbor distance between two carbon aroms, R is the CNT radius, and $\theta = \arctan[\sqrt{3}m/(2n+m)]$ is a chiral angle.

For example for a (30,0) zigzag CNT the curvature-induced gap is about 6 meV or **1.5 THz**.

No need for a 10T magnetic field!

Curvature-induced THz gap

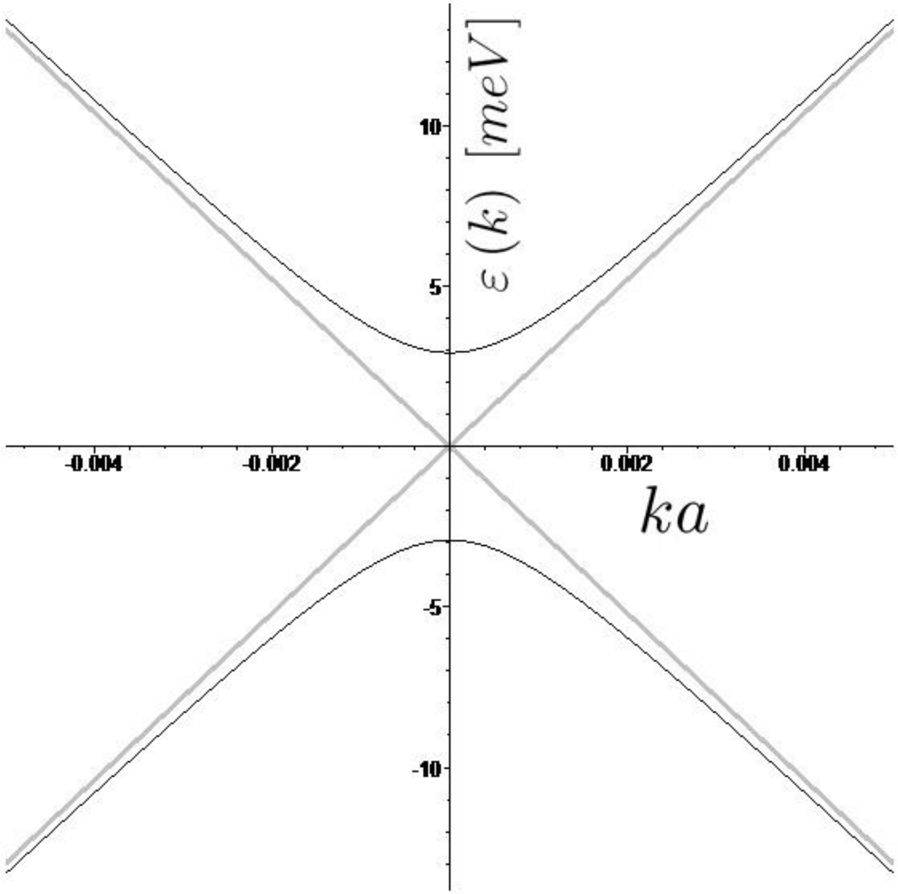

Low-energy spectrum of a (30,0) CNT

[R. Hartmann & MEP, 2009]

Optical transitions across the curvature-induced gap

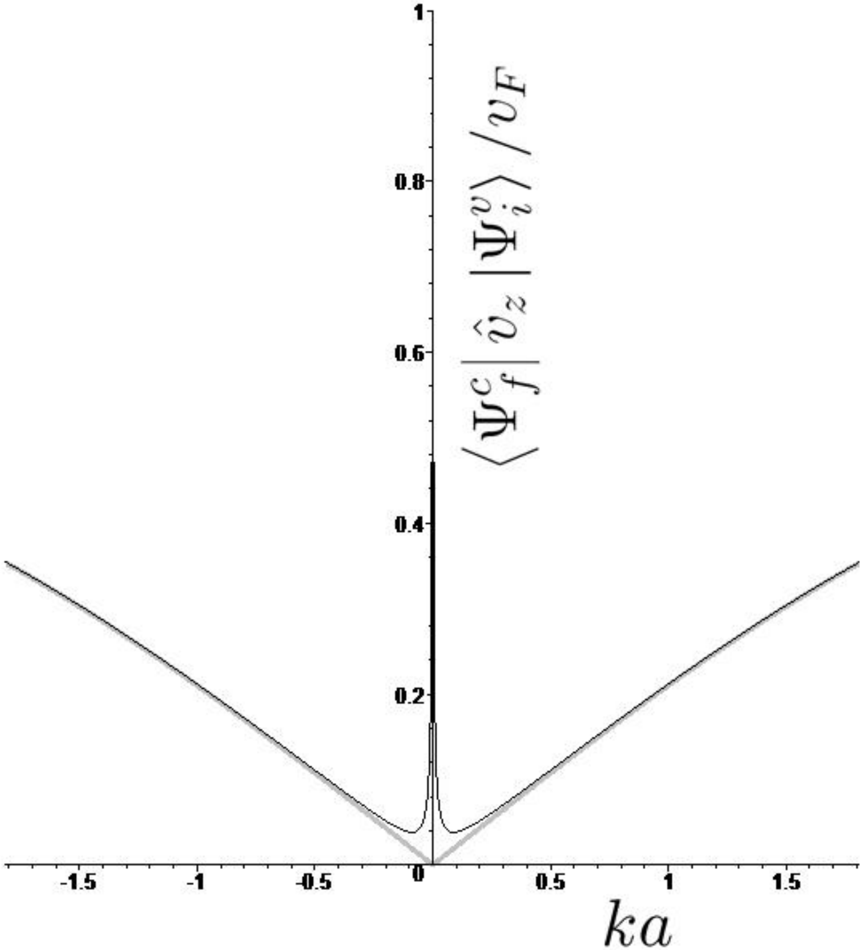

Matrix elements of optical tranzitions polarized alond the nanotube axis for a (30,0) CNT [RH & MEP - 2009]

Excitonic effects?

From J.Kono talk, HMF-18, Sao Pedro, Brazil, 2008

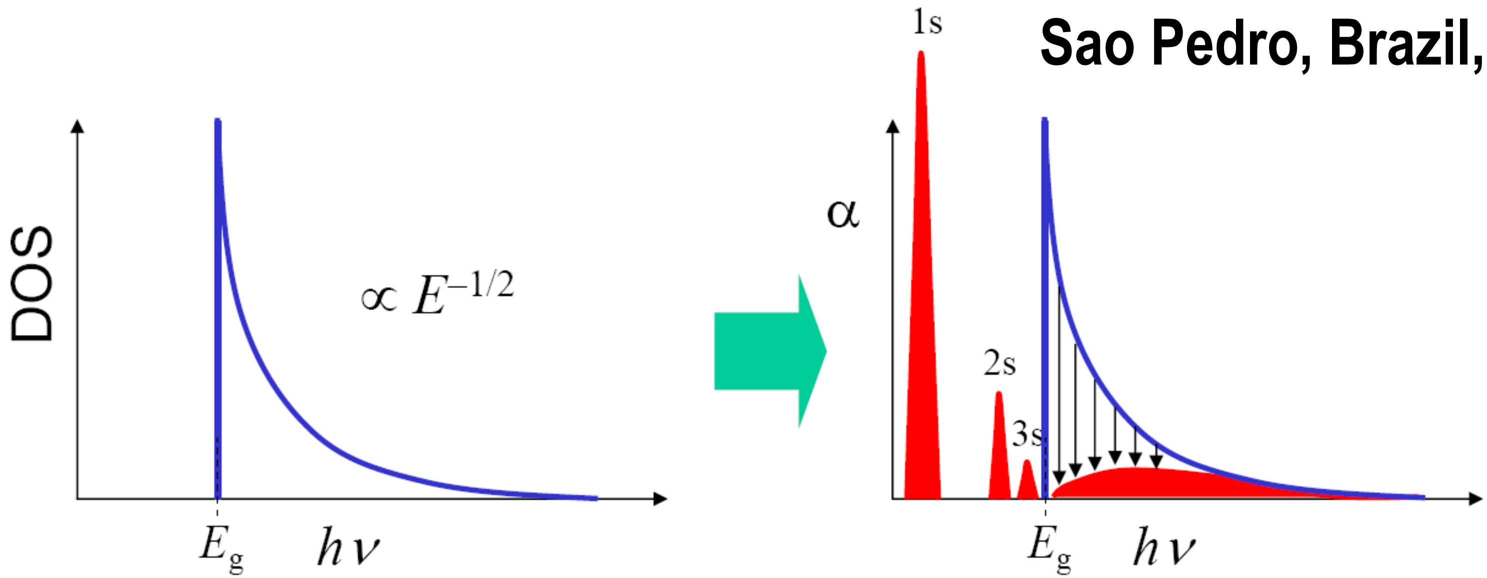

- Huge binding energy → extremely stable
- Lineshape: 1-D VHS (asymmetric) → 1-D excitons (symmetric)
- Sommerfeld factor < 1 (*collapse* of 1-D VHS)

A typical exciton binding energy for a semiconductor CNT is 400 meV (for a (7,6) CNT). Our 1 THz gap is ~ 4meV.

Dark excitons? Gap renormalisation? Loss of control?

Excitons in narrow-gap carbon nanotubes

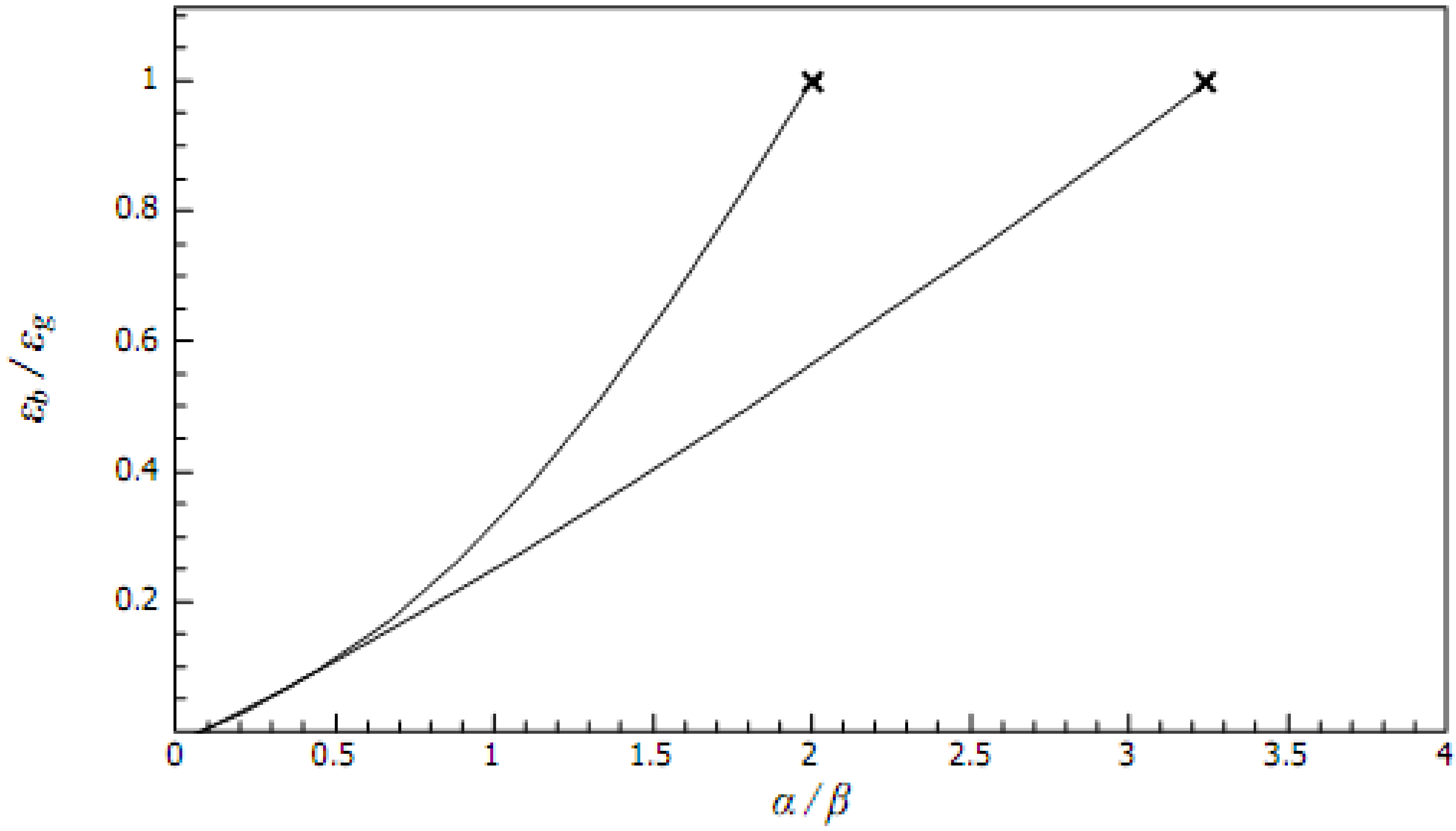

R.R.Hartmann, I.A.Shelykh & MEP, PRB 84, 035437 (2011)

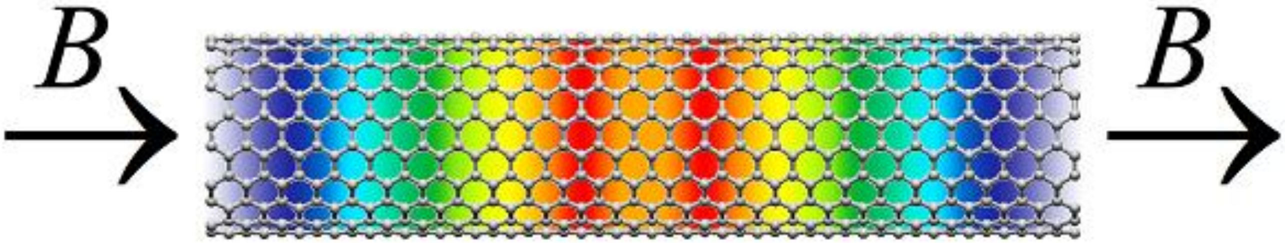

Our results *vs* the effective mass approximation

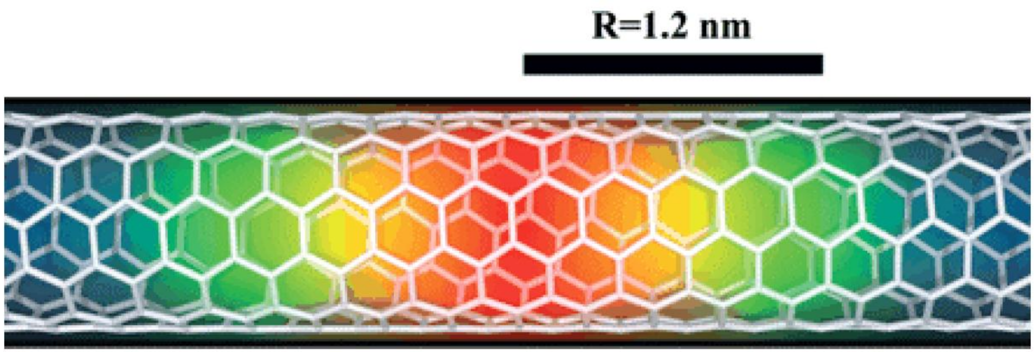

Density of the 1*s*-exciton envelope wave function for a (6,5) SWNT. The wave function has been calculated using the experimentally determined exciton binding energy and the truncated Coulomb electron-hole interaction. The density represents the probability of finding the electron and hole composing the exciton at the indicated relative separation. The half width of the exciton along the nanotube is $R = 1.2$ nm, compared to the 0.8-nm diameter of the nanotube. [F. Wang *et al*, Science 308, 838 (2005)]

THz applications of graphene

Graphene as a THz emitter

- Highly-efficient frequency multiplication due to non-parabolic electronic spectrum [S.A. Mikhailov, EPL **79**, 27002 (2007); JPCM **20**, 384204(2008)]
- Graphene-based SL, THz plasmonics etc…

Graphene as a THz detector

- Zero-gap semiconductor => THz absorption
- Gate control of the Fermi level position => tuneable low-frequency limit via the Moss-Burstein effect
- Momentum alignment of photoexcited carriers => polarisation sensitivity (for p-n junction structures)

Klein tunneling and Graphene p-n junctions

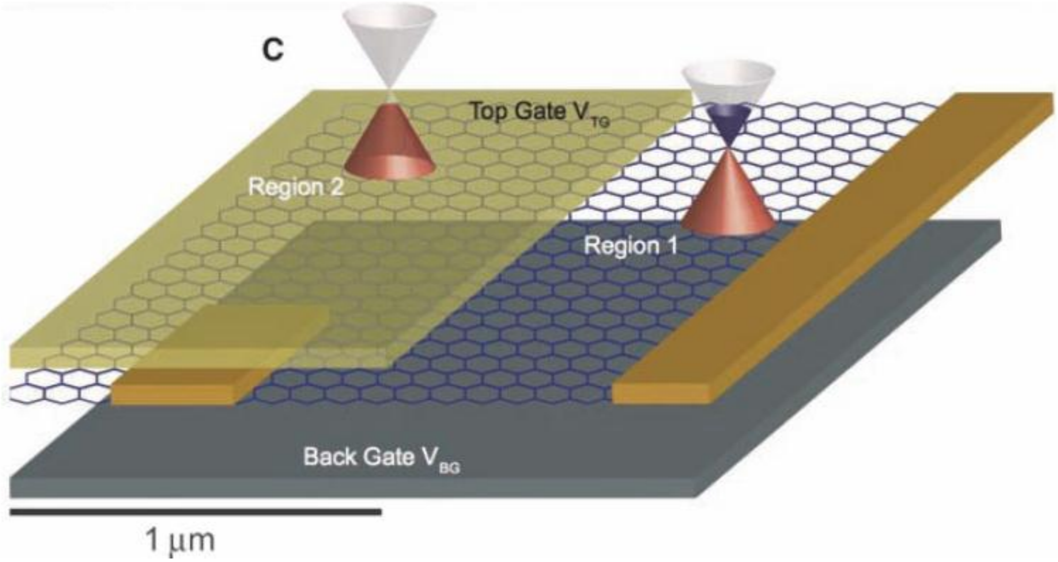

From J.R. Williams, L. DiCarlo, and C.M. Marcus, Science 317, 638

M.I. Katsnelson, K.S. Novoselov, A.K. Geim, Nature Phys. 2, 620 (2006).
V.V. Cheianov, V.I.Fal'ko, Phys. Rev. B 74, 041403(R) (2006)
V.V. Cheianov, V. Fal'ko, B. L. Altshuler, Science 315, 1252 (2007)
B. Huard, J.A. Sulpizio, N. Stander, K. Todd, B. Yang, and D. Goldhaber-Gordon, Phys. Rev. Lett. 98, 236803 (2007)
B. Özyilmaz, P. Jarillo-Herrero, D. Efetov, D. A. Abanin, L. S. Levitov, and P. Kim, Phys. Rev. Lett. 99, 166804 (2007)

Exeter structures (A.K. Savchenko & Co, 2008)

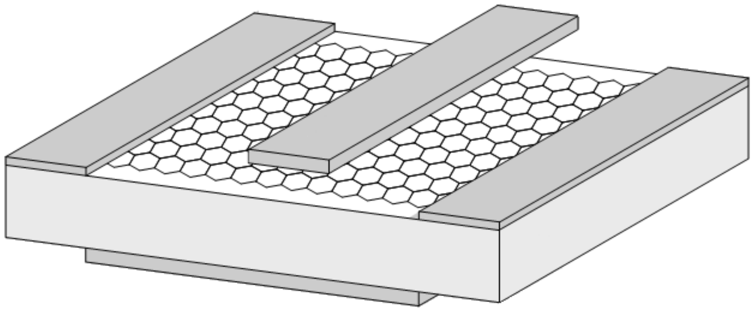

Alex Savchenko
1953 - 2010

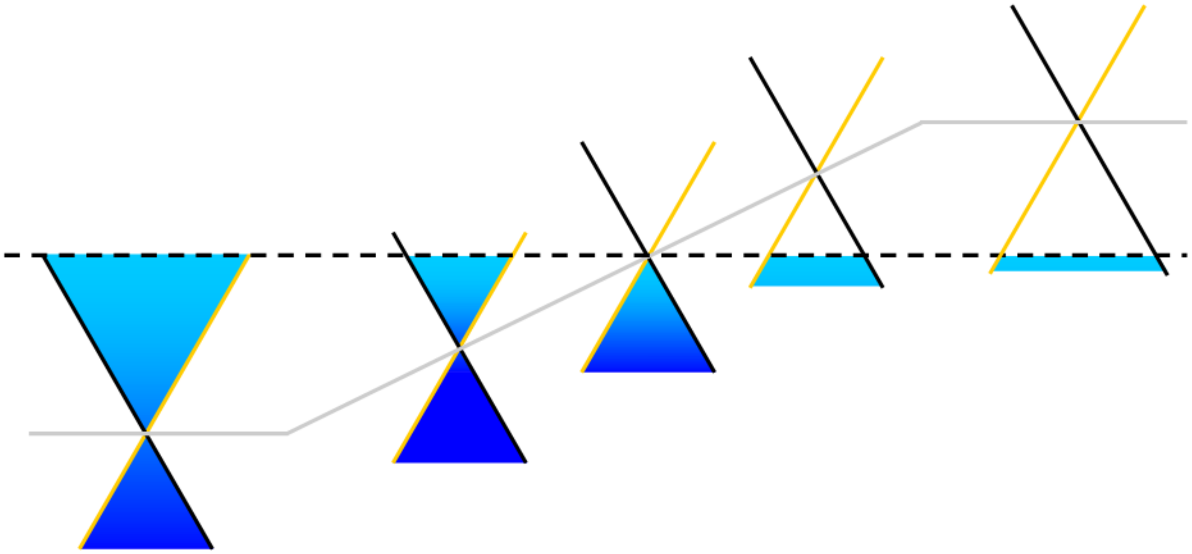

Klein tunneling in a graphene p-n junction

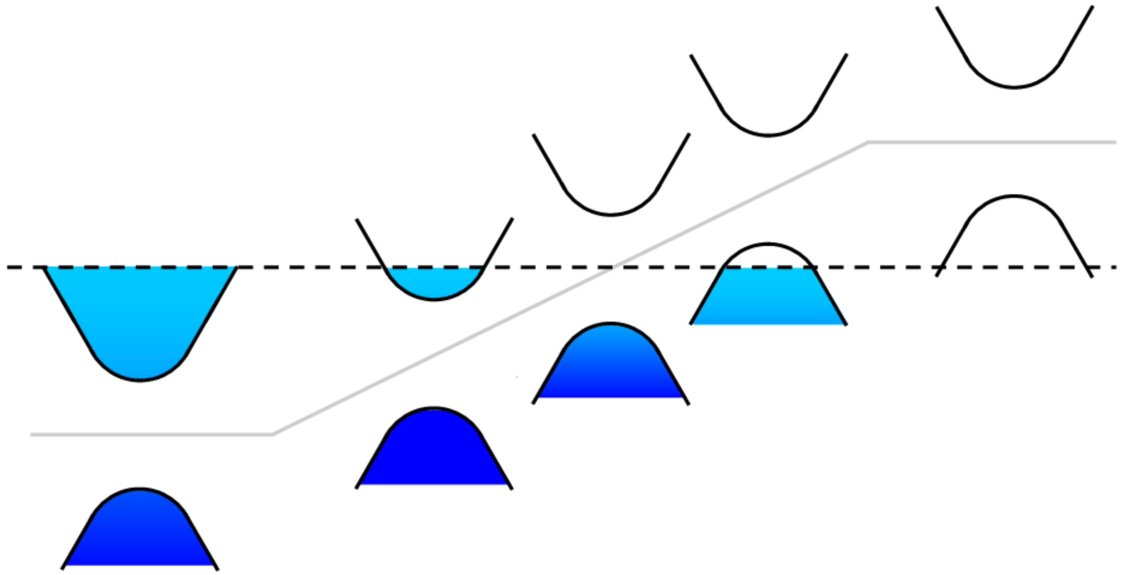

Conventional p-n junction

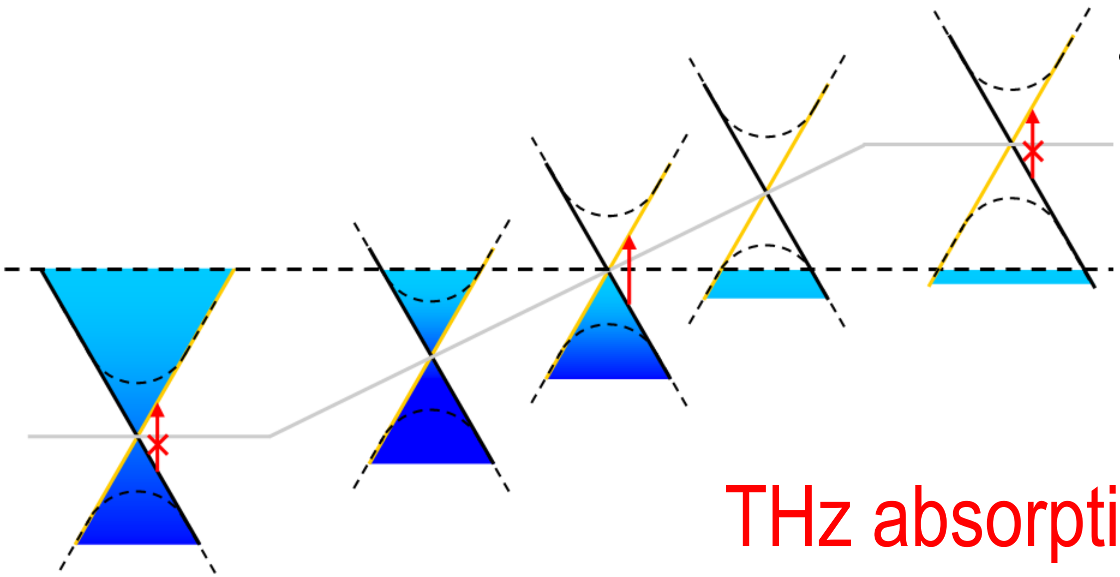

$$\varepsilon = \pm\hbar v_{\mathrm{F}}\sqrt{k_{\parallel}^{2}+k_{\perp}^{2}} \Rightarrow$$

angle-dependent tunneling

THz absorption

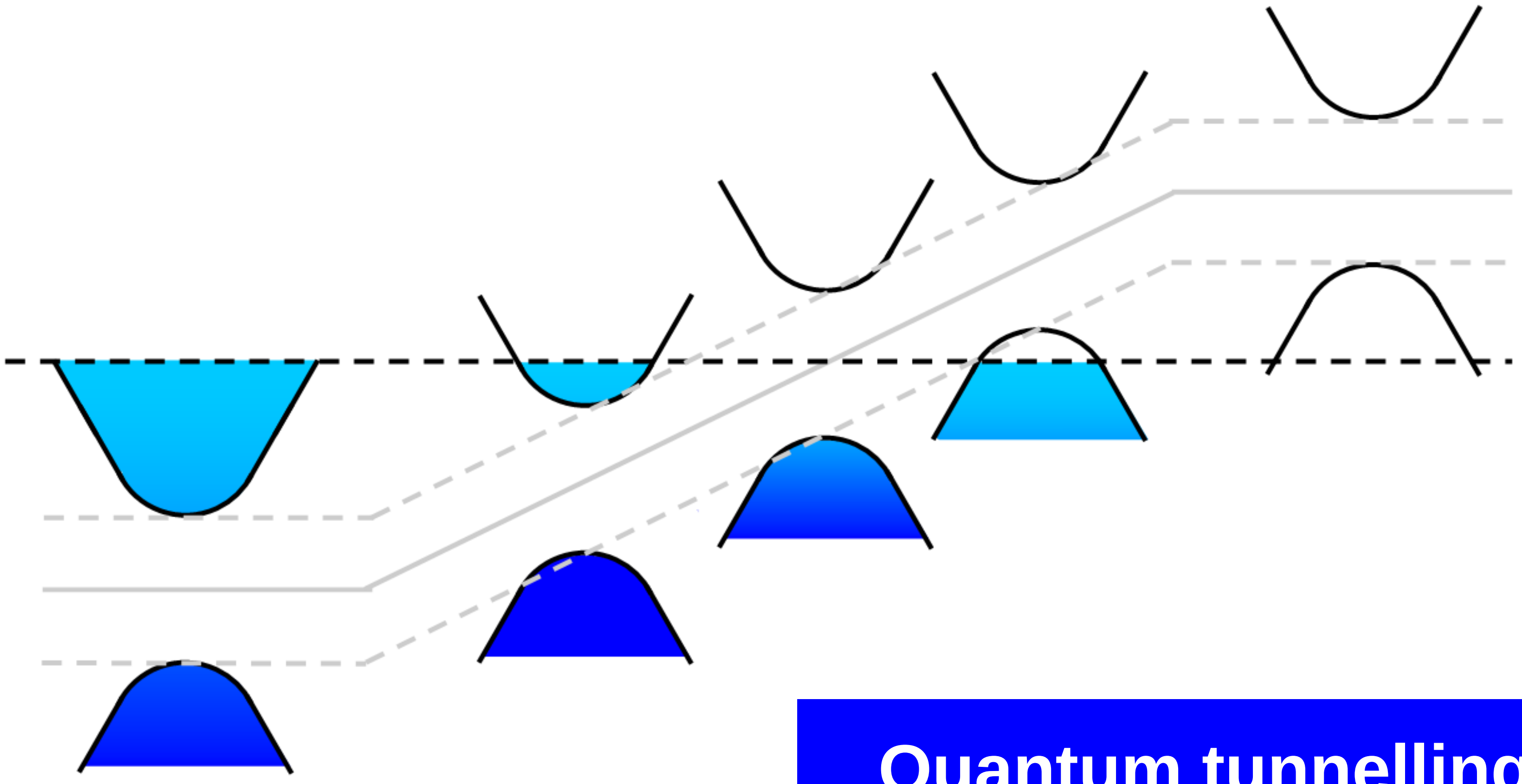

Quantum tunnelling

in a conventional system

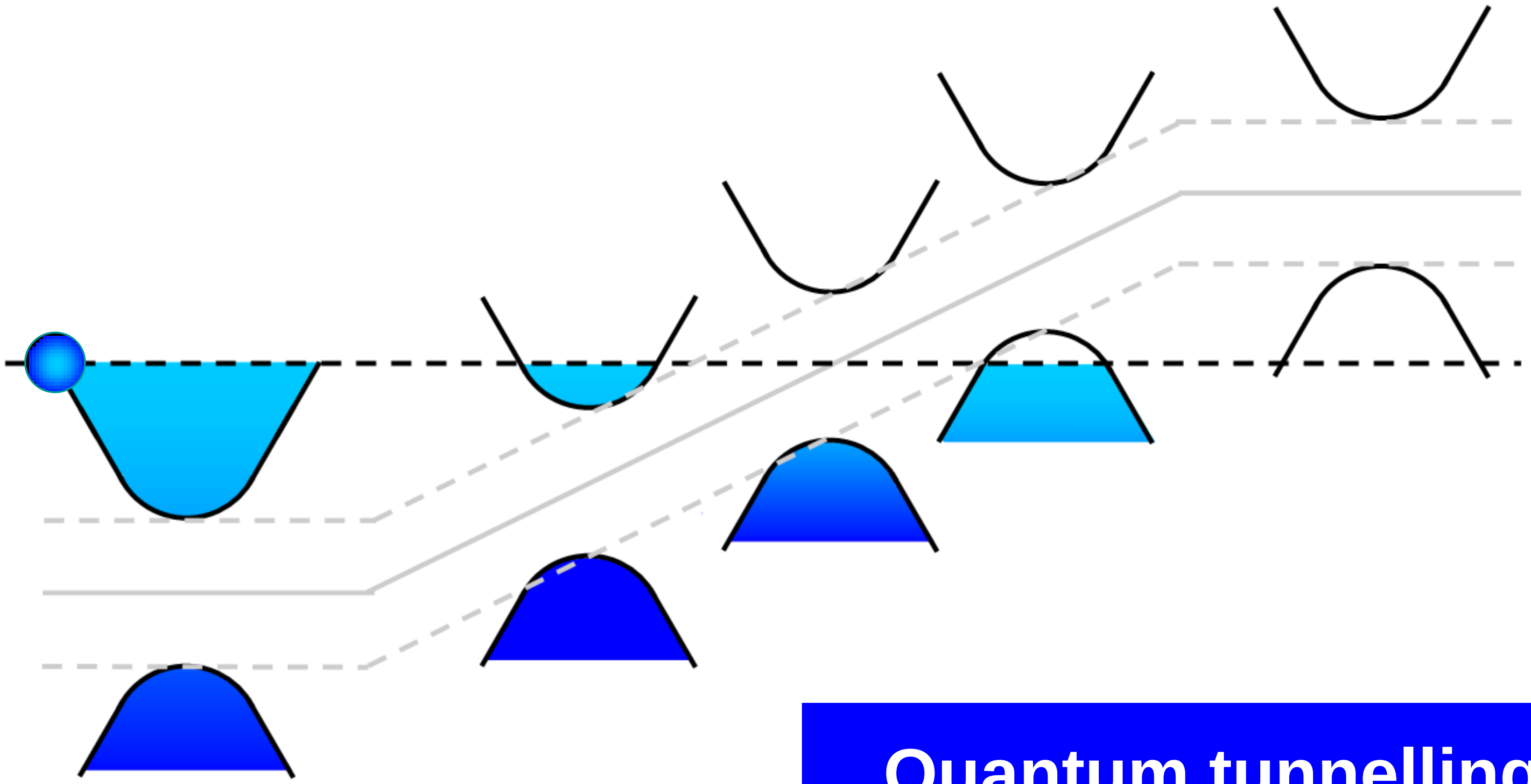

Quantum tunnelling

in a conventional system

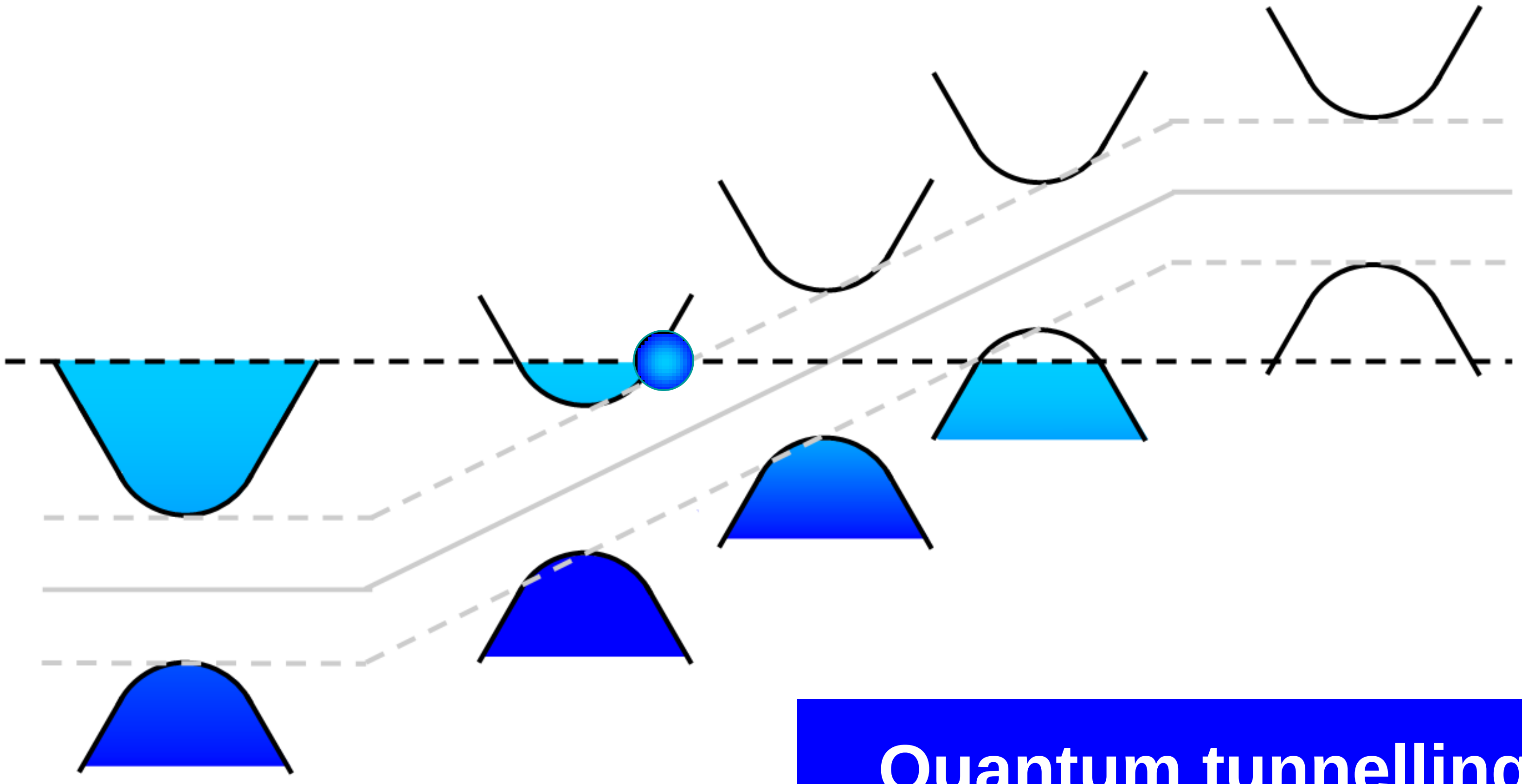

Quantum tunnelling

in a conventional system

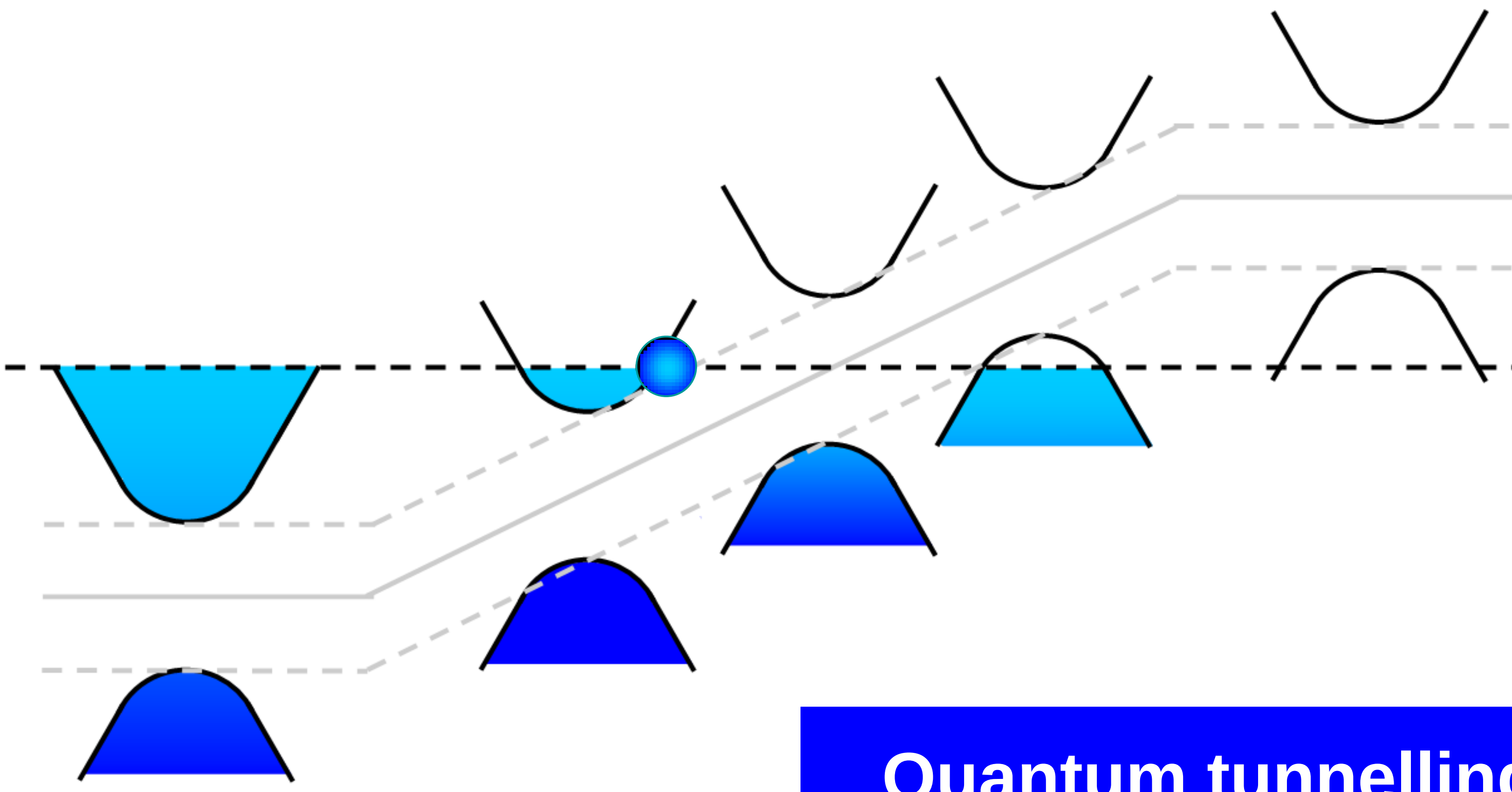

Quantum tunnelling

in a conventional system

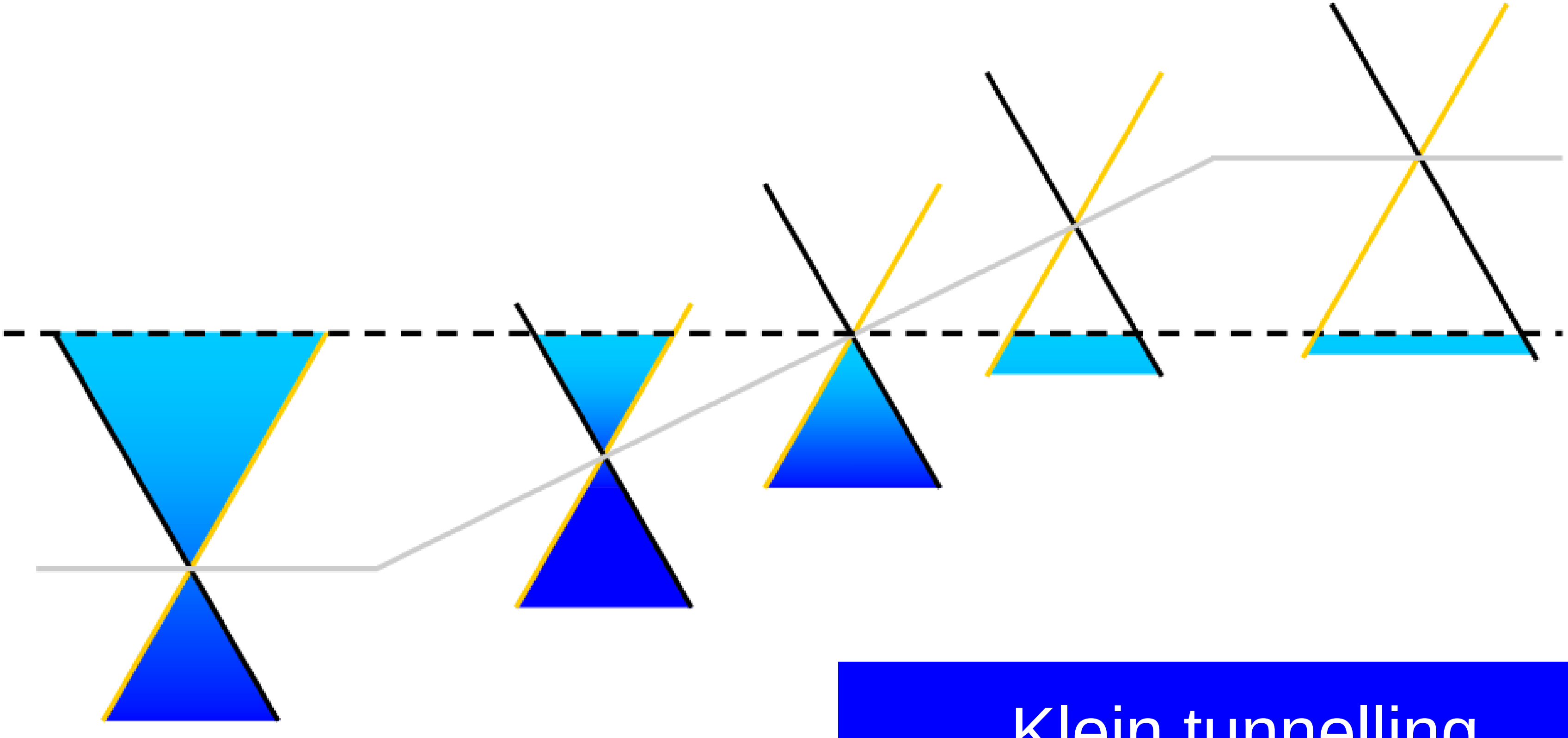

Klein tunnelling

in a Graphene p-n junction

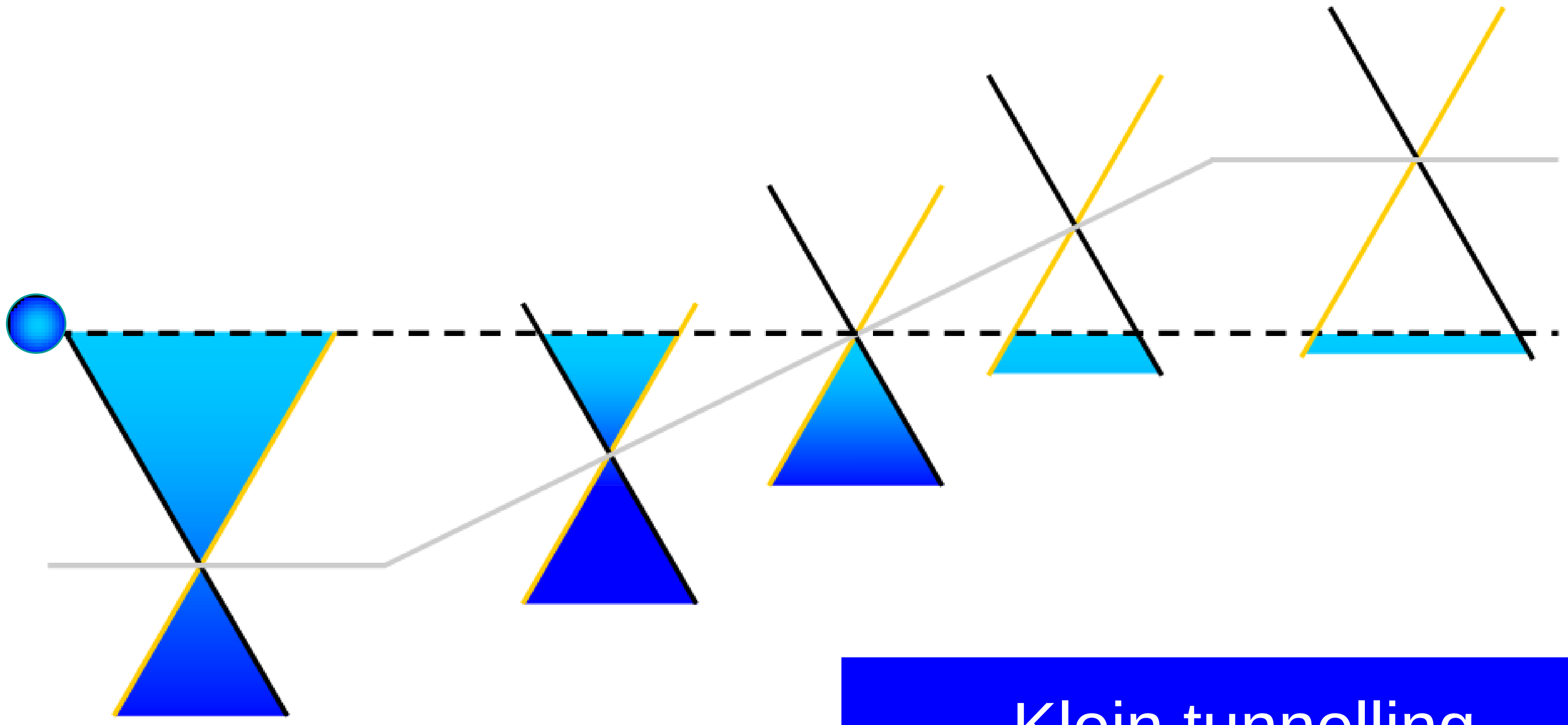

Klein tunnelling

in a Graphene p-n junction

What if the incidence is not normal to a barrier?

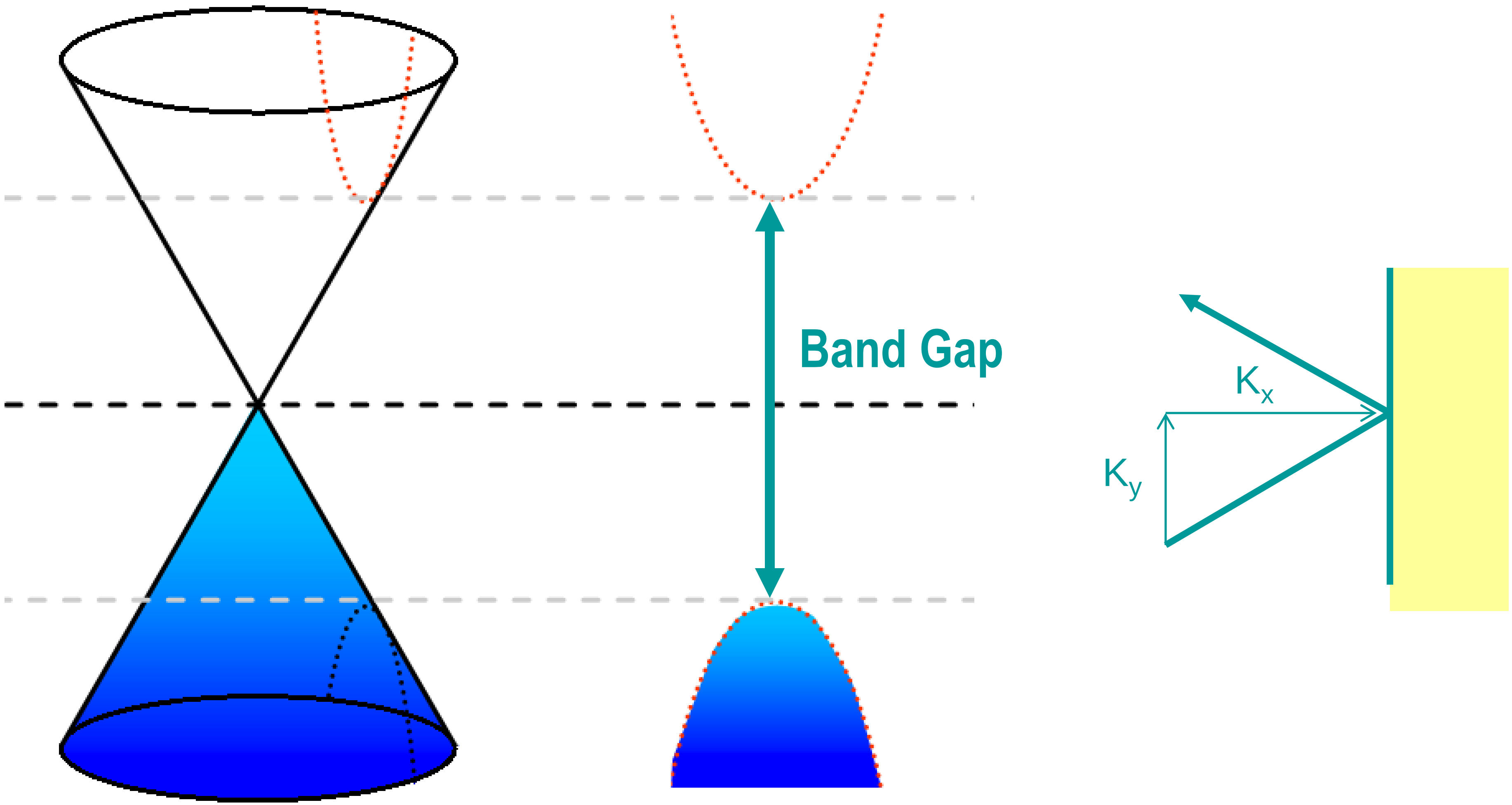

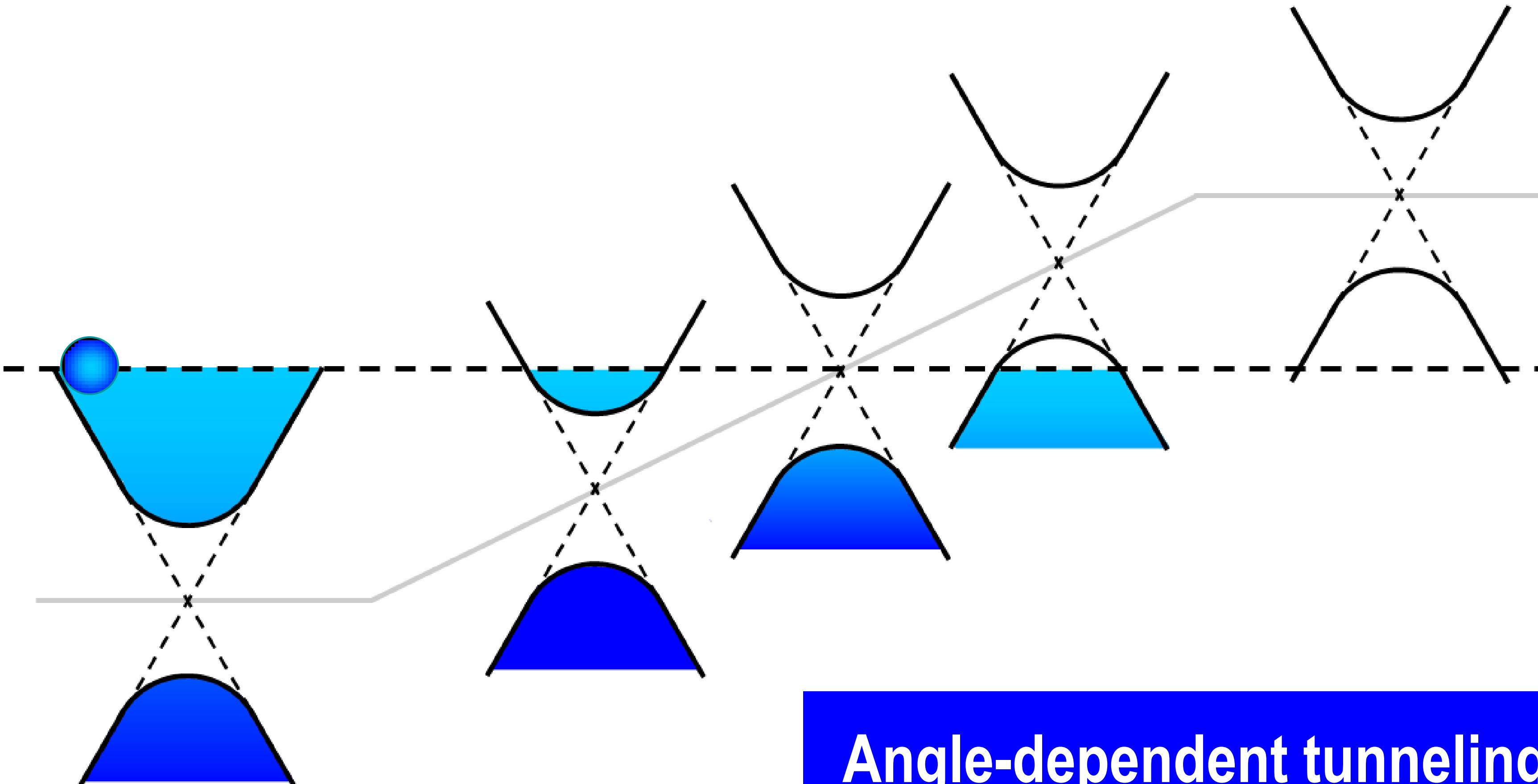

Angle-dependent tunneling in a Graphene p-n junction

Tunneling probability

in a Graphene p-n-p junction

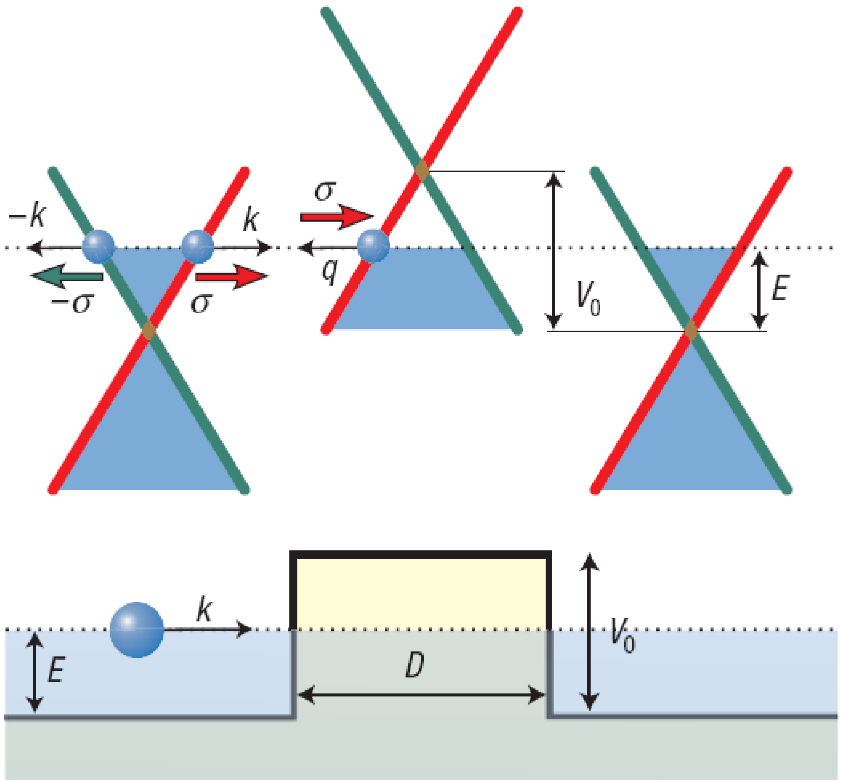

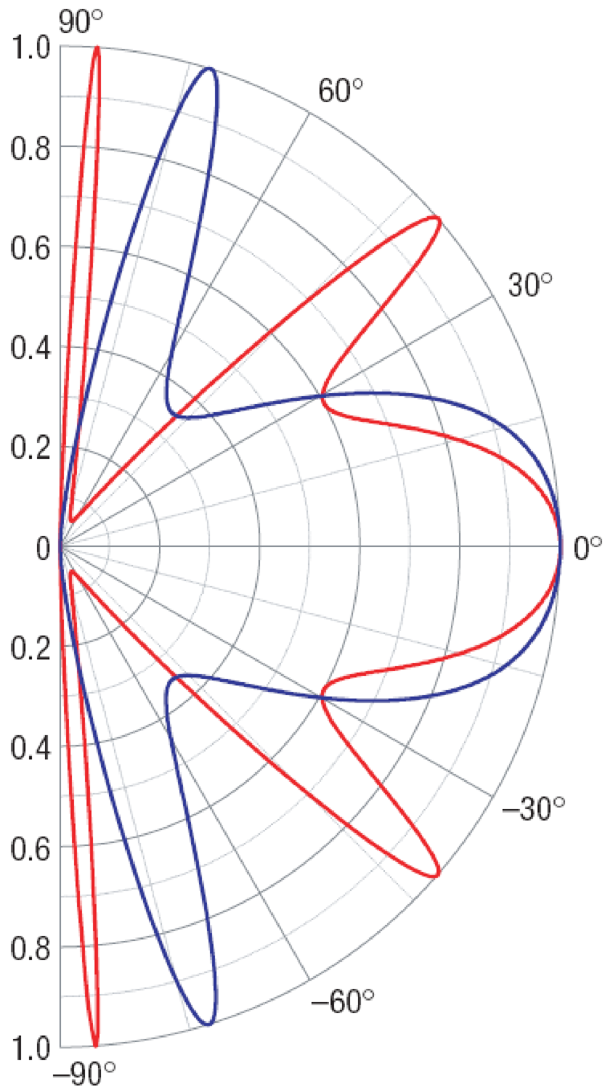

From M.I. Katsnelson, K.S. Novoselov, and A.K. Geim, Nature Physics 2, 620 (2006).

Momentum alignment of photoexcited carriers in graphene

For $\hbar\omega << \gamma_0$, $\left|\langle C|\hat{\mathbf{v}}|V\rangle\right|^2 = v_F^2 \sin^2(\varphi_{\mathbf{p}} - \varphi_{\mathbf{k}}) \Rightarrow$

$f(\mathbf{k}) \propto 1 + \alpha_0 \cos[2(\varphi_{\mathbf{p}} - \varphi_{\mathbf{k}})]$ **with** $\alpha_0 = -1$

(**p** is the light polarization vector)

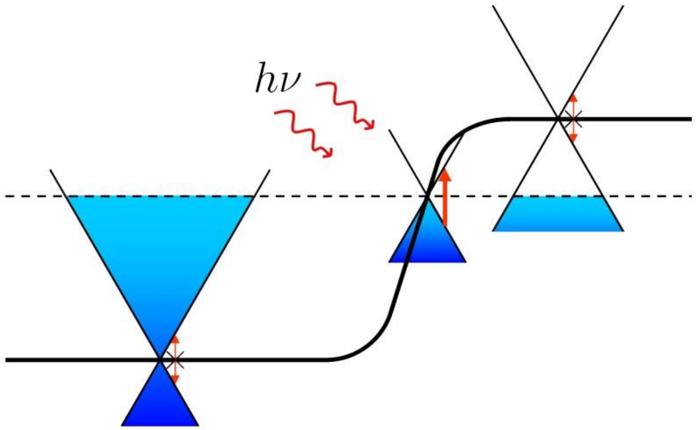

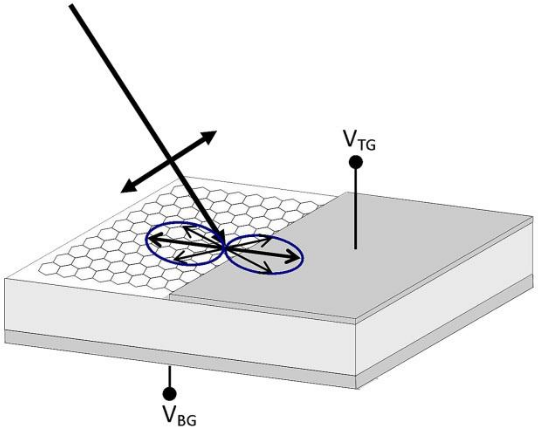

Momentum alignment of photoexcited carriers

Conical approximation

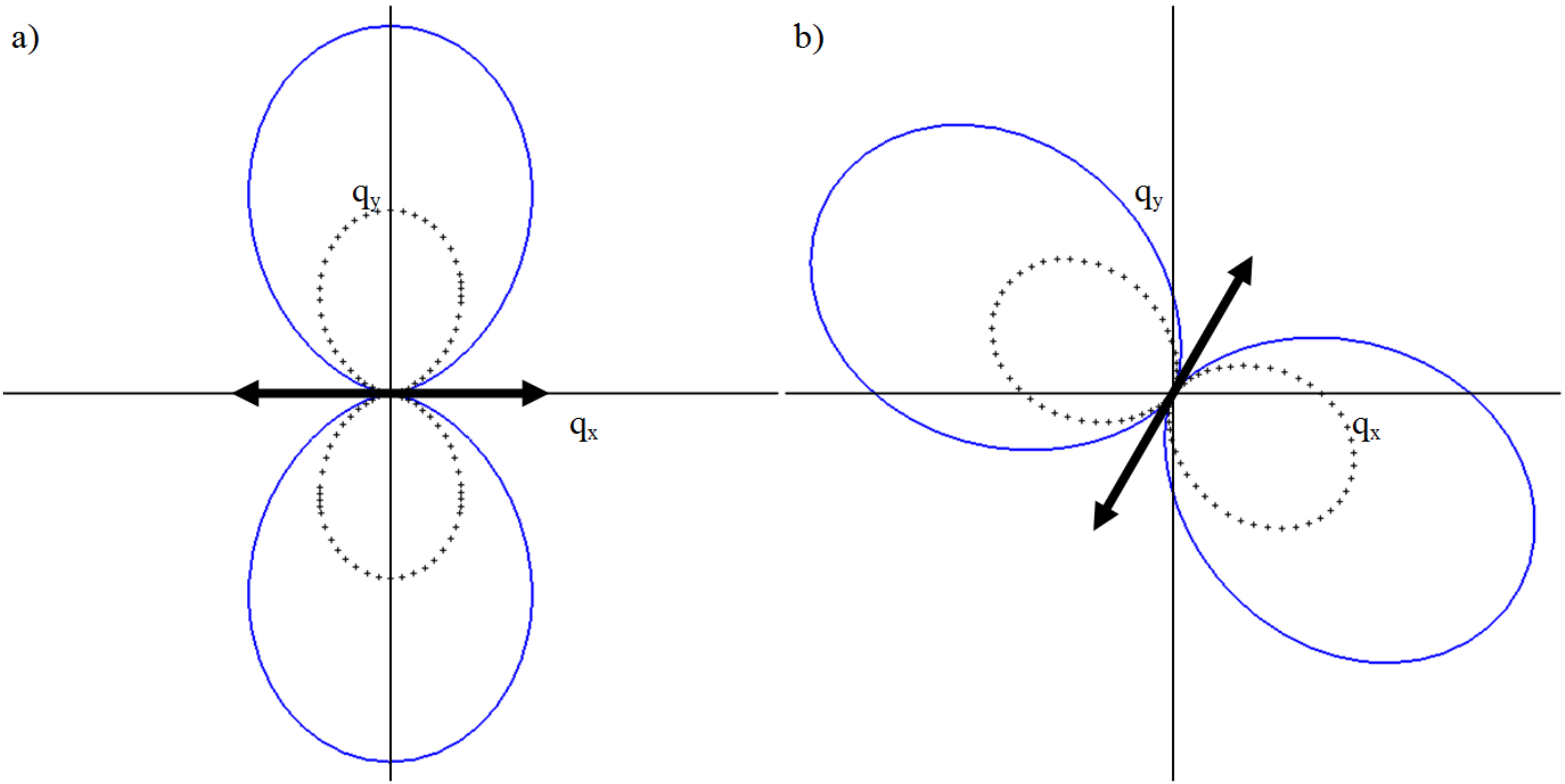

Polarisation angle at zero degrees from the x-axis

Polarisation angle at π/3 degrees from the x-axis

Momentum alignment of photoexcited carriers

Conical approximation

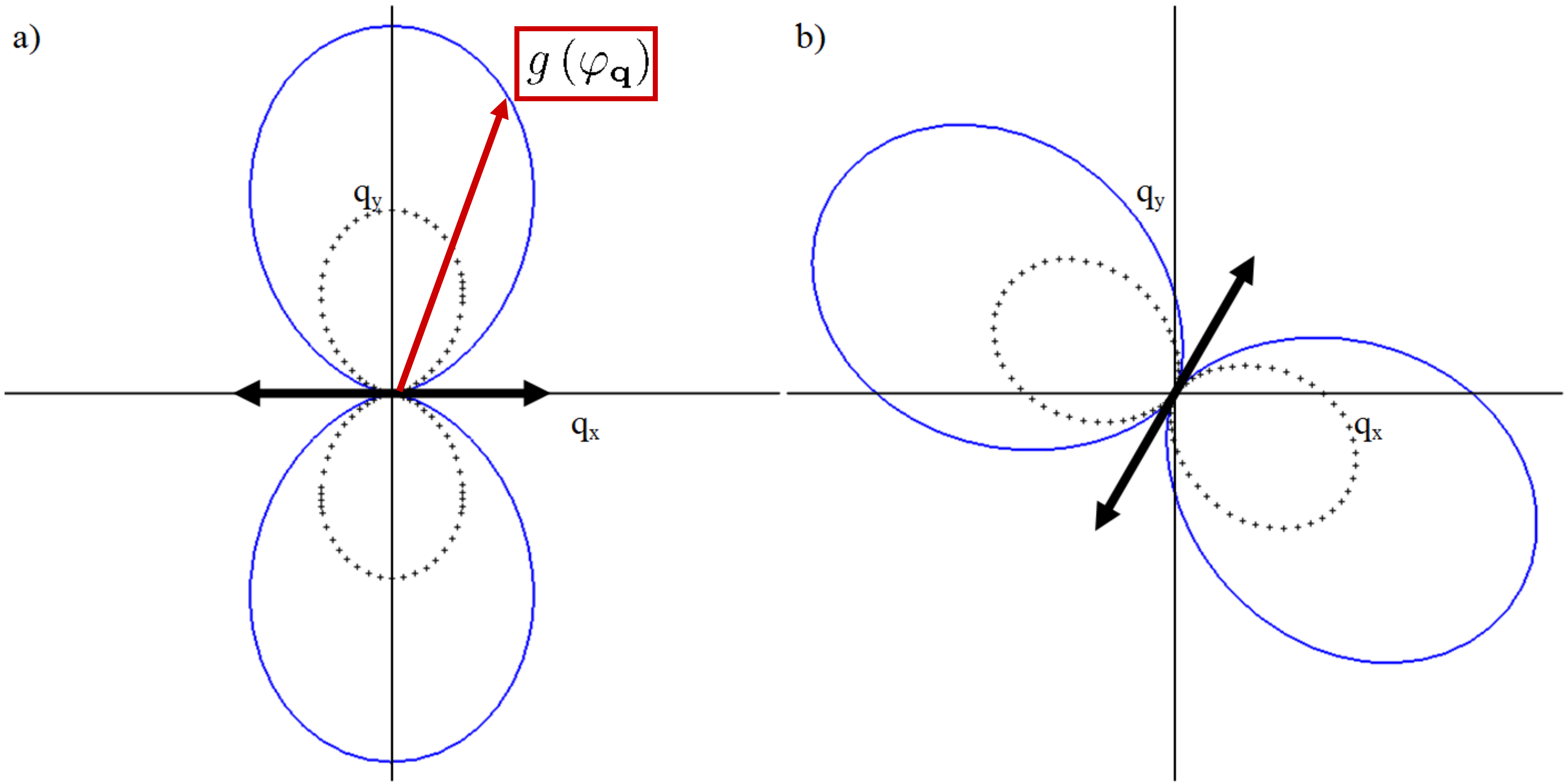

Polarisation angle at zero degrees from the x-axis

Polarisation angle at π/3 degrees from the x-axis

Reminder: alignment in conventional III-V quantum wells

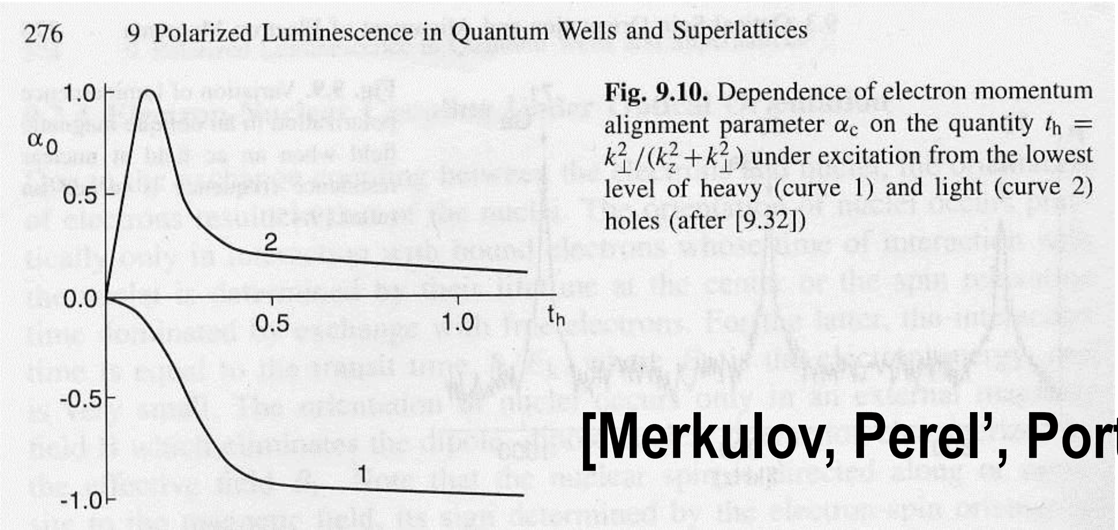

Fig. 9.10. Dependence of electron momentum alignment parameter α_c on the quantity $t_h = k_\perp^2/(k_z^2+k_\perp^2)$ under excitation from the lowest level of heavy (curve 1) and light (curve 2) holes (after [9.32])

From E.L. Ivchenko and G.E. Pikus "Superlattices and other heterostructures", (Springer, 1997).

[Merkulov, Perel', Portnoi, Sov.Phys.-JETP (1991)]

Influence of warping

Experiment:

D.N. Mirlin & Co (1990)

Theory:

MEP (1991)

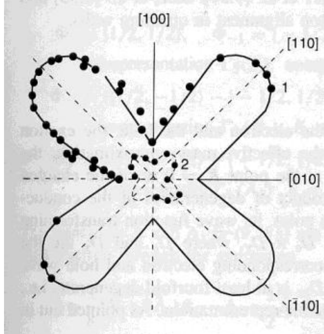

Fig. 9.11. Angular indicatrix of linear luminescence polarization for excitation and recombination to the lowest heavy hole level. Curve 1 – low temperatures (radiation is due to electrons with the highest energy); curve 2 – high temperatures (radiation comes from all excited electrons) (after [9.46])

Fig. 9.12. Angular indicatrix of linear polarization of luminescence in GaAs/AlGaAs superlattice at the high frequency edge of emission line. Curve 1, $E_0 = 215$ meV; curve 2, $E_0 = 60$ meV (after [9.48])

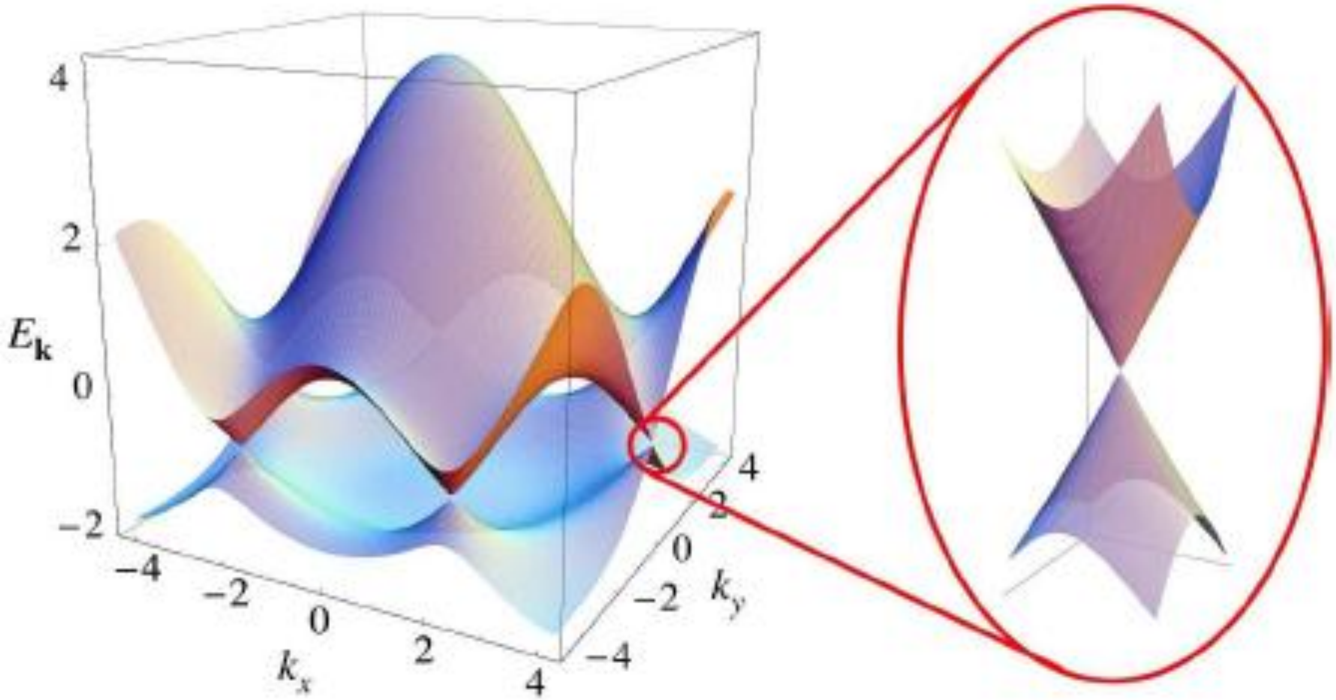

Graphene dispersion.

P.R. Wallace, The band theory of graphite. *Phys. Rev.* **71,** 622–634 (1947).

Calculations

Transition probability for a fixed q (here q=k-K):

$$W_{\mathbf{k}}^{\mathbf{k}} = \frac{2\pi h e^2 I_{\mathbf{e}}}{c(\hbar\omega)^2} \left| \mathbf{e} \cdot \left\langle \psi^C \left| \hat{\mathbf{v}} \right| \psi^V \right\rangle \right|^2 \delta\left(\xi_C - \xi_V - \hbar\omega\right)$$

with $\hat{\mathbf{v}} = \frac{i}{\hbar}\left[\hat{\mathcal{H}}, \mathbf{r}\right]$.

Total transition rate: $\sum_{\mathbf{q}} W = \left(\frac{1}{2\pi}\right)^2 \int \boxed{W q dq} d\varphi_{\mathbf{q}}$

Total absorption probability= $\pi \frac{e^2}{\hbar c}$ =0.023 – the same result as from dynamic conductivity calculations

Angular probability of absorption

$$g\left(\varphi_{\mathbf{q}}\right) = \left(\frac{1}{2\pi}\right)^2 \int W_{\mathbf{k}}^{\mathbf{k}}\left(q, \varphi_{\mathbf{q}}\right) q dq$$

Interpretation

"Pseudospin" – $\tilde{s} = (\boldsymbol{\sigma}\mathbf{p})/|\mathbf{p}|$.

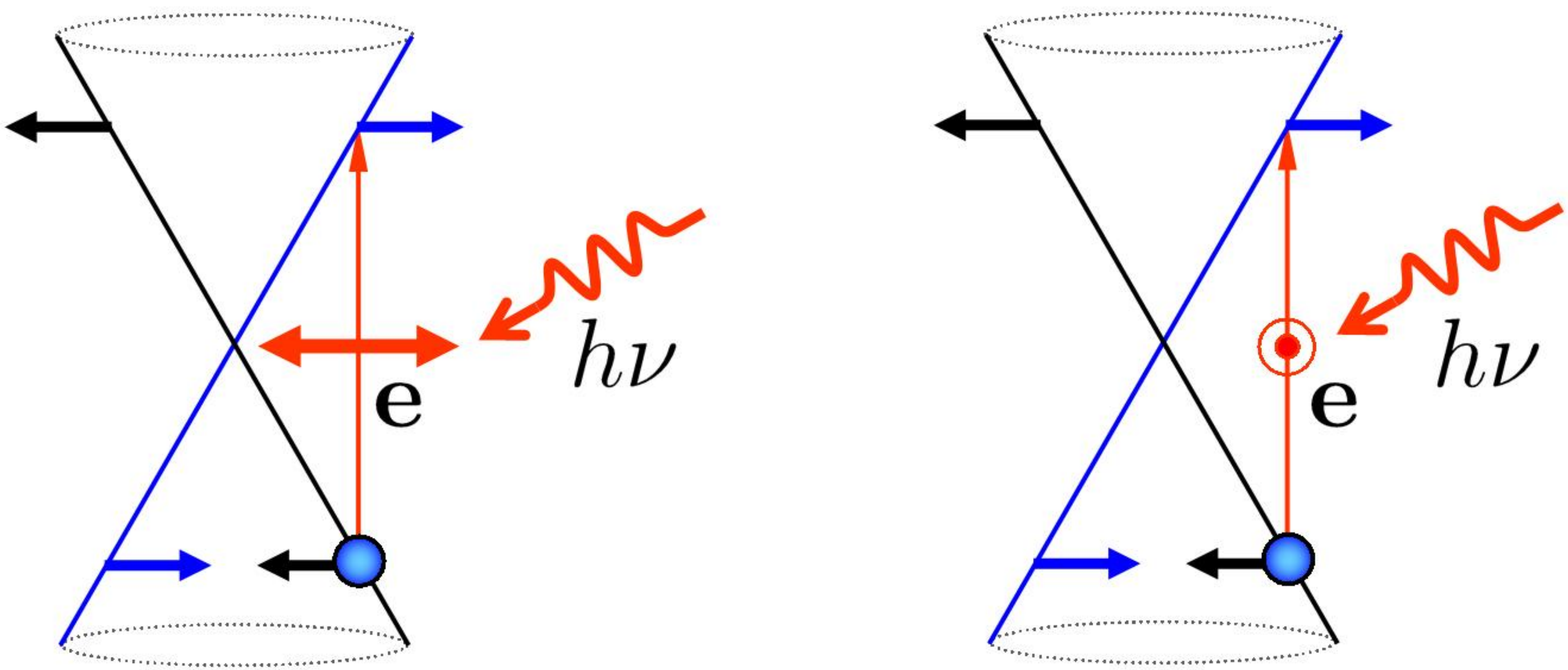

Pseudospin-orbit interaction as a reason for alignment

Momentum alignment of photoexcited carriers

Trigonal warping energy regime

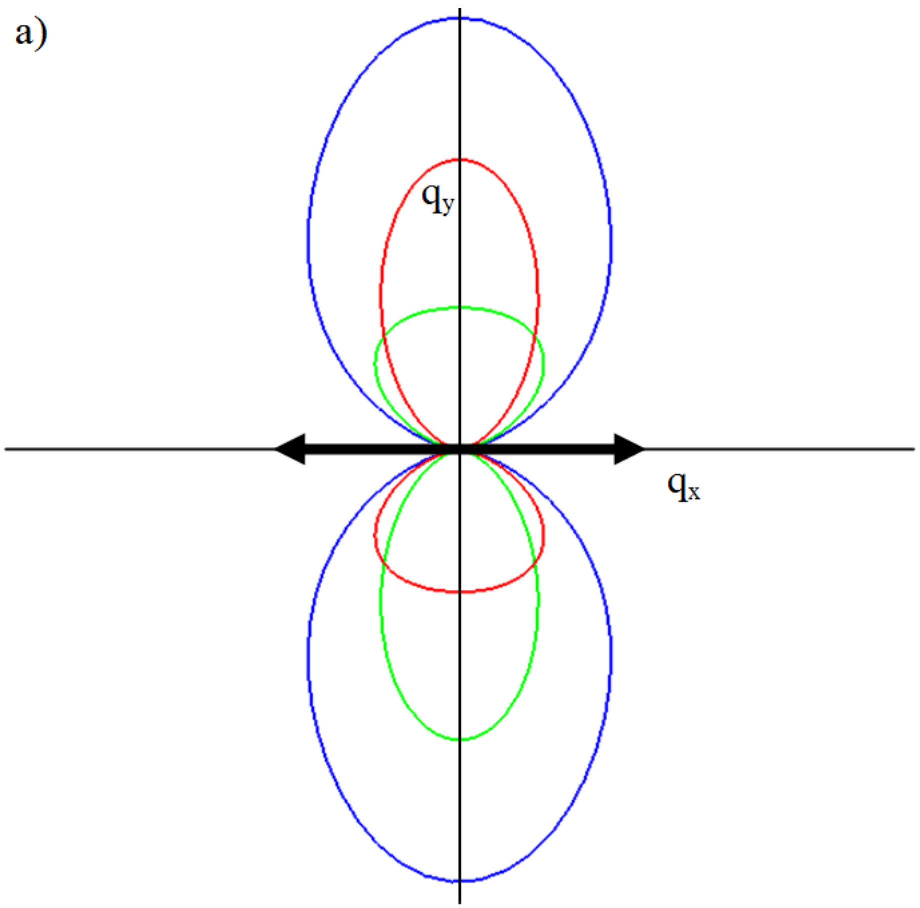

Polarisation angle at zero degrees from the x-axis

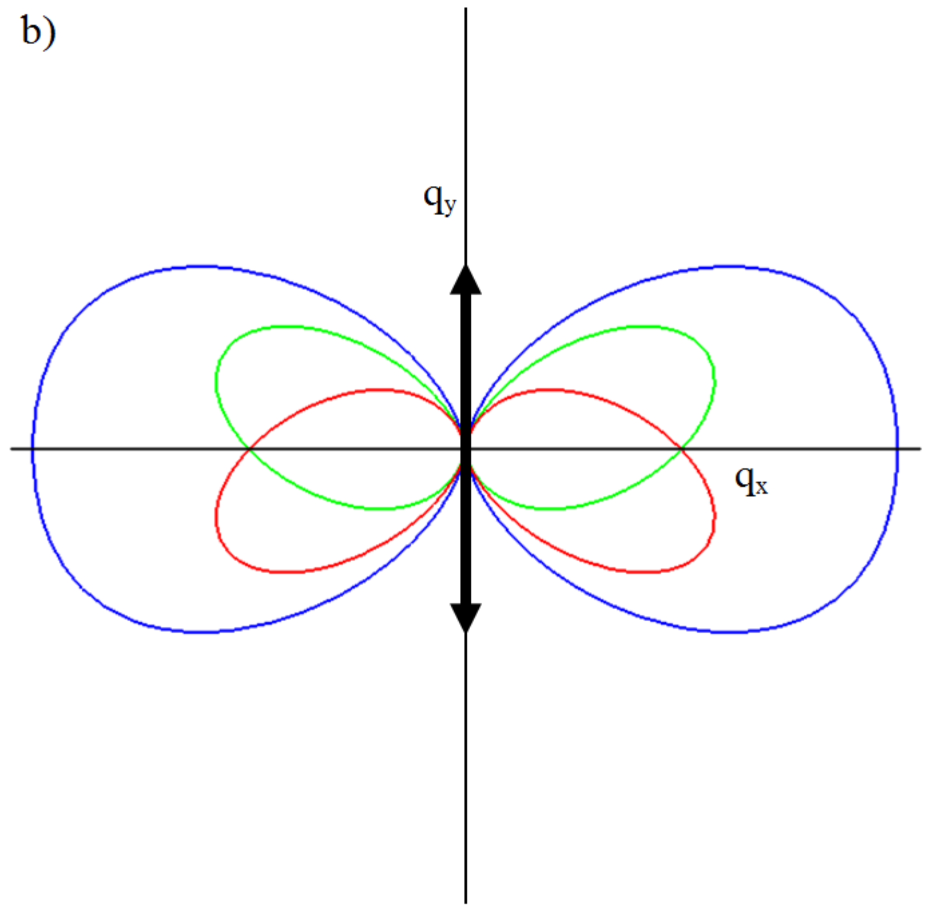

Polarisation angle at π/2 degrees from the x-axis

Comparison of high and low excitation frequency

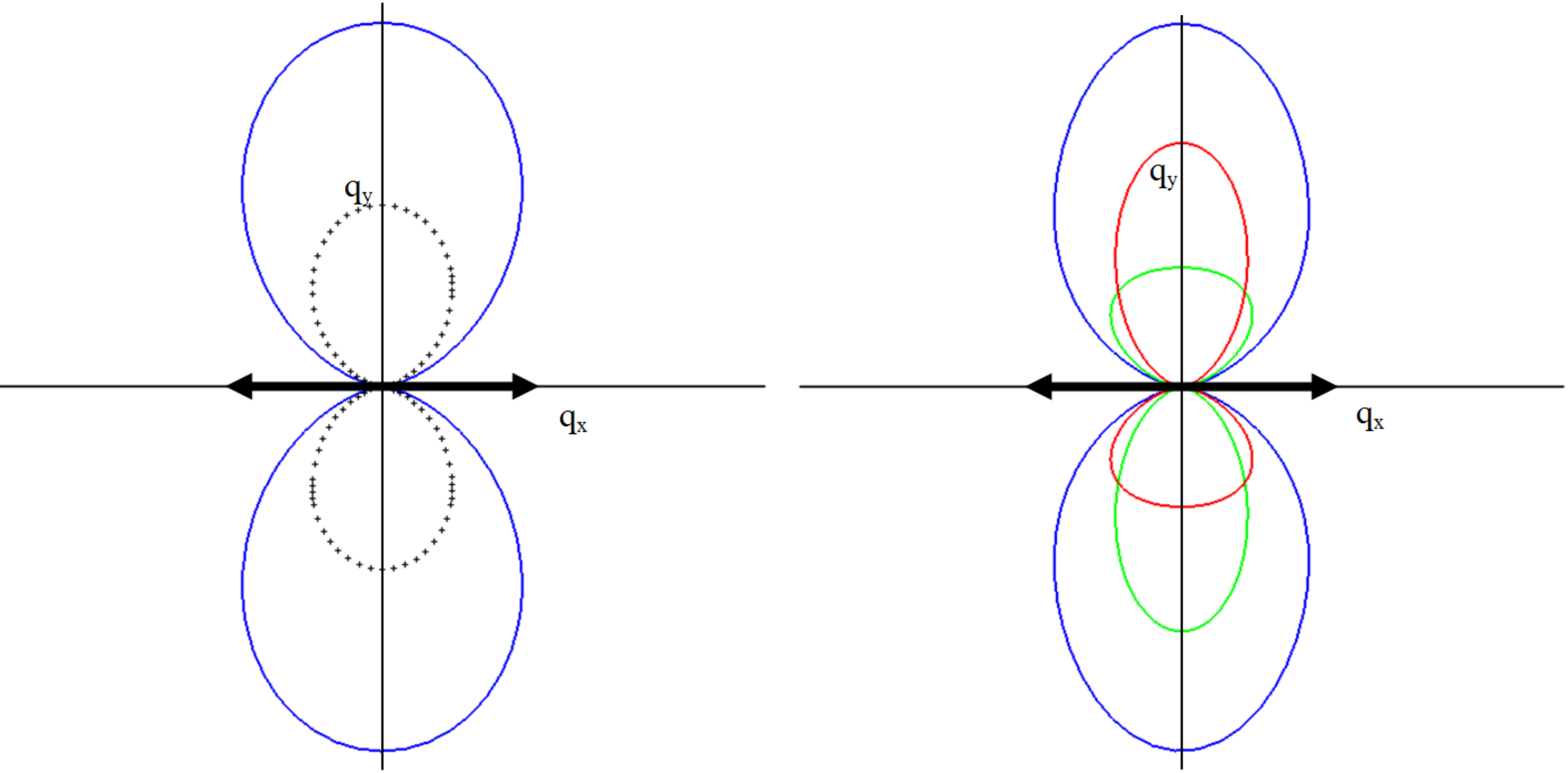

Valley mixing is essential to preserve symmetry!

The effect of trigonal warping

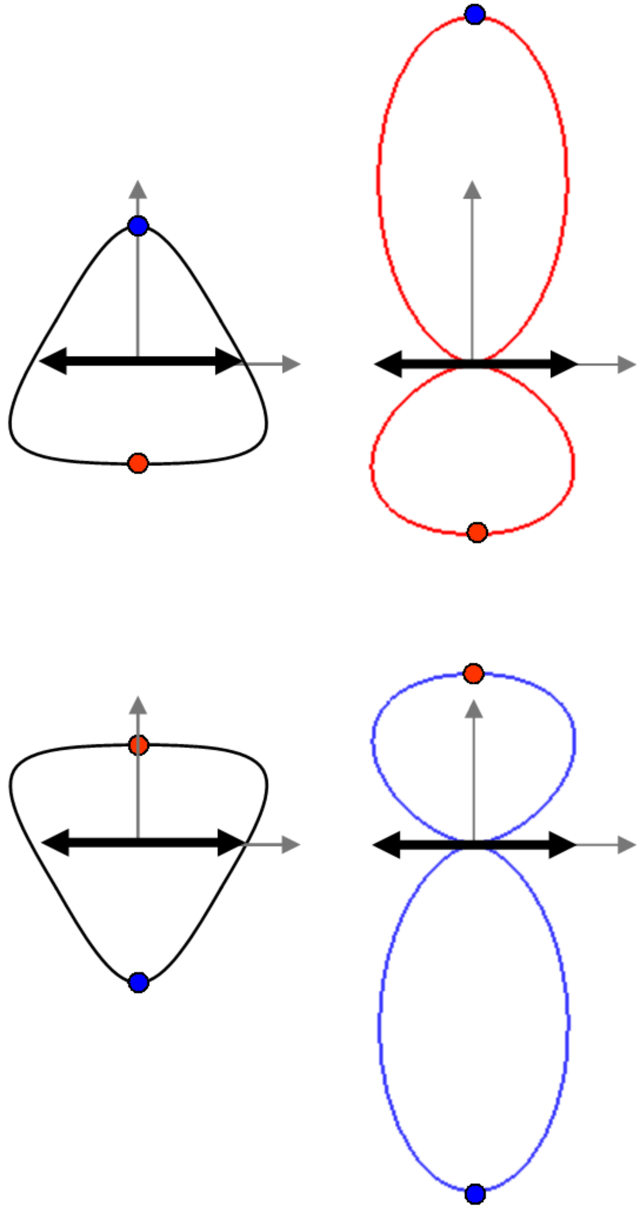

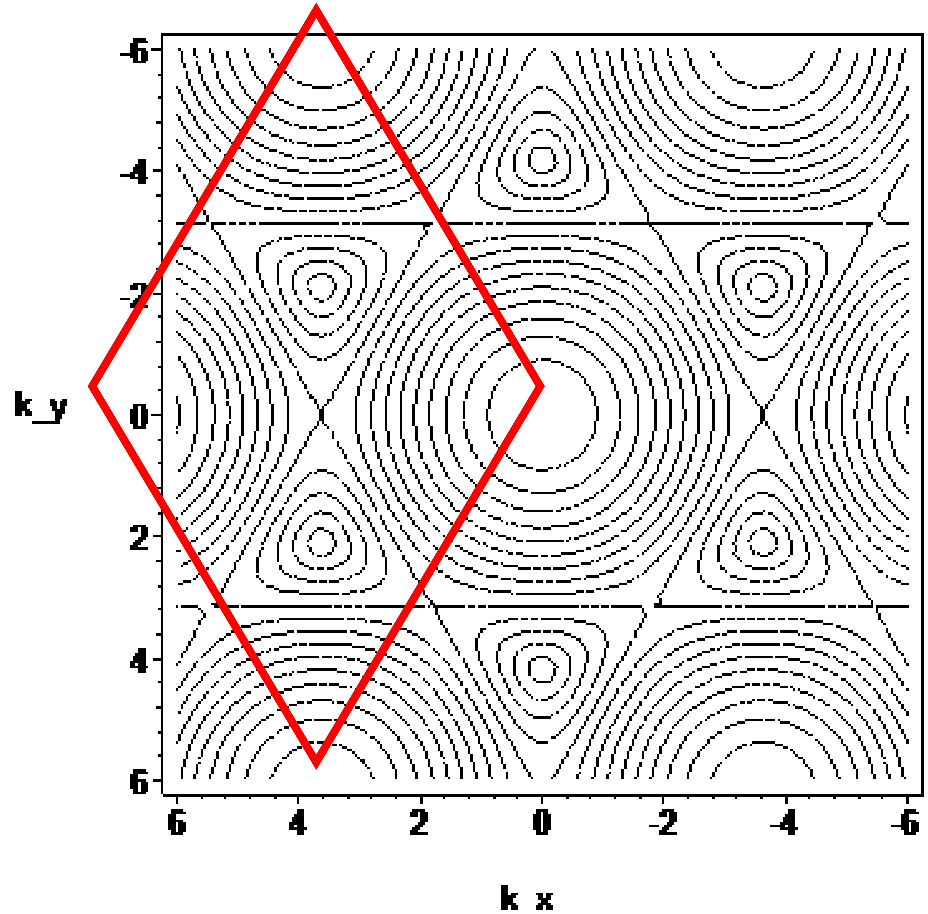

Optovalleytronics

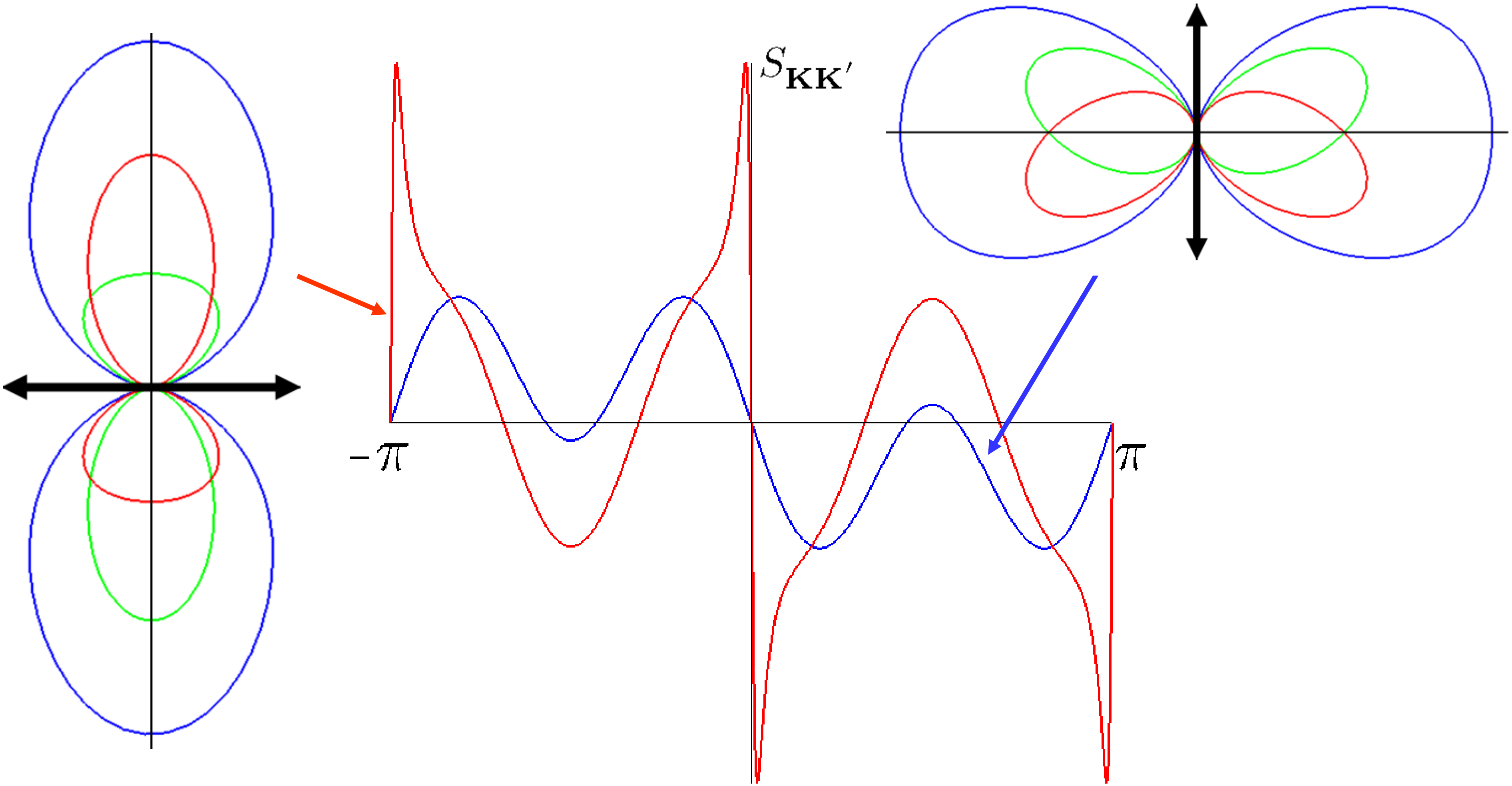

$$S_{\mathbf{KK'}} = \frac{F_{\mathbf{K}} - F_{\mathbf{K'}}}{F_{\mathbf{K}} + F_{\mathbf{K'}}}$$

Summary

- We demonstrate that a quasi-metallic carbon nanotube emits radiation in the mid-infrared range, when the potential difference is applied to its ends. The typical required voltages and nanotube parameters are similar to those available in the state-of-the-art transport experiments. The maximum of the spectral density of emission is shown to have the strong voltage dependence, which is universal for all quasi-metallic carbon nanotubes in the ballistic regime.
- We show that an electric field, which is applied normally to the axis of long-period chiral nanotubes, significantly modifies their band structure near the edge of the Brillouin zone. This results in the negative effective mass region at the energy scale below the high-energy phonon emission threshold. This effect can be used for an efficient frequency multiplication in the THz range.
- We discuss the feasibility of using the effect of magnetic field, which opens the energy gaps and allows optical transitions in armchair nanotubes, for detecting THz radiation. This effect also results in a very narrow emission line with the peak position controlled by the value of applied magnetic field..
- A similar effect is due to the curvature-induced gap in quasi-metallic CNTs
- Graphene can be used as a polarization-sensitive THz detector with sub-wavelength spatial resolution

Where can you read about it?

- PRB **71**, 035411 (2005)
- Proc. of SPIE 6328-5 (2006); arXiv:cond-mat/0608596
- Nano Letters **7**, 3414 (2007)

Generation of Terahertz Radiation by Hot Electrons in Carbon Nanotubes
O. V. Kibis, M. Rosenau da Costa, and M. E. Portnoi
pp 3414 - 3417; **(Letter)** DOI: 10.1021/nl0718418

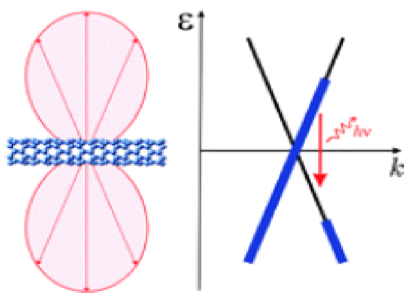

- Superlattices and Microstructures (2008); Physica E (2008); Int. J. Mod. Phys. B (2009); (reviews – 2010): J. Nanophotonics ; *The Handbook of Nanophysics, Vol. 4: Nanotubes and Nanowires.*

Where else can you read about it?

- Excitons in narrow-gap carbon nanotubes: PRB **84**, 035437 (2011)
- Graphene-based THz detectors + THz amplifiers based on narrow-gap CNTs:

R.R. Hartmann and M.E. Portnoi,

Optoelectronic Properties of Carbon-based Nanostructures: Steering electrons in graphene by electromagnetic fields **(LAP LAMBERT Academic Publishing, 2011)**

FUNDING:

UK EPSRC; 4 EU FP7 Networks; MCT, IBEM & FINEP (Brazil).

Thank you!

PEOPLE

Oleg Kibis[a,b]

Marcelo Rosenau[a], Vivaldo Campo Jr[a]

Richard Hartmann[a,c,d]

Neil Robinson[c], Lois Hugget[c]

Charles Downing[c], David Stone[c]

Ivan Shelykh[a,d,e]

(c)School of Physics
University of Exeter
United Kingdom

UNIVERSITY OF EXETER

(a)ICCMP
Universidade de Brasília

(b) DOCENDO DICIMUS НГТУ

(d) Instituto Internacional de Física
Universidade Federal do Rio Grande do Norte

(e) University of Iceland
(Háskóli Íslands - Forsíða)